Department of Mathematics and Statistics

Differential Equation and Complex Network Approaches for Epidemic Modelling

Chang Phang

This thesis is presented for the Degree of

Doctor of Philosophy of

Curtin University

June 2012

Declaration

The work presented in this thesis is my own work and all references are duly acknowledged.

This work has not been submitted, in whole or in part, in respect of any academic award at Curtin University or elsewhere.

Chang Phang

25 June, 2012

Acknowledgments

I would like to thank my supervisor, Professor Yong Hong Wu, for his guidance . His helpful suggestions and encouragement have been of great value to me in the research and the preparation of this thesis. I would also like to thank my associate supervisor,Associate Professor Benchawan Wiwatanapataphee, for her helpful advices and suggestions.

I am very grateful to Malaysia Government for the financial support during the period of my study. I would also like to thank Ministry of Higher Education Malaysia and Universiti Tun Hussein Onn Malaysia for giving me the opportunity to study in Perth.

Finally, I would like to thank the Department of Mathematics and Statistics, Curtin University for providing me with all the necessary facilities for my research. Acknowledgment is also made to all the staff and students in the Department of Mathematics and Statistics for their friendship and encouragement during my study at Curtin University.

Abstract

This study consists of three parts. The first part focuses on bifurcation analysis of epidemic models with sub-optimal immunity and saturated treatment/recovery rate as well as nonlinear incidence rate. Different from classical models, sub-optimal immunity models are more realistic for modelling the spread of the microparasitic infectious diseases such as Pertussis and Influenza A. By carrying out the bifurcation analysis, we find that for certain values of the model parameters, Hopf bifurcation, Bogdanov-Takens bifurcation and its associated homoclinic bifurcation occur. From the bifurcation curves established, one can predict the persistence or extinction of the diseases.

The second part of the research focuses on the problem of estimating the domain of attraction (DOA) for compartmental ordinary differential equation epidemic models. Determination of the domain of attraction for epidemic models is important for understanding the dynamic behaviour of the spread of diseases as a function of the initial population distribution. In this work, we focus on the sub-optimal immunity models investigated in the first part of this thesis. The theories of autonomous dynamical systems are utilized for the analysis, and a procedure has been established successfully to determine the maximal Lyapunov function in the form of rational functions and consequently the DOA.

In the third part of the research, we develop a bond percolation model for community clustered networks with an arbitrarily specified joint degree distribution. Our model is based on the probability generating function (PGF) formalism for

multitype networks, but incorporate also the free-excess degree distribution, which makes it applicable for clustered networks. In the context of contact network epidemiology, our model serves as a special case of community clustered networks which are more suitable for modelling the disease transmission in community networks with clustering effects. Beyond the percolation threshold, we have obtained the probability that a randomly chosen community-i node leads to the giant component; and in the context of contact network epidemiology, this probability refers to the probability that an individual in a community is affected by the infectious disease. Besides that, we have established the method to determine the size of the giant component and the average small-component size (excluding the giant component). When taking into account the clustering effect through the free-excess degree distribution, our study shows that the clustering effect will lead to the decrease in the size of the giant component. In short, our model enables one to numerically simulate the disease transmission in community networks taking into account the community structure effects and clustering effects.

List of Publications Related to This Thesis

1. Chang Phang and Yong Hong Wu, Bifurcation of an epidemic model with sub-optimal immunity and saturated recovery rate , *Proceeding of 2011 IEEE International Conference on Systems Biology (ISB)*, 2011, 155 - 160 .

Contents

List of Figures

List of Tables

Nomenclature

C	clustering coefficient
DOA	domain of attraction
E_i	equilirium point
G_p	generating function
$H_0(x)$	total number of vertices reachable from a randomly chosen vertex
$H_1(x)$	total number of vertices reachable from a randomly chosen edge
I	infective population
N	population
$O(x)^n$	polynomial with order n and higher
PGF	probablity generating function
R	recovered population
R_0	basic reproductive number
S	susceptible population
T	disease transmissibilty rate (network models)
p_k	probability that a randomly chosen vertex on the graph has degree k
q_{k-1}	probability that a vertex has excess degree $k-1$
t	time
z	average degree
β	disease transmisson rate (ODE models)
μ	natural death rate
$\langle s \rangle$	average cluster size

Chapter 1

Introduction

1.1 Background

The spread of infectious diseases has always been a big concern both in developed and developing countries. For instance, in the pass 30 years, the Human Immunodeficiency Virus (HIV), which cause Acquired Immunodeficiency Syndrome (AIDS) has become a serious sexually-transmitted disease throughout the world. In 2009, the World Health Organization (WHO) estimated that there were 33.4 million people worldwide living with HIV/AIDS, with 2.7 million new HIV infections per year and 2.0 million annual deaths due to AIDS.

Epidemics such as the 2002 outbreak of SARS, the 2009 outbreak of H1N1, and the Ebola virus outbreaks bring certain chaos to the society. It poses a threat to public health, economic and social development of the human society. For instance, the 1918 Spanish flu epidemic caused millions of deaths. Far before that, the bubonic plague (Black Death) had affected half of the population in Europe in 600 AD. The recurrent of this disease between 1346 and 1350 had caused the death of more than 10 000 people every day, and the death is as much as one-third of the population. Thus, the prevention and control of epidemics become very important and in fact, fighting with infectious diseases has a long history.

In less developed countries, every year, millions of people die of measles, respiratory infections, diarrhea and other infectious diseases that can be treated and not considered dangerous in the developed countries. Besides that, diseases such

as malaria, schistosomiasis, typhus, sleeping sickness, dengue and cholera, are endemic in many parts of the world.

In order to prevent and to control infectious diseases more effectively, or even to eradicate the diseases, at very first, it is very important to fully understand the mechanism of the transmission dynamics of the diseases. This kind of work includes the use of mathematical models to describe the diseases transmission processes. Based on the occurrence and progression of diseases and the surroundings, mathematical models can be formulated to characterize the infectious agents, to analyze the origins of the diseases and the factors involved in the transmissions, and even to predict the prevalence of the diseases and their patterns. Based on the analysis, the authorities can provide useful guidance or predictions so that better strategies and plans can be managed. In other words, quantitative studies based on mathematical models are able to describe the mechanisms of disease transmission and provide a foundation for prevention and control of the infectious diseases. Hence, there emerges a field of study which is called mathematical epidemiology. More specifically, for epidemic modelling, one will study both epidemics which are sudden outbreaks of a disease, and endemic situations in which a disease is always present. The existing mathematical models can be categorized in few groups, based on the described diseases, environments and populations, as linear, nonlinear, autonomous, or non-autonomous models. There exist, moreover, modelling variations in each category.

Mathematicians and physicists are among the academic workers who contribute to the knowledge of mathematical epidemiology. They keep up working in modelling the epidemics outbreak. One of the main parts of epidemiological research is focused on rate-based differential-equation models, i.e. compartmental models on completely mixing population. This epidemiology modelling has been used in planning, implementing and evaluating various prevention therapy and control programs. Before the era of research in complex networks, the theoretical approach to epidemic spreading is based on compartmental models in term of system of ordinary differential equations. Two typical epidemiology models in the ODEs

form, are the SIS (susceptible-infected-susceptible) model and the SIR (susceptible-infected-refractory) model [66]. In the SIS model, an individual has two possible statuses: susceptible and infected. A susceptible individual may become infected once it contacts an infected one. After certain time, the infected individuals recover and return to the susceptible state. In the SIR model, an individual has three possible statuses: susceptible, infected, and refractory (i.e. removal). The infected individuals cannot go back to the susceptible status but can become refractory, which describes the phenomenon of long-time immunity. In addition to these two typical models, there are many other models, such as the SI (susceptible-infected) model and the SIRS (susceptible-infected-refractory-susceptible) model, and the sub-optimal immunity model which lies in between the SIS and the SIR models. The sub-optimal immunity model is our major concern in this thesis. Examples of this kind of diseases include Pertussis (temporary immunity) and Influenza A (partial immunity). This kind of models is less studied in comparison to the existing SIS and SIR models. In this thesis, we will study the bifurcation of this kind of models.

Basically, the ODEs form of epidemic models uses the assumption that all the details, such as the individual habits, the geographical location and the presence of community structures, are averaged out. The mixing of individuals is considered as homogeneous mixing. But what in the reality is that the spreading of an infectious disease, i.e. epidemic process, on a social network is a heterogeneous process. Furthermore, humans tend to respond to the emergence of an epidemic by avoiding contacts with infected individuals. Such situation needs to be considered when we come to the epidemic modelling. In this context, we have to use nonlinear incidence rate which is more appropriate for describing the homogeneous mixing of population. On the other hand, the complex networks play an important role to obtain good representation for heterogeneous mixing in epidemics modelling.[8, 9, 12, 23, 31, 37, 62, 77–79]

In this aspect, the last decade has witnessed the active researches in complex networks, i.e. the networks in which the structure is irregular, complex and dynamically evolving in time. In the real world application, the dynamics of com-

plex networks has recently received much attention [14, 28, 84]. In this area, most researches have been directed in two major directions. The first direction is the dynamics of networks: the research in this direction focuses on structure of the networks, revealing that simple dynamical rules, such as preferential attachment or selective rewiring, can be used to generate complex topologies. The second direction is the dynamics on networks: research in this direction has focused on large ensembles of dynamical systems, where the interaction between individual units is described by a complex networks [38].

On top of that, researchers from various disciplines are trying to model the real world into certain type of network models. Apart from the random graph by Erdos and Renyi in 1959, other important work has been done by Watts and Strogatz in 1998 [92], Barabasi and Albert in 1999 [6] where two important properties, the small-world effect and the scale-free networks (i.e. power law distribution), were discovered. Another property which many networks have in common is clustering, or community structure, where a seminal paper appeared in 2002 by Girvan and Newman [34] who proposed a new algorithm for detecting community structure in networks [70, 71]. Various analytic and numerical studies have been carried out for the model itself [21, 64, 68, 72, 86] and one of the important applications is in epidemics modelling [56, 73]. Apart from that, many authors proposed modifications and generalization to make the complex network model to more realistically represent real networks.[6, 74].One of the phenomena that shows this feature is the spreading process such as opinions and diseases on social networks. In this project, apart from the bifurcation analysis for the sub-optimal immunity model, we also focus on the study of the spreading of diseases in community networks. Our objective is to obtain the more realistic model for epidemics outbreaks so as to obtain the analytical solution for counting the size of epidemic. Our model is based on the probability generating function which can be used to represent any degree distribution. In more general context, according to their degree distribution, networks can be categorized into homogeneous networks and heterogeneous networks. In the context of epidemic spreading, for homogeneous networks, the dynamics can be

shown by the mean field or fully mixed approaches [63], while for the heterogeneous networks, the influence of degree distribution must be considered. Examples of the homogeneous network include the Erdos and Renyi (ER) random network and the small-world network (SW) in which the node degree distribute around a mean value and decay exponentially. An example of heterogeneous networks is the Barabasi and Albert's scale free network in which the degree distribution satisfies the power law. Hence the use of the probability generating function has an advantage here because it enables the derivation of network models with arbitrary degree distributions.

In short, apart from the bifurcation analysis for the sub-optimal immunity models, we aim to model the epidemics outbreak in the sense of complex networks. We will build the complex network model based on the probability generating function formalism.

1.2 Objectives

The main purpose of the work is to study the rich dynamics of the sub-optimal immunity model with saturated treatment rate through bifurcation analysis and computation of the domain of attraction. Apart from that, we will build the model based on the probability generating function formalism to cater the need of investigating the disease transmission in community networks. More specifically, this project has the following objectives:

(i) Investigate the rich dynamics of an epidemic model with sub-optimal immunity and saturated treatment/recovery rate through bifurcation analysis.

(ii) Formulate an epidemic model with sub-optimal immunity, nonlinear incidence and saturated treatment/recovery rate and investigate its rich dynamics through bifurcation analysis.

(iii) Determine the domain of attraction of the sub-optimal immunity models.

(iv) Develop a model based on the probability generating function formalism to

study the disease transmission in community networks and obtain the analytical solution through the bond percolation method.

1.3 Main contributions of this thesis

The main contributions of this thesis include the following aspects:

(i) Development of analytical results to demonstrate the existence of Bogdonov-Takens bifurcation in the sub-optimal immunity model with saturated recovery rate.

(ii) Construction of a new model which combines nonlinear incidence rate and nonlinear treatment/recovery rate for sub-optimal immunity type models.

(iii) Development of a new robust procedure for determining the maximal Lyapunov function in the form of rational functions.

(iv) Development of a bond percolation model of community clustered networks with an arbitrary joint degree distribution (i.e. the degree distribution is arbitrarily specified).

1.4 Outline of the thesis

This thesis consists of seven chapters. Chapter One provides a brief introduction of the research and presents the objectives of the study. Chapter Two discusses some necessary background information and knowledge highly relevant to this research and also reviews previous work closely related to the scope of this project. The more specific literature review for each topic in this research is in the first section of each chapter from Chapter Three to Six.

Chapter Three discusses the epidemic model with sub-optimal immunity and saturated treatment/recovery rate. Different from classical models, sub-optimal immunity models are more realistic to explain the microparasitic infectious diseases such as Pertussis and Influenza A. By carrying out the bifurcation analysis of the

model, we show that for certain values of the model parameters, Hopf bifurcation, Bogdonov-Takens bifurcation and its associated homoclinic bifurcation occur. By studying the bifurcation curves, one can predict the persistence or extinction of the diseases.

Chapter Four presents a new epidemic model with sub-optimal immunity, nonlinear incidence and saturated treatment/recovery rate. Beside the bifurcation analysis similar to that in Chapter Three, due to the combination of the nonlinearities in both incidence rate and recovery rate, the work involves a more complex analysis of equilibrium through a higher order polynomial and thus, some analysis involves numerical analysis.

Chapter Five deals with the problem of estimating the domain of attraction (DOA) for epidemic models. In this work, we establish a procedure to determine the maximal Lyapunov function in the form of rational functions. The estimation of domain of attraction for epidemic models is important for understanding the dynamic behaviour of the spread of diseases as a function of the initial population distribution. We focus on the sub-optimal immunity models with saturated treatment rate which we study in Chapter Three and Four.

Chapter Six presents a bond percolation model for community clustered networks with an arbitrary joint degree distribution (i.e. the degree distribution is specified). Our model is based on the probability generating function (PGF) formalism for multitype networks and incorporate the free-excess degree distribution, which makes it applicable for clustered networks. In the context of contact network epidemiology, our model serves as a special case of community clustered networks which are more suitable for modelling the disease transmission in community networks with clustering effects. Beyond the percolation threshold, we obtain the probability that a randomly chosen community-i node leads to the giant component and in the context of contact network epidemiology, the probability refers to the probability that an individual in a community is affected by the infective disease. In addition, we establish formulae to calculate the size of the giant component and the average small-component size (excluding the giant component). When taking into

account the clustering effect through the free-excess degree distribution, our model shows that the clustering effect will lead to decrease in the size of the giant component. In short, our model enables us to find the numerical calculation related to the disease transmission in community networks with various community structure effects and clustering effects.

Chapter Seven presents the conclusions from this study. Further research is also provided in this chapter.

We conclude the Chapter 1 by showing the structure of this thesis and the links of chapters in the thesis.

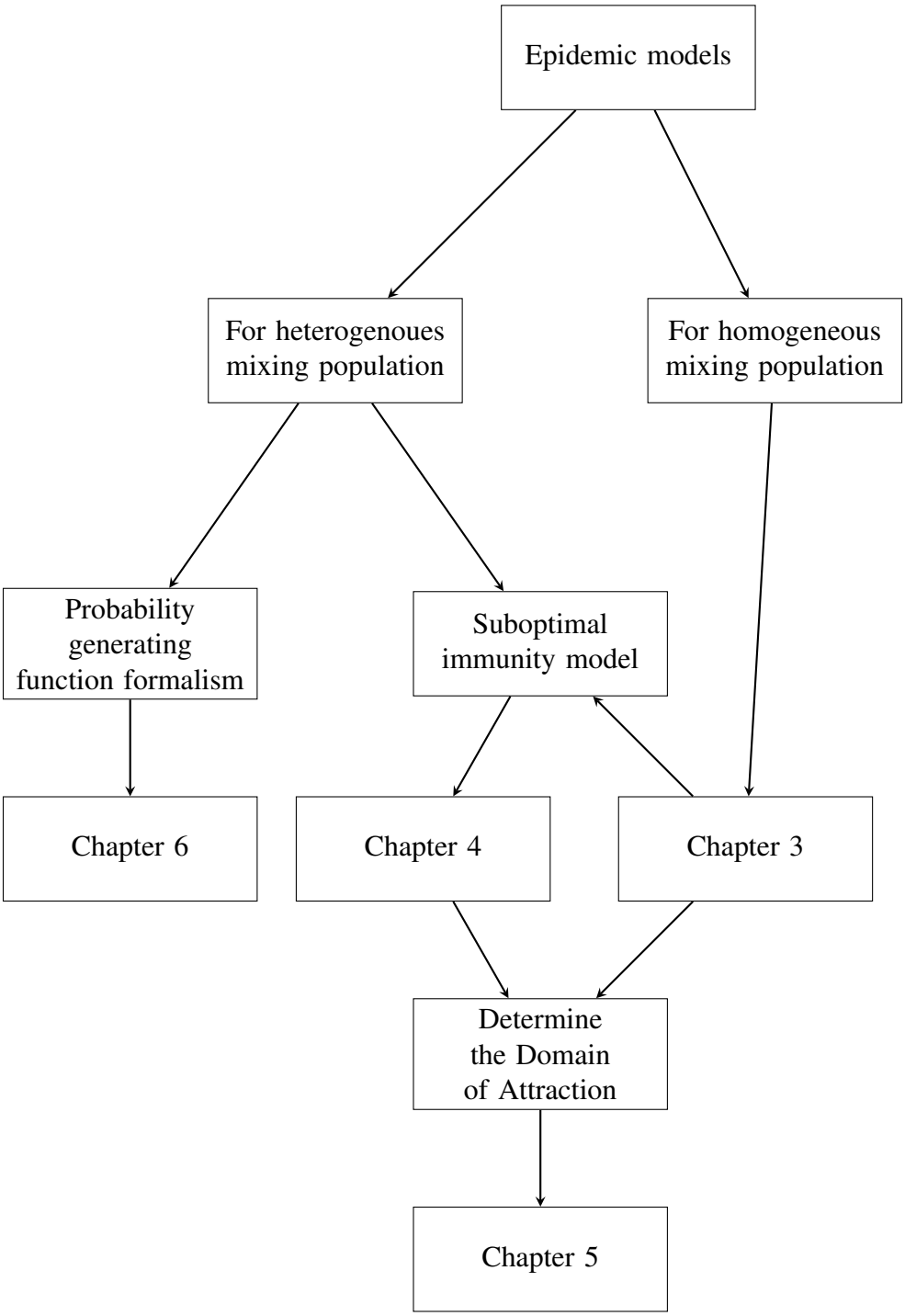

Figure 1.1: The structure of this thesis and the links of chapters in the thesis

Chapter 2

Literature Review

The transmission of infectious diseases is one of the biological problems. By using certain assumption, one can describe it by mathematical models, and through mathematical analysis, solution can be obtained. Simulation will be done to compare the mathematical models with the actual biological problems, before it can be used for prediction of real phenomena. These rely very much on the assumptions used in the models.

In the past few decades, many different types of mathematical models have been developed for the study of disease transmission, including the differential equation models and complex network models. Different models offer different advantages over others on some aspects but also have limitation on other aspects. Generally, it is almost impossible to establish an unified epidemic model to represent all the aspects. In this research, we focus on a compartmental model, namely the suboptimal immunity model, which is more realistic in explaining the microparasitic infectious diseases such as Pertussis and Influenza A. We will extend the existing models to include some special features such as nonlinear incidence rate and saturated treatment recovery rate, so that the model is capable of simulating nonlinear phenomena such as outbreak of diseases. We will also develop a bond percolation model which is more appropriate for the study of disease transmission in community structure networks with extra consideration of the clustering effect. We will review and discuss previous works relevant to our research in this chapter.

The rest of this chapter is organized as follows. In Section 2.1, we review

the basic modelling aspect of compartmental ordinary differential equation (ODE) models, including the structure of the SIR type models, the threshold condition, equilibrium and stability analysis, types of incidence rate, types of recovery rate and sub-optimal immunity models. In Section 2.2, we focus on the mathematical analysis aspect for compartmental ODE models, including particularly the Hopf bifurcation, Bogdanov-Takens bifurcation and domain of attraction (DOA). In Section 2.3, we will review some basic concepts to be used for our community structure networks, with particular focus on the probability generating function (PGF) formalism.

2.1 General overview for compartmental models

Besides complex network models, there are two main branches in epidemic modeling, namely stochastic models and deterministic models. Deterministic models provide a useful approximation to the epidemic evolution of highly infectious agents that appear ubiquitous throughout large populations [4], while stochastic models replace the actual values of the numbers of susceptible and infectious individuals with probability distributions.

In deterministic models, the most common approach is using a compartmental representation of the various stages in the spreading of diseases. Normally, the models are expressed by a system of ordinary differential equations (ODEs). The first compartmental model was developed by Kermack and McKendrick in 1927 where the compartments in the model represent the subpopulations including susceptible, infectious and removal individuals. The model is applicable for the viral diseases such as measles and chickenpox for which the individuals gain immunity to the same virus. Later in 1932, Kermack and McKendrick proposed a SIS model which explains the disease transmission dynamics in bacterial diseases such as encephalitis and gonorrhea where the recovered individuals gain no immunity and can be reinfected. Since then, various researches extended the classical models in many aspects so that they can describe well the complex epidemiological characteristics.

Typical models include the sub-optimal immunity models [35, 76], the models with latent period [52, 53], the models with nonconstant population [16, 25], and the models with the effects of quarantine on disease transmissions [32, 75, 94]. Epidemic models have been used in many applications and for more details, we refer the reader to the references [4, 15, 19, 26, 44]. Various studies have also been undertaken specific to certain kinds of diseases such as the Chikungunya disease [65], the hands-foot-mouth disease [81], dengue fever [33], tuberculosis [11, 20], West Nile virus [93] and Malaria [22].

2.1.1 SIR framework models

For the compartmental epidemic models, the host population is divided into three non-overlapping classes that distinguish an individual's state of disease as either susceptible, S, infective, I or recovered, R. Assuming a fixed population, $N = S(t) + I(t) + R(t)$, which means the population is closed and hence there is no change in demographic as no individuals leave or enter the population, Kermack and McKendrick (1927) derived the following equations:

$$\begin{aligned} \frac{dS}{dt} &= -\beta SI \\ \frac{dI}{dt} &= \beta SI - \mu I \\ \frac{dR}{dt} &= \mu I, \end{aligned} \tag{2.1}$$

with initial condition : $S(0) = S_0 > 0$, $I(0) = I_0 > 0$, $R(0) = 0$ and where all the parameters are positive. β is the disease transmission rate, while μ is the natural death rate . βSI is called incidence rate while μI is removal rate.

From $\frac{dI}{dt} = \beta SI - \mu I$, we have $\frac{dI}{dt}|_{t=0} = \beta S_0 I_0 - \mu I_0$. Let $\rho = \mu/\beta$, if $S_0 > \rho$,then $\frac{dI}{dt}|_{t=0} = \beta S_0 I_0 - \mu I_0 > 0$ and so $I(t) > I_0$ for some $t > 0$, i.e. epidemic occurs. If $S_0 < \rho$,then $\frac{dI}{dt} = \beta SI - \mu I_0 \leq 0$ for all $t \geq 0$, and so the infection dies out, i.e. no epidemic can occur. $\rho = \mu/\beta$ is sometimes called the relative removal rate and its reciprocal β/μ is the infection contact rate.

For β, we can let it be fb, where the parameter f is the rate at which an individual makes contacts with others and b is the transmission probability that a

contact between an infective and susceptible leads to transmission of the infection. Equation $\frac{dR}{dt} = \mu I$ is redundant, as one can calculate R as $N - S - I$. The quantities S, I and R are all bounded above by N. Hence, mathematical analysis can be carried out with the reduced system having lower dimension.

Besides the typical three compartment SIR model, many other similar types of epidemiology models have been developed such as the MSEIR, MSEIRS, SEIR, SEIRS, SIRS, SEI, SEIS, SI and the SIS model, where M is the passively immune class and E is the latent period class. Each model is used to study certain particular infectious diseases. For instance, the SEIR model, which includes an exposed or latent period class of individuals who are not yet infectious, is appropriate for the yellow fever.

2.1.2 Threshold condition

In compartmental epidemic models, one of the important parameters is the basic reproduction number R_0, which is the average number of secondary infections caused by an average infective. For the classical model (2.1), the basic reproduction number is given by $R_0 = fb/\mu$ or more generally $R_0 = Nfb/\mu$. If $R_0 > 1$, epidemic can occur. R_0 gives the average number of secondary infection that arise when an infectious individual is introduced into an otherwise entirely susceptible population. The value of R_0 does not depend on the distribution of infectious periods. By definition, the basic reproductive number R_0 can be written as

$$R_0 = \left(\frac{\text{infection}}{\text{contact}}\right)\left(\frac{\text{contact}}{\text{time}}\right)\left(\frac{\text{time}}{\text{infection}}\right). \tag{2.2}$$

Mathematically, the basic reproduction number, R_0, can be computed by using the survival function or the next generation matrix method [27].

In the next generation matrix method, the basic steps for calculating the basic reproduction number,R_0, for the compartmental epidemic models are as follows.

Step 1: Find $F_i(x_0)$ and $V_i(x_0)$, where F_i are the new infections in compartment i , V_i denote the infections transformed from other compartments to compartment i, x_0 is the disease-free equilibrium state.

Step 2: Find the next generation matrix G where $G = FV^{-1}$ and , $F = \left[\frac{\partial F_i(x_0)}{\partial x_j}\right]$,$V = \left[\frac{\partial V_i(x_0)}{\partial x_j}\right]$.

Step 3: The spectral radius of $G = FV^{-1}$ is the basic reproduction number, R_0.

Further notes on the basic reproduction number,R_0, for the compartmental epidemic models are available in [41, 87].

2.1.3 Equilibrium and stability analysis

A general way to determine the stability at an equilibrium point is by calculating the eigenvalues of the Jacobian matrix, J, at the equilibrium point. For example, for the SIR model (2.1), the Jacobian matrix for the reduced system is

$$J = \begin{pmatrix} -\beta I^* & -\beta S^* \\ \beta I^* & \beta S^* - \mu \end{pmatrix},$$

where (S^*, I^*) is the state at an equilibrium point. For the disease free equilibrium, $(S^*, I^*) = (N, 0)$, and the eigenvalues of the Jacobian matrix are $\lambda_1 = 0$ and $\lambda_2 = \beta N - \mu$. In order for the system (2.1) to be stable, we need $Re(\lambda) < 0$, that is $R_0 = \beta N/\mu < 1$. At the stable equilibrium point (S^*, I^*), the solutions in the neighbourhood of the equilibrium point are attracted to the point.

In summary, for the epidemic model $\dot{x} = f(x)$ with n equations and n unknowns, the procedure for the equilibrium and stability analysis is as follows:
Input: $\dot{x} = f(x)$.
Output: Stability analysis for the equilibrium point(s).

Step 1: Determine the fixed points x^* where $f(x^*) = 0$, including the disease free equilibrium (DFE),P_0, and the endemic equilibrium (EE), P^*.

Step 2: Find the Jacobian matrix, $J(P)$, at the equilibrium point.

Step 3: Find the eigenvalues of $J(P)$.

Step 4: If all the eigenvalues have negative real parts, the equilibrium point is locally asymptotically stable.

2.1.4 Types of incidence

There are two categories of incidence rate, namely bilinear incidence rate and saturated incidence rate. Bilinear incidence is simply $\beta N\frac{S}{N}I$, or βSI and models based on this have a trivial equilibrium (corresponding to the disease-free state) and nontrivial equilibrium (corresponding to the endemic state) which are usually asymptotically stable. The bilinear incidence rate is based on the law of mass action, which is appropriate for communicable diseases such as influenza, but not for sexually transmitted diseases. But as the number of susceptible population is large, it is unreasonable to consider the bilinear incidence rate because the number of contact between the susceptible population and the infective population within a certain time is limited. Furthermore, the assumption of homogeneous mixing of population may be invalid.

Hence, one may prefer saturated incidence such as the standard incidence, $\beta\frac{S}{N}I$, which is the proportionate mixing incidence, when the total population size N is not too large. Other forms of saturated incidence include $\beta SI/(1+aI)$,$\beta SI/(1+aS)$ and $\beta SI^h/(1+aI^h)$, where $1/(1+aI)$ measures the inhibition effect from the behavioral change due to the increasing number of susceptible individuals. Apart from that, it is more appropriate to explain the crowding effect of the infective individuals. Besides that, one may use nonlinear incidence in the form of βS^pI^q. All these incidence rates are more appropriate to explain the situation when the number of infectives is very high and the exposure to the disease agent is virtually limited. Hence these incidence rates will respond more slowly than the linear form of incidence rate. We will study a special case of nonlinear incidence, βSI^2, in Chapter Four.

For compartmental epidemic models, different incidence rate was discussed in the references [2, 42, 51, 57, 58, 83], and most of the articles focus on discussion on the dynamics of the related epidemic models.

2.1.5 Types of recover/removal/treatment rates

In classical epidemic models, the classical removal rate is represented by the linear function, μI . But this classical removal rate, μI, is unsatisfactory because the treatment capacity such as medicines and sickbeds may be limited or insufficient in some epidemic outbreak. In [24], the authors proposed a saturation recovery function, $h(I) = vI + cI/(b + I)$, as the recovery rate function in which $c/(b + I)$ and v are respectively the recovery rate of the infected population with and with no treatment. The authors studied how the saturation recovery affects the dynamics of epidemic models and showed that the saturation recovery would cause multiple endemic equilibria and backward bifurcation. Apart from this saturated recovery rate, in [91], the authors suggested an epidemic model with a constant removal rate of infective individuals and showed that it can be used to study the effect of limited resources for treatment of the infective to the spread of infectious disease. In contrast with these, the author in [90] proposed a piecewise saturation recovery function to study the dynamical behavior of epidemic models.

In short, there are various considerations for epidemic models. For some other consideration such as the type of population, one may consider constant population or varying population. The varying population is considered if the disease causes fatal reduction in the population. Besides that, there are different types of transmissions which include vertical transmission (i.e. from mother to son, without monotonicity) and horizontal transmission (with monotonicity).

2.1.6 Sub-optimal immunity models

Although the SIR and SIS frameworks for infectious diseases have been successfully applied, most of the diseases do not fall into either of these extreme categories. It is because for certain diseases, the recovered individuals may obtain immunity to prevent her/him to get re-infection as the immune protection may wane over time (temporary immunity), or immunity may not be fully protective but reduces the risk of re-infection (partial immunity) [35]. The temporary immunity normally happens for some childhood diseases which are controlled by vaccination such as Pertus-

sis. The partial immunity protection will be received by infected individuals who suffer from diseases such as Influenza, Neisseria meningitides and Mycobacterium tuberculosis. The classical SIR epidemic model is appropriate for diseases such as measles and mumps which give permanently immune to the infected population, while the SIS type structures are most appropriate for diseases such as gonorrhoea which does not produce sufficient immunity against reinfection [19]. In this thesis, we will focus on the bifurcation analysis for this sub-optimal immunity epidemic models. We will study the models with nonlinear incidence rate and saturated recovery rate.

2.2 Qualitative analysis of compartmental epidemic models

For the compartmental epidemic models without delay and constant polpulation, for the sake of simplicity, one can always use the reduced system to do the analysis. The basic steps for the qualitative analysis are as follows,

1. Determine the basic reproduction number by the next generation matrix or other appropriate methods. Find the disease free equilibrium (DFE) and the endemic equilibrium (EE), the Jacobian matrix, the characteristic equation and its eigenvalues.

2. Investigate whether the DFE or EE are locally asymptotically stable by using the Routh-Hurwitz criteria or globally asymptotically stable by the Lyapunov function.

3. Study the limit cycle phenomena by using Dulac's criterion, Bendixson's criterion and the Poincare-Bendixson Theorem.

4. Undertake bifurcation analysis including backward bifurcation, Hopf bifurcation and Bogdanov-Takens bifurcation.

2.2.1 Hopf bifurcation

In this thesis, we mainly focus on bifurcation analysis including analysis of Hopf bifurcation and Bogdanov-Takens bifurcation for the sub-optimal immunity models. Mathematically, the Hopf bifurcation point in compartmental epidemic models can be determined when its Jacobian matrix at the equilibrium point of the system ODEs has a pair of purely imaginary eigenvalues and the remaining eigenvalues have nonzero real parts. In other words, Hopf or Poincaré-Andronov-Hopf bifurcation is a local bifurcation in which a fixed point of a dynamical system loses stability, as a pair of complex conjugate eigenvalues of the linearization around the fixed point cross the imaginary axis of the complex plane. More generally, for a dynamical system such as the compartmental epidemic models, for example an autonomous system $\dot{\mathbf{x}} = f(\mathbf{x}, \mu)$ where μ is the bifurcation parameter, the following methods may be used to check whether Hopf bifurcation occurs or not.

1. Let $\mu_0 = 0$. If the eigenvalues for the Jacobian matrix is purely imaginary pair, Hopf bifurcation may occur. This condition is named as transversality condition, i.e. $\frac{d}{d\mu} Re(\lambda(\mu))|_{\mu=\mu_0} \neq 0$.

2. Numerical analysis or linear algebra methods. The methods allow us to get the Hopf bifurcation point without checking its eigenvalues. Among that the famous ones include Hopf algorithms using polynomial resultants [40], bialternate product algorithms or additive compound matrix method [40], Bordering Methods [36]. The application of such methods in epidemic models can be found in [39, 43, 54]. More specifically, there are direct methods and indirect methods for obtaining the Hopf bifurcation point. In direct methods,the Hopf bifurcation point is obtained directly from its linearized system (i.e. Jacobian matrix). Typical direct methods include tensor product (Kronecker product method) , bialtenate product and induced matrices method. On the other hand, indirect methods allow one to determine the Hopf bifurcation point from the characteristic polynomial derived from the linearized system. Typical indirect methods include Hopf algorithms using polynomial

resultants [40], Hurtwitz Determinant, Hermite criterion, Markov criterion and Lienard-Chipart criterion.

3. Apply the center manifold theorem to reduce the dimension of the ODEs system and hence compare with the normal forms.

4. Use the Levinson-Smith Theorem if the autonomous system can be written as a Lienard's system.

In compartmental epidemic models or any autonomous systems, once the Hopf bifurcation point is determined, it is important to know whether the Hopf bifurcation is supercritical or subcritical. The supercritical Hopf bifurcation appears when the equilibrium becomes unstable, while the periodic solutions are stable. On the contrary, the subcritical Hopf bifurcation appears when the equilibrium becomes stable, while the periodic solutions are unstable.

Consider a two dimensional ODE systems as follows,

$$\begin{aligned} \frac{dI}{dt} &= G(I,R), \\ \frac{dR}{dt} &= H(I,R), \end{aligned} \tag{2.3}$$

the procedure for the Hopf bifurcation analysis is as follows:

Step 1: Find all equilibrium points, say (I_1, R_1) which fulfill the Hopf bifurcation condition.

Step 2: Translate (I_1, R_1) to the origin by using the transformation , $x = I - I_1$,$y = R - R_1$

$$\begin{aligned} \frac{dx}{dt} &= a_{11}x + a_{12}y + f_1(x,y) \\ \frac{dy}{dt} &= a_{21}x + a_{22}y + f_2(x,y), \end{aligned} \tag{2.4}$$

where $f_1(x,y)$ and $f_2(x,y)$ represent the higher order terms.

Step 3: Transform the system of ODEs to the new form by using the transformation $X = x$, $Y = a_{11}x + a_{12}y$. More specifically, from

$$\frac{dx}{dt} = a_{11}x + a_{12}y + f_1(x,y),$$

we get,

$$\frac{dX}{dt} = Y + f_1\left(X, \frac{Y - a_{11}X}{a_{12}}\right).$$

From

$$\frac{dy}{dt} = a_{21}x + a_{22}y + f_2(x, y),$$

we get

$$\begin{aligned}
\frac{dY}{dt} &= \frac{dY}{dx}\frac{dx}{dt} + \frac{dY}{dy}\frac{dy}{dt} \\
&= a_{11}(a_{11}x + a_{12}y + f_1(x, y)) + a_{12}(a_{21}x + a_{22}y + f_2(x, y)) \\
&= (a_{11}^2 + a_{12}a_{21})X + (a_{11}a_{12} + a_{12}a_{22})\left(\frac{Y - a_{11}X}{a_{12}}\right) \\
&+ a_{11}f_1\left(X, \frac{Y - a_{11}X}{a_{12}}\right) + a_{12}f_2\left(X, \frac{Y - a_{11}X}{a_{12}}\right) \\
&= (a_{11}^2 + a_{12}a_{21})X + (a_{11}a_{12} + a_{12}a_{22})\left(\frac{Y}{a_{12}}\right) - (a_{11}^2 + a_{11}a_{22})X \\
&+ a_{11}f_1\left(X, \frac{Y - a_{11}X}{a_{12}}\right) + a_{12}f_2\left(X, \frac{Y - a_{11}X}{a_{12}}\right) \\
&= (a_{12}a_{21} - a_{11}a_{22})X + (a_{11} + a_{12})Y + a_{11}f_1\left(X, \frac{Y - a_{11}X}{a_{12}}\right) \\
&+ a_{12}f_2\left(X, \frac{Y - a_{11}X}{a_{12}}\right).
\end{aligned} \tag{2.5}$$

It is shown that

$$a_{11} + a_{12} = 0.$$

Hence

$$\frac{dY}{dt} = -k_1X + a_{11}f_1\left(X, \frac{Y - a_{11}X}{a_{12}}\right) + a_{12}f_2\left(X, \frac{Y - a_{11}X}{a_{12}}\right),$$

where $k_1 = a_{11}a_{22} - a_{12}a_{21}$.

Step 4: Transform the system of ODE in step 3 to the normal form by using the transformation $u = -X$, $v = Y/\sqrt{k_1}$ to obtain

$$\begin{aligned}
\frac{du}{dt} &= -\sqrt{k_1}v + f(u, v) \\
\frac{dv}{dt} &= \sqrt{k_1}u + g(u, v),
\end{aligned} \tag{2.6}$$

where $f(u, v)$ and $g(u, v)$ represent the higher order terms.

Step 5: Find the first Lyapunov coefficient

$$\begin{aligned}\Lambda_1 = &\frac{1}{16}(f_{uuu} + f_{uvv} + g_{uuv} + g_{vvv}) \\ &+ \frac{1}{16\sqrt{k_1}}(f_{uv}(f_{uu} + f_{vv}) - g_{uv}(g_{uu} + g_{vv}) - f_{uu}g_{uu} + f_{vv}g_{vv}).\end{aligned} \tag{2.7}$$

If $\Lambda_1 > 0$, we have subcritical Hopf bifurcation, while if $\Lambda_1 < 0$, we have supercritical Hopf bifurcation.

2.2.2 Bogdanov-Takens bifurcation

Apart form Hopf bifurcation, Bogdanov-Takens bifurcation is another important dynamical behaviour of compartmental epidemic models [83, 85, 103]. Bogdanov-Takens bifurcation is co-dimension two, namely two parameters must be varied for the bifurcation to occur. An epidemic system will undergoes Bogdanov-Takens bifurcation if its linearized system around a fixed point has a double eigenvalue at zero when the technical nondegeneracy conditions are satisfied.

In a seminal paper [83], the writers used the normal form theory to show that the epidemic model considered undergoes Bogdanov-Takens bifurcation. The normal form is given by

$$\begin{aligned}\frac{dx}{dt} &= y \\ \frac{dy}{dt} &= \tau_1 + \tau_2 x + x^2 + xy \pm O(|x, y, \lambda|^3).\end{aligned} \tag{2.8}$$

Then, the system of epidemic model admits the following bifurcation

(a) there is a saddle-node bifurcation curve when $\tau_1 = \frac{1}{4}\tau_2^2$,

(b) there is a Hopf bifurcation curve when $\tau_1 = 0$ and $\tau_2 < 0$,

(c) there is a homoclinic bifurcation curve when $\tau_1 = -\frac{6}{25}\tau_2^2$.

2.2.3 Domain of attraction

The study of the domain of attraction (DOA) for the compartmental epidemic models has a great importance in forecasting and predicting the status of the infection

and evaluating the efficiency of the control strategies. Basically, if the initial state lies within the DOA, the disease will evolve towards an endemic state. On the other hand, if the initial state is outside the DOA, the system will converge to the disease free state. Although a considerable number of studies on DOA estimation and optimized DOA for the epidemic dynamical models have been conducted, such as those in [45, 49, 60] , all the epidemic models investigated in the literature mentioned above are limited to relatively simple epidemic models, and none of them include either nonlinear incidence rates or saturated recovery rates. In Chapter Five, we will thus study the DOA for the models we proposed in Chapter Three and Four, namely the sub-optimal immunity models with nonlinear incidence rates and saturated recovery rates by using the maximal Lyapunov function derived by [88].

2.3 Probability generating function

As mentioned in Chapter One, since the emerge of random graph theory by Erdos and Renyi in 1959, the theory had been extended in a variety of ways to make the random graphs a better representation of real world networks, such as those works done by [7, 92] addressing two important network properties, small-world effect and scale-free networks (i.e. power law distribution). Apart from that, Newman et. al. [18, 69, 74] had used the probability generating function (PGF) to generate graphs with a given degree distribution, in which the degree of nodes are independently distributed random integers drawn from a given p_k. This formalism is able to include the network models with non-Poisson degree distribution. Furthermore, it has been shown that the percolation problems can be solved in random graphs by means of the generating functions formalism, and hence one can obtain exact solutions for the presence and the size of an epidemic in random graphs with arbitrary degree distributions [18, 69, 74].

In this section, we briefly discuss some basic properties for PGF formalism and its application in percolation problems to obtain some solution in epidemic modelling on complex networks. In Chapter Six, we use this PGF formalism in

order to obtain the solution for the spreading of epidemic diseases in the community clustered networks through the bond percolation model.

Definition 2.1. *A probability distribution* $G_0(x) = \sum_{k=0}^{\infty} p_k x^k$ *is called the generating function where* p_k *is the probability that a randomly chosen vertex (i.e. node) on the graph has degree* k*, where* $\sum_{k=0}^{\infty} p_k = 1$ *and* $0 \leq x \leq 1$.

Definition 2.2. *A probability distribution* $G_1(x) = \sum_{k=1}^{\infty} q_{k-1} x^{k-1}$ *is the generating function for the excess degree where* q_{k-1} *is the probability that a vertex (i.e. node) has excess degree* $k-1$ *, where* $\sum_{k=0}^{\infty} q_k = 1$ *and* $0 \leq x \leq 1$.

q_{k-1} can be found by using $q_{k-1} = \frac{kp_k}{\langle k \rangle}$. $G_1(x)$ can be calculated by using $G_1(x) = \frac{G_0'(x)}{G_0'(1)} = \frac{1}{\langle k \rangle} G_0'(x)$. Normally $\langle k \rangle = z$ where z is the average degree of a node. Below are some of the properties of PGF.

Proposition 2.1. *Let* p *be a probability distribution and* G_p *its generating function.*

1. $G_p(1) = 1$. *i.e.*$G_0(1) = 1$ *and* $G_1(1) = 1$.
2. $G_p(x)$ *converges for* $0 \leq x \leq 1$.
3. *Derivatives,* $p_k = \frac{1}{k!} \frac{\partial^k G_0}{\partial x^k}|_{x=0}$.
4. *Mean or moment,* $\langle k \rangle = \sum_k k p_k = G_p'(1)$. *Generally, we have* $\langle k^n \rangle = \sum_k k^n p_k = \left[(x \frac{d}{dx})^n G_0(x) \right]_{x=1}$.
5. $Var = \sum_k k(k-1)p(k)$.

In the context of epidemic spreading on complex networks, we can obtain the basic reproduction number by $R_0 = TG_1'(1)$ where T denotes the disease transmissibility and $G_1'(1) = \langle k_e \rangle$ is the mean excess degree. If all the contacts transmit the disease, we will have $T = 1$. However, in reality, the probability that exactly m infections are transmitted by an infective node of degree k is

$$\binom{k}{m} T^m (1-T)^{k-m}. \tag{2.9}$$

To represent the transmissibility of a disease, we let $\Gamma_0(x,T)$ be the generating function for the distribution of the infection transmitted by a randomly chosen individual for any (fixed) transmissibility T (Sometime written as $G_0(x,T)$). The relationship between Γ_0 and G_0 is given below.

$$\begin{aligned}\Gamma_0(x,T) &= \sum_{m=0}^{\infty}\left[\sum_{k=m}^{\infty} p_k \binom{k}{m} T^m (1-T)^{k-m}\right] x^m \\ &= \left[\sum_{k=0}^{\infty} p_k \binom{k}{0} T^0 (1-T)^{k-0}\right] x^0 + \left[\sum_{k=1}^{\infty} p_k \binom{k}{1} T^1 (1-T)^{k-1}\right] x^1 + \dots \\ &= \sum_{k=0}^{\infty} p_k \left[\sum_{m=0}^{\infty} p_k \binom{k}{m} (xT)^m (1-T)^{k-m}\right] \\ &= \sum_{k=0}^{\infty} p_k \left[xT + (1-T)\right]^k = G_0(1+(x-1)T).\end{aligned} \tag{2.10}$$

The above equality can be obtained through the Binomial Theorem. It is always important to consider secondary infection. In this case, we define $\Gamma_1(x,T)$ be the generating function for the probability distribution of occupied edges leaving a node arrived at by following a randomly chosen edge is generated by (2.11).

$$\begin{aligned}\Gamma_1(x,T) &= \sum_{m=1}^{\infty}\left[\sum_{k=m}^{\infty} q_{k-1} \binom{k-1}{m} (xT)^m (1-T)^{k-1-m}\right] x^{m-1} \\ &= \left[\sum_{k=1}^{\infty} q_{k-1} \binom{k-1}{m} (xT)^m (1-T)^{k-1-m}\right] = \sum_{k=1}^{\infty} q_{k-1} \left[xT + (1-T)\right]^{k-1} \\ &= \sum_{k=0}^{\infty} q_k \left[xT + (1-T)\right]^k = G_1(1+(x-1)T).\end{aligned} \tag{2.11}$$

Remark 2.1. *We can also derive the above equation from*

$$\Gamma_1(x,T) = \sum_{m=0}^{\infty}\left[\sum_{k=m}^{\infty} q_k \binom{k}{m} (xT)^m (1-T)^{k-m}\right] x^m. \tag{2.12}$$

If we let $T = 1$, Equations (2.10) and (2.11) will be $\Gamma_1(x,1) = G_0(x)$ and $\Gamma_1(x,1) = G_1(x)$, or more precisely, it is the generating functions in Definition 2.1 and Definition 2.2. Note that $G_0(x,1) = G_0(x)$, $G_0(1,T) = G_0(1)$, $G_0'(1,T) =$

$TG_0'(x)$, and that the basic reproduction number , $R_0 = TG_1'(1) = \Gamma_1'(x,T)$. In this equation, we can calculate the critical transmissibility, T_c, which is defined by $T_c = G_1'(1) = 1$. This value is equivalent to the R_0 value obtained from compartmental ODE models.

2.3.1 The distribution of disease outbreak and epidemic size

In this section, for simplicity, we will first discuss in detail the distribution of disease outbreak and epidemic size without considering transmissibility, T. Hence, we briefly present the formalism with the transmissibility, T, taken into account.

2.3.1.1 The distribution of disease outbreak and epidemic size without considering transmissibility

Let $H_1(x)$ be the total number of vertices (i.e. nodes) reachable by following an edge and satisfy the self consistency condition.

$$\begin{aligned} H_1(x) &= xq_0 + xq_1H_1(x) + xq_2[H_1(x)]^2 + xq_3[H_1(x)]^3 + \dots \\ &= x\sum_k q_k[H_1(x)]^k \end{aligned} \tag{2.13}$$

or in short form

$$H_1(x) = xG_1(H_1(x)). \tag{2.14}$$

The above equation says that when we follow an edge, we find at least one node at the other end (the factor of x on the RHS), plus some other clusters of vertices (each represented by H_1) which are reachable by following other edges attached to that node. The number of the clusters is distributed according to q_k , and hence the appearance of G_1 . In fact, this is the burning (breath-first-search) algorithm.

Let $H_0(x)$ be the total number of vertices reachable from a randomly chosen node, i.e. the size of the component to which such a node belongs to, is generated by

$$H_0(x) = xG_0(H_1(x)) \tag{2.15}$$

or written as $H_0(x) = x\sum_k p_k[H_1(x)]^k$. We know that the mean size of disease

outbreak is given by $H_0'(x)$. By implicit differentiation of (2.14), we get

$$H_1'(x) = G_1(H_1(x)) + xG_1'(H_1(x))H_1'(x). \tag{2.16}$$

Lemma 2.1. *The equation* $H_1'(x) = G_1(H_1(x)) + xG_1'(H_1(x))H_1'(x)$ *can be written as*

(a) $H_1'(1) = \frac{1}{1-G_1'(1)}$,

(b) $H_1'(1) = 1 + G_1'(1)H_1'(1)$.

Proof. (a) Rearrange $H_1'(x) = G_1(H_1(x)) + xG_1'(H_1(x))H_1'(x)$, we have $H_1'(x) = \frac{G_1(H_1(x))}{1-xG_1'(H_1(x))}$. Hence, we get $H_1'(1) = \frac{G_1(H_1(1))}{1-G_1'(H_1(1))}$. From $G_0(1) = 1$, $G_1(1) = 1$, we have $H_0(1) = 1$, $H_1(1) = 1$, and hence $H_1'(1) = \frac{G_1(1)}{1-G_1'(1)} = \frac{1}{1-G_1'(1)}$.

(b) From $H_1'(x) = G_1(H_1(x)) + xG_1'(H_1(x))H_1'(x)$, we have $H_1'(1) = G_1(H_1(1)) + G_1'(H_1(1))H_1'(1) = G_1(1) + G_1'(1)H_1'(1) = 1 + G_1'(1)H_1'(1)$.

□

By implicit differentiation of (2.15) and using Lemma 2.1, we get

$$\begin{aligned} H_0'(x) &= G_0(H_1(x)) + xG_0'(H_1(x))H_1'(x) \\ &= G_0(H_1(x)) + xG_0'(H_1(x)) \left[\frac{G_1(H_1(x))}{1 - xG_1'(H_1(x))}\right]. \end{aligned} \tag{2.17}$$

Since $H_1(1) = 1$ and $G_1(H_1(1)) = G_1(1) = 1$, by using Lemma 2.1, we have

$$\begin{aligned} H_0'(1) &= G_0(H_1(1)) + G_0'(H_1(1)) \left[\frac{G_1(H_1(1))}{1 - G_1'(H_1(1))}\right] \\ &= G_0(1) + G_0'(1) \left[\frac{1}{1 - G_1'(1)}\right] \\ &= 1 + G_0'(1) \left[\frac{1}{1 - R_0}\right]. \end{aligned} \tag{2.18}$$

Alternatively we can write (2.18) as

$$\langle s \rangle = H_0'(1) = 1 + G_0'(1)H_1'(1), \tag{2.19}$$

where $\langle s \rangle$ is the average cluster size. From Lemma 2.1(a), we get the mean component size as follows,

$$\langle s \rangle = H_0'(1) = 1 + G_0'(1)\left[\frac{1}{1 - G_1'(1)}\right] = 1 + \frac{z_1^2}{z_1 - z_2}, \tag{2.20}$$

where $z_1 = \langle k \rangle$ and z_2 is the mean number of the second neighbours of a node. This tells us that the critical point is given by $G_1'(1)$. Hence, we have the following two cases :

Case I: $G_1'(1) < 1$. Assumption : No giant component in the network (i.e. no giant cluster).

Case II: $G_1'(1) > 1$. Assumption : There is a giant component in the network, but by definition, $H_0(x)$ generates the probability distribution of the sizes of the components excluding the giant component. Hence $H_0(1) \neq 1$, but $H_0(x) = 1 - S$, where S is the fraction of the graph occupied by the giant component. $S - 1 - G_0(u)$ where $u \equiv H_1(1)$ is the smallest non-negative real solution of $u = G_1(u)$.

We illustrate the calculation of the distribution through the following example.

Example 2.1. *Based on the Random graphs (i.e. network) / Erdos-Renyi graphs, for Poisson-distribution graphs* $G_0(x) = e^{z(x-1)}$,$G_1(x) = \frac{1}{z}G_0'(x) = \frac{1}{z}ze^{z(x-1)} = e^{z(x-1)}$ *, find the probability that a randomly chosen node belongs to a component of size* s*, where* s *is an integer.*

Let $H_1(x) = q_0 x$ *where* $q_0 = e^{-z}$*. From*

$$\begin{aligned} e^{z(x-1)} &= e^{-z}e^{zx} = e^{-z}\left[1 + \frac{zx}{1!} + \frac{z^2x^2}{2!} + \frac{z^3x^3}{3!} + \dots\right] \\ &= e^{-z}\sum_{k=0}^{\infty}\frac{z^k x^k}{k!} \end{aligned}$$

$$\begin{aligned} H_1^{(1)}(x) = xG_1(H_1(x)) &= xe^{-z}\left[1 + \frac{z(e^{-z}x)}{1!} + \frac{z^2(e^{-z}x)^2}{2!} + \frac{z^3(e^{-z}x)^3}{3!} + \dots\right] \\ &= xe^{-z} + O(x^2) \end{aligned}$$

$$
\begin{aligned}
H_1^{(2)}(x) &= xG_1(H_1^{(1)}(x)) = xe^{-z}\left[1 + \frac{z(e^{-z}x)}{1!} + \frac{z^2(e^{-z}x)^2}{2!} + \frac{z^3(e^{-z}x)^3}{3!} + \ldots\right] \\
&= xe^{-z} + x^2ze^{-2z} + O(x^3) \\
H_1^{(3)}(x) &= xG_1(H_1^{(2)}(x)) \\
&= xe^{-z}\{1 + \frac{z(xe^{-z} + x^2ze^{-2z})}{1!} + \frac{z^2(xe^{-z} + x^2ze^{-2z})^2}{2!} \\
&+ \frac{z^3(xe^{-z} + x^2ze^{-2z})^3}{3!} + \ldots\} \\
&= xe^{-z} + x^2ze^{-2z} + \frac{3}{2}x^3z^2e^{-3z} + O(x^4).
\end{aligned}
$$

Similar to this and after some algebra works, we obtain

$$
H_1^{(4)}(x) = xe^{-z} + x^2ze^{-2z} + \frac{3}{2}x^3z^2e^{-3z} + \frac{5}{3}x^4z^3e^{-4z} + O(x^5).
$$

Since $G_0(x) = G_1(x) = e^{z(x-1)}$ *and* $H_1(x) = xG_1(H_1(x))$,$H_0(x) = xG_0(H_1(x))$ *, from the result above, we have*

$$
H_0(x) = xe^{-z} + x^2ze^{-2z} + \frac{3}{2}x^3z^2e^{-3z} + \frac{5}{3}x^4z^3e^{-4z} + O(x^5).
$$

Compared with $H_0(x) = \sum_{s=0}^{\infty} P_s x^s = P_0 + P_1x + P_2x^2 + P_3x^3 + P_4x^4 + \ldots$*, we get the probability,* P_s *that a randomly chosen node belongs to the component of size* s *is* $P_0 = 0$*,* $P_1 = e^{-z}$,$P_2 = ze^{-2z}$,$P_3 = \frac{3}{2}z^2e^{-3z}$,$P_4 = \frac{5}{3}z^3e^{-4z}$.

2.3.1.2 The distribution of disease outbreak and epidemic size with consideration of transmissibility

Let $H_1(x,T)$ be the generating function for the distribution of the size of clusters of connected vertices reached by following a randomly chosen edge, and let $H_0(x,T)$ be the generating function for the distribution of the outbreak size corresponding to a randomly chosen individual for any (fixed) transmissibility T(corresponding to a randomly chosen node). Note that

$$
H_0(x,T) = \sum_{s=0}^{\infty} P_s(T)x^s. \tag{2.21}
$$

Let

$$
\begin{aligned}
H_1(x,T) &= xG_1(H_1(x,T);T), \\
H_0(x,T) &= xG_0(H_1(x,T);T).
\end{aligned} \tag{2.22}
$$

More precisely,

$$\begin{aligned} H_1(x,T) &= x\sum_{m=0}^{\infty}\left[\sum_{k=m}^{\infty} q_k \binom{k}{m}(T)^m(1-T)^{k-m}\right](H_1(x,T))^m \\ &= xG_1(1+(H_1(x,T)-1)T). \end{aligned} \tag{2.23}$$

The mean size of the disease outbreak is $H_0'(1;T)$.

Similar to the previous subsection, differentiating the first equation in (2.22) and after some calculation, we get

$$\begin{aligned} H_1'(x;T) &= xG_1'(H_1(x;T);T)H_1'(x;T) + G_1(H_1(x;T);T) \\ H_1'(1;T) &= G_1'(H_1(1;T);T)H_1'(1;T) + G_1(H_1(1;T);T). \end{aligned} \tag{2.24}$$

From $G_0(1)=1$,$G_1(1)=1$, we have $H_0(1)=1$,$H_1(1)=1$. Hence

$$\begin{aligned} H_1'(1;T) &= G_1'(1;T)H_1'(1;T) + G_1(1;T) \\ H_1'(1;T) &= 1 + G_1'(1;T)H_1'(1;T) \end{aligned} \tag{2.25}$$

or

$$H_1'(1;T) = \frac{1}{1-G_1'(1;T)}. \tag{2.26}$$

From the above, we obtain the mean outbreak size, $\langle s\rangle$(i.e. average cluster size), as follows

$$\begin{aligned} \langle s\rangle = H_0'(1;T) &= 1 + G_0'(1;T)H_1'(1;T) \\ &= 1 + \frac{G_0'(1;T)}{1-G_1'(1;T)} = 1 + \frac{TG_0'(1)}{1-TG_1'(1)}. \end{aligned} \tag{2.27}$$

Obviously, the $\langle s\rangle$ diverges when $TG_1'(1)=1$. Hence the critical transmissibility is $T_c = \frac{1}{G_1'(1)}$.

This tells us that the critical point is given by $G_1'(1)=1$. Hence, we have the following two cases :

Case I: $G_1'(1)<1$. Assumption : No giant component in the network (i.e. no giant cluster).

Case II: $G_1'(1)>1$. Assumption : There is a giant component in the network. But by definition, $H_0(x;T)$ generates the probability distribution of the sizes of the components excluding the giant component. Hence $H_0(1;T)\neq 1$. But

$H_0(1;T) = \sum_s P_s = 1 - S(T)$, where S is the fraction of the graph occupied by the giant component. $S(T) = 1 - G_0(u;T)$ where $u \equiv H_1(1;T)$ is the smallest non-negative real solution of $u = G_1(u;T)$.

2.4 Concluding remarks

Throughout this chapter, a wide range of epidemic characteristics have been described within the framework of this PhD study, namely epidemic modelling by differential equations and complex networks. The focus for the first part of the framework is bifurcation analysis for the sub-optimal immunity epidemic models and calculation of the domain of attraction, while the later part focuses on the probability generating function formalism.

Chapter 3

Bifurcation of an Epidemic Model with Sub-optimal Immunity and Saturated Recovery Rate

In this chapter, we study the bifurcation of an epidemic model with sub-optimal immunity and saturated treatment/recovery rate. Different from classical models, sub-optimal immunity models are more realistic for modelling the microparasitic infectious diseases such as Pertussis and Influenza A. By carrying out the bifurcation analysis of the model, we show that for certain values of the model parameters, Hopf bifurcation, Bogdonov-Takens bifurcation and its associated homoclinic bifurcation occur. By studying the bifurcation curves, one can predict the persistence or extinction of diseases.

3.1 General

In recent years, extensive research has been carried out worldwide to develop more realistic epidemic models. For compartmental ODE models, several new models for different incidence rate and treatment/recovery rate have been introduced. Subsequent analytical studies show that some of these epidemic models possess rich dynamics.

In a seminal paper [83], the authors presented a SIR epidemic model with the nonlinear incidence rate in the form of $(\beta SI^2)/(1 + aI^2)$. In the paper, they con-

sider a reduced system and perform an elaborative analysis of equilibrium through a quadratic equation. Using transformation to normal form, they show that the model undergoes Hopf bifurcation, homoclinic bifurcation and Bogdonov-Takens bifurcation. Following the paper, a few other papers discuss about the same dynamical behavior in the SIR model but with different forms of incidence rates such as $(\beta SI)/(1 + aI + bI^2)$[103] and $(\beta SI^2)/(1 + aI + bI^2)$[85] .

Similarly, different treatment/recovery/removal rate are considered in order to predict the trend of disease transmission more accurately. Unlike the earlier models, the recent models may have two endemic equilibria when $R_0 < 1$. Hence, the eradication of diseases depends not only on R_0 , but also on the initial sizes of all sub-populations. The work in [91] is a pioneer work for bifurcation analysis which shows the existence of Hopf bifurcation and Bogdonov-Takens bifurcation for the model with constant removal rate. After the work of [91], various studies of bifurcation for the models with other forms of treatment/recovery rate have been carried out. Backward bifurcation is shown in a SIR model with piecewise function treatment in [90], meanwhile the work in [100] claims the existence of Hopf bifurcation in a SIR model with saturated treatment rate. Furthermore, in the SIR model with saturated incidence rate and saturated treatment rate [99], only backward bifurcation is shown to exist, while reference [24]suggests that a SIS model with a saturated recovery rate possesses Bogdonov-Takens bifurcation. However, to date, no analysis has been done to study the existence of Bogdonov-Takens bifurcation in the SIR model with saturated recovery rate. Hence, we intend to further study the bifurcation of the SIR model, and we will use the more generalized form of the model, namely the sub-optimal immunity model which lies in between the SIS and SIR models.

In this chapter, we undertake the bifurcation analysis for an epidemic model with sub-optimal immunity and saturated treatment/recovery rate. Apart from using the saturated treatment/recovery rate, an additional parameter σ is used to form the sub-optimal immunity model as in [76]. The new model lies in between the SIS and SIR models. The sub-optimal immunity model will be more appropriate

for the study of microparasite infections which usually occurs during childhood. After a primary infection, one may get temporary immunity (immune protection will wane over time) or partial immunity (immunity that may not fully protective). Examples of this kind of diseases include Pertussis (temporary immunity) and Influenza (partial immunity) [35]. Different to that in [76], we show in this chapter that Bogdonov-Takens bifurcation and its associated homoclinic bifurcation exist in this sub-optimal immunity model.

Throughout the chapter, for simplicity, we choose some specific values for the parameters as [103] did. The parameter values can be easily replaced by other values as long as the conditions are fulfilled. Our analysis was carried out for the case where the basic reproduction number, R_0, is less than unity. Apart from the discussion of Hopf bifurcation, we show that the sub-optimal immunity model undergoes Bogdonov-Takens bifurcation and its associated homoclinic bifurcation.

The rest of the chapter is organized as follows. In Section 3.2, we discuss the qualitative analysis of the model. In Sections 3.3 and 3.4, we study the Hopf bifurcation and Bogdanov-Takens Bifurcation. Some conclusions are given in Section 3.5.

3.2 Qualitative analysis

We consider a model with sub-optimal immunity and saturated recovery rate

$$\begin{aligned} \frac{dS}{dt} &= A - \beta SI + \sigma T(I) - \mu S, \\ \frac{dI}{dt} &= \beta SI - T(I) - \mu I, \\ \frac{dR}{dt} &= (1-\sigma)T(I) - \mu R. \end{aligned} \tag{3.1}$$

where all the parameters are positive, A is the recruitment rate of susceptible population, β is the disease transmission rate, μ is the natural death rate and $T(I)$ is the recovery rate.

In our analysis at equilibrium point, we assume that $S + I + R = A/\mu$, and we take $T(I) = vI + cI/(1 + aI)$ in which $c/(1 + aI)$ and v are respectively the recovery rate of the infected population with and with no treatment.

Defining the basic reproduction number by $R_0 = \beta A/(\mu(\mu + T'(0)))$ with $T(I) = vI + cI/(1 + aI)$, we obtain $R_0 = \beta A/(\mu(\mu + v + c))$. Define $R_1 = \beta Aa/(\beta k(v + c) + \beta\mu + \mu a(\mu + v))$.

Now, we consider the following reduced system

$$\begin{aligned} \frac{dI}{dt} &= \beta(\frac{A}{\mu} - I - R)I - vI - \frac{cI}{1 + aI} - \mu I, \\ \frac{dR}{dt} &= k(vI + \frac{cI}{1 + aI}) - \mu R, \end{aligned} \tag{3.2}$$

where $k = 1 - \sigma$. At equilibrium,$dI/dt = 0$,$dR/dt = 0$, and hence from (3.2), we obtain $R = kI(v(1 + aI) + c)/(\mu(1 + aI))$. Then by substituting this into the first equation in (3.2), after some algebra work, we obtain

$$(\beta a(kv+\mu))I^2+(\beta(kv+kc+\mu-Aa)+\mu a(\mu+v))I+\mu(\mu+v+c)-\beta A = 0. \tag{3.3}$$

Let

$$\triangle = (\beta(kv+kc+\mu-Aa)+\mu a(\mu+v))^2-4\beta a(kv+\mu)(\mu(\mu+v+c)-\beta A). \tag{3.4}$$

Lemma 3.1. *(a) System* (3.2) *has a unique positive equilibrium* $E^*(I^*, R^*)$ *under any of the following three conditions.*

(i) $R_0 = 1$ *and* $(\beta(kv + kc + \mu - Aa) + \mu a(\mu + v)) < 0$ *for which*

$$I^* = \frac{-(\beta(kv + kc + \mu - Aa) + \mu a(\mu + v))}{\beta a(kv + \mu)}, R^* = \frac{kI^*(v(1 + aI^*) + c)}{\mu(1 + aI^*)}$$

(ii) $R_0 > 1$ *for which*

$$I^* = \frac{-(\beta(kv + kc + \mu - Aa) + \mu a(\mu + v)) + \sqrt{\triangle}}{2\beta a(kv + \mu)}, R^* = \frac{kI^*(v(1 + aI^*) + c)}{\mu(1 + aI^*)}$$

(iii) $\triangle = 0$ *and* $(\beta(kv + kc + \mu - Aa) + \mu a(\mu + v)) < 0$ *for which*

$$I^* = \frac{-(\beta(kv + kc + \mu - Aa) + \mu a(\mu + v))}{2\beta a(kv + \mu)}, R^* = \frac{kI^*(v(1 + aI^*) + c)}{\mu(1 + aI^*)}$$

.

(b) System (3.2) *has two positive equilibria* $E_1(I_1, R_1)$ *and* $E_2(I_2, R_2)$ *if and only if* $R_0 < 1$, $\triangle > 0$ *and* $(\beta(kv + kc + \mu - Aa) + \mu a(\mu + v)) < 0$ *where*

$$I_1 = \frac{-(\beta(kv + kc + \mu - Aa) + \mu a(\mu + v)) - \sqrt{\triangle}}{2\beta a(kv + \mu)}, R_1 = \frac{kI_1(v(1 + aI_1) + c)}{\mu(1 + aI_1)}$$

$$I_2 = \frac{-(\beta(kv + kc + \mu - Aa) + \mu a(\mu + v)) + \sqrt{\triangle}}{2\beta a(kv + \mu)}, R_2 = \frac{kI_2(v(1 + aI_2) + c)}{\mu(1 + aI_2)}$$

The Jacobian matrix for system (3.2) is

$$M = \begin{pmatrix} -\beta I + \beta(\frac{A}{\mu} - I - R)I - v - \frac{c}{1+aI} + \frac{caI}{(1+aI)^2} - \mu & -\beta I \\ k(v + \frac{c}{1+aI} - \frac{caI}{(1+aI)^2}) & -\mu \end{pmatrix}.$$

The determinant of M is as follows

$$det(M) = \frac{S_1}{(1 + aI)^2},$$

where

$$S_1 = 2\beta a^2(kv + \mu)I^3 + (\beta a(4kv + kc + 4\mu - Aa) + \mu a^2(\mu + v))I^2$$
$$+ (2\beta(\mu - Aa + kc + kv) + 2\mu a(v + \mu))I + \mu(\mu + v + c) - \beta A.$$

The sign of the determinant is determined by the sign of S_1.

Using (3.3), we get

$$S_1 = (\beta a(2kv - kc + 2\mu + Aa) - \mu a^2(\mu + v))I^2$$
$$+ (2\beta(\mu + kc + kv) - 2\mu ca)I + \mu(\mu + v + c) - \beta A.$$

Lemma 3.2.

(a) The unique positive equilibrium $E^*(I^*, R^*)$ *in system* (3.2) *is*

(i) a degenerate equilibrium if $\triangle = 0$,$(\beta(kv + kc + \mu - Aa) + \mu a(\mu + v)) < 0$.

(ii) a center-type equilibrium if $R_0 > 1$ *while* $tr(M) = 0$.

(b) The positive equilibrium $E_1(I_1, R_1)$ *in system* (3.2) *leads to* $S_1(I_1) < 0$ *while* $\triangle > 0$, $R_0 < 1$ *and* $(\beta(kv + kc + \mu - Aa) + \mu a(\mu + v)) < 0$. *It is thus a saddle point.*

(c) The positive equilibrium $E_2(I_2, R_2)$ *in system* (3.2) *leads to* $S_1(I_2) < 0$ *while* $\triangle > 0$, $R_0 < 1$ *and* $(\beta(kv + kc + \mu - Aa) + \mu a(\mu + v)) < 0$. *It is thus a node, focus or center.*

3.3 Hopf bifurcation

In this section, we will show that the model in (3.2) undergoes Hopf bifurcation for some values.

Let $(\beta, v, c, a, \mu, k) = (1/2, 8, 8, 3, 1, 1/4)$ for (I_2, R_2) and set $tr(M) = 0$, then we obtain $A = 51/2$ while $(I_2, R_2) = (1, 5/2)$. This happens when $R_0 = 3/4 < 1$. Replacing I and R by x and y, namely $(I_2, R_2) = (x_2, y_2)$, we have

$$\begin{aligned} \frac{dx}{dt} &= \frac{1}{2}(\frac{51}{2} - x - y)x - 9x - \frac{8x}{1+3x}, \\ \frac{dy}{dt} &= 2x + \frac{2x}{1+3x} - y. \end{aligned} \tag{3.5}$$

To translate (x_2, y_2) to the origin, we set , $X = x - 1$, $Y = y - 5/2$ and rename X,Y as x,y respectively. Then

$$\begin{aligned} \frac{dx}{dt} &= \frac{1}{2}(\frac{51}{2} - (x+1) - (y + \frac{5}{2}))(x+1) - 9(x+1) - \frac{8(x+1)}{1+3(x+1)}, \\ \frac{dy}{dt} &= 2(x+1) + \frac{2(x+1)}{1+3(x+1)} - (y + \frac{5}{2}). \end{aligned} \tag{3.6}$$

Using the Taylor expansion for (3.6), we have

$$\begin{aligned} \frac{dx}{dt} &= -\frac{1}{2}y + (1 - \frac{1}{2}y)x - \frac{1}{8}x^2 - \frac{9}{32}x^3 + \frac{27}{128}x^4 + O(|x, y|^5), \\ \frac{dy}{dt} &= -y + \frac{17}{8}x - \frac{3}{32}x^2 + \frac{9}{128}x^3 - \frac{27}{512}x^4 + O(|x, y|^5). \end{aligned} \tag{3.7}$$

The Jacobian matrix for (3.7) at (x_2, y_2) is

$$M = \begin{pmatrix} 1 & -\frac{1}{2} \\ \frac{17}{8} & -1 \end{pmatrix}.$$

We thus have $tr(M) = 0$ and $det(M) = \frac{1}{16} > 0$, and hence Hopf bifurcation occurs. By carrying out transformation $X = x$, $Y = x - \frac{1}{2}y$, and then renaming X,Y as x,y respectively, (3.7) becomes

$$\begin{aligned} \frac{dx}{dt} &= y - \frac{9}{8}x^2 + xy - \frac{9}{32}x^3 + \frac{27}{128}x^4 + O(|x, y|^5), \\ \frac{dy}{dt} &= -\frac{1}{16}x - \frac{69}{64}x^2 + xy - \frac{81}{256}x^3 + \frac{243}{1024}x^4 + O(|x, y|^5). \end{aligned} \tag{3.8}$$

Making the change of variables $u = -x$, $v = 4y$, we obtain

$$\begin{aligned}\frac{du}{dt} &= -\frac{1}{4}v + \frac{9}{8}u^2 + \frac{1}{4}uv - \frac{9}{32}u^3 - \frac{27}{128}u^4 + O(|u,v|^5),\\ \frac{dv}{dt} &= \frac{1}{4}u - \frac{69}{64}u^2 - uv - \frac{81}{64}u^4 + \frac{243}{256}u^4 + O(|u,v|^5).\end{aligned} \tag{3.9}$$

Let $k_1 = \dfrac{1}{16}$, from (3.9), we obtain

$$\begin{aligned}\frac{du}{dt} &= -\sqrt{k_1}v + F_1(u,v),\\ \frac{dv}{dt} &= \sqrt{k_1}u + F_2(u,v).\end{aligned} \tag{3.10}$$

where

$$\begin{aligned}F_1(u,v) &= \frac{9}{8}u^2 + \frac{1}{4}uv - \frac{9}{32}u^3 - \frac{27}{128}u^4 + O(|u,v|^5),\\ F_2(u,v) &= -\frac{69}{64}u^2 - uv + \frac{81}{256}u^4 + \frac{243}{256}u^4 + O(|u,v|^5).\end{aligned}$$

We can get the first Liapunov constant, σ , by

$$\begin{aligned}\sigma = &\frac{1}{16}\left[\frac{\partial^3 F_1}{\partial u^3} + \frac{\partial^3 F_1}{\partial u \partial v^2} + \frac{\partial^3 F_2}{\partial u^2 \partial v} + \frac{\partial^3 F_2}{\partial v^3}\right]\\ &+ \frac{1}{16\sqrt{k_1}}\left[\frac{\partial^2 F_1}{\partial u \partial v}\left(\frac{\partial^2 F_1}{\partial u^2} + \frac{\partial^2 F_1}{\partial v^2}\right) - \frac{\partial^2 F_2}{\partial u \partial v}\left(\frac{\partial^2 F_2}{\partial u^2} + \frac{\partial^2 F_2}{\partial v^2}\right)\right]\\ &+ \frac{1}{16\sqrt{k_1}}\left[-\frac{\partial^2 F_1}{\partial u^2}\frac{\partial^2 F_2}{\partial u^2} + \frac{\partial^2 F_1}{\partial v^2}\frac{\partial^2 F_2}{\partial v^2}\right] = \frac{699}{256}.\end{aligned}$$

Hence, there is an unstable periodic orbit when$A$ increases from $51/2$.

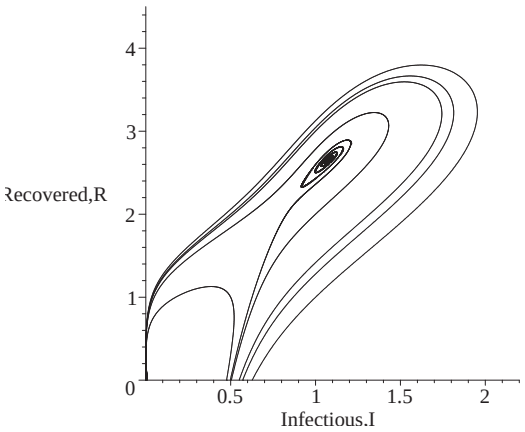

Figure 3.1: An unstable orbit for $(\beta, v, c, a, \mu, k) = (1/2, 8, 8, 3, 1, 1/4)$ and $A = 25.52$

Figure 3.1 shows an unstable orbit for the system (3.2) when $(\beta, v, c, a, \mu, k) = (1/2, 8, 8, 3, 1, 1/4)$ and $A = 25.52$.

In the following, we choose A as a bifurcation parameter. Let $A = 51/2 + \epsilon$. From (3.5), we obtain,

$$\begin{aligned} \frac{dx}{dt} &= \frac{1}{2}(\frac{51}{2} + \epsilon - x - y)x - 9x - \frac{8x}{1+3x}, \\ \frac{dy}{dt} &= 2x + \frac{2x}{1+3x} - y. \end{aligned} \tag{3.11}$$

It is easy to show that

$$(x_2^*, y_2^*) = \left(\frac{35}{36} + \frac{\epsilon}{6} + \frac{\sqrt{36\epsilon^2 + 564\epsilon + 1}}{36}, \frac{2021}{828} + \frac{43\epsilon}{138} + \frac{49\sqrt{36\epsilon^2 + 564\epsilon + 1}}{828} \right)$$

is the positive equilibrium of the system (3.11). The Jacobian matrix is given by

$$M = \begin{pmatrix} M_{11} & -\frac{x_2^*}{2} \\ M_{21} & -1 \end{pmatrix},$$

where

$$M_{11} = -x_2^* + \frac{15}{4} + \frac{\epsilon}{2} - \frac{y_2^*}{2} - \frac{8}{1+3x_2^*} + \frac{24x_2^*}{(1+3x_2^*)^2},$$
$$M_{21} = 2 + \frac{2}{1+3x_2^*} - \frac{6x_2^*}{(1+3x_2^*)^2}.$$

Hence, the characteristic equation is given by

$$\lambda^2 + (1 - M_{11})\lambda - M_{11} + \frac{x_2^*}{2} M_{21} = 0.$$

We thus obtain $\lambda = \dfrac{m_A \pm \sqrt{m_B}}{m_C}$, where

$$\begin{aligned} m_A &= 1339 - 36378\epsilon - 6156\epsilon^2 - 216\epsilon^3 + (-1339 - 744\epsilon - 36\epsilon^2)\sqrt{1 + 564\epsilon + 36\epsilon^2}, \\ m_B &= -32696110 - 1957294879\epsilon - 13313554632\epsilon^2 - 2408256576\epsilon^3 \\ &\quad - 149198112\epsilon^4 - 1399680\epsilon^5 + 93312\epsilon^6 \\ &\quad + \{-397285586 - 826878324\epsilon - 246740976\epsilon^2 - 21607776\epsilon^3 \\ &\quad - 355104\epsilon^4 + 15552\epsilon^5\}\sqrt{1 + 564\epsilon + 36\epsilon^2}, \\ m_C &= 72(1105 + 564\epsilon + 36\epsilon^2 + (47 + 6\epsilon)\sqrt{1 + 564\epsilon + 36\epsilon^2}). \end{aligned}$$

Hence, we have

(a) $Re\lambda(\epsilon) = 0$ when $\epsilon = 0$.

(b) $Im\lambda(\epsilon) = \dfrac{\sqrt{429981696}}{82944} \neq 0$ when $\epsilon = 0$.

(c) $Re\dfrac{d}{d\epsilon}\lambda(\epsilon) = -5 \neq 0$ when $\epsilon = 0$.

Theorem 3.1. *There exist a* $\sigma_1 > 0$ *and a function* $\epsilon = \epsilon(x_1)$ *defined on* $0 < x_1 - 1 \leq \sigma_1$ *, which satisfy* $\epsilon(1) = 0$ *and when* $\epsilon = \epsilon(x_1) < 0$*, system* (3.11) *has a unique unstable limit cycle which passes through* $(x_1, 5/2)$ *.*

3.4 Bogdanov-Takens bifurcation

In this section, we will study the Bogdanov-Takens bifurcation for some values of the model in (3.2).

We choose $(\beta, v, a, \mu, k) = (1/2, 2, 1/2, 1, 1/4)$ for model (3.2) and let $\triangle = 0$, and we obtain $c = 8$. Setting $A = 19$, we obtain $(I^*, R^*) = (2, 3)$, $tr(M) = 0$ and $det(M) = 0$. Writing I and R as x and y, namely $(I^*, R^*) = (x^*, y^*)$, we have

$$\begin{aligned} \frac{dx}{dt} &= \frac{1}{2}(19 - x - y)x - 3x - \frac{8x}{1 + \frac{1}{2}x}, \\ \frac{dy}{dt} &= \frac{1}{2}x + \frac{2x}{1 + \frac{1}{2}x} - y. \end{aligned} \tag{3.12}$$

To translate (x^*, y^*) to the origin, we set $X = x - 2$, $Y = y - 3$ and rename X,Y as x,y respectively. Then

$$\begin{aligned} \frac{dx}{dt} &= \frac{1}{2}(19 - (x+2) - (y+3))(x+2) - 3(x+2) - \frac{8(x+2)}{1 + \frac{1}{2}(x+2)}, \\ \frac{dy}{dt} &= \frac{1}{2}(x+2) + \frac{2(x+2)}{1 + \frac{1}{2}(x+2)} - (y+3). \end{aligned} \tag{3.13}$$

Using the Taylor expansion for (3.13), we have

$$\begin{aligned} \frac{dx}{dt} &= -y + (1 - \frac{1}{2}y)x - \frac{1}{8}x^3 + \frac{1}{32}x^4 + O(|x, y|^5), \\ \frac{dy}{dt} &= -y + x - \frac{1}{8}x^2 + \frac{1}{32}x^3 - \frac{1}{128}x^4 + O(|x, y|^5). \end{aligned} \tag{3.14}$$

The Jacobian matrix for (3.14) at (x^*, y^*) is

$$M = \begin{pmatrix} 1 & -1 \\ 1 & -1 \end{pmatrix}.$$

We thus have $tr(M) = 0$ and $det(M) = 0$. Clearly, the matrix M has two zero eigenvalues, and thus the Bogdanov-Takens bifurcation occurs. By carrying out transformation $X = x$, $Y = x - y$, and renaming X,Y as x,y respectively, (3.14) becomes

$$\begin{aligned} \frac{dx}{dt} &= y - \frac{1}{2}x^2 + \frac{1}{2}xy - \frac{1}{8}x^3 + \frac{1}{32}x^4 + O(|x, y|^5), \\ \frac{dy}{dt} &= -\frac{3}{8}x^2 + \frac{1}{2}xy - \frac{5}{32}x^3 + \frac{5}{128}x^4 + O(|x, y|^5). \end{aligned} \tag{3.15}$$

In order to obtain the canonical normal form, we follow the procedure as in [80]. Setting $u = x - \frac{1}{4}x^2$, $v = y - \frac{1}{2}y^2$, we obtain

$$\begin{aligned} \frac{du}{dt} &= v + O(|u, v|^3), \\ \frac{dv}{dt} &= \frac{1}{2}uv - \frac{3}{8}u^2 + O(|u, v|^3). \end{aligned} \tag{3.16}$$

In the following, we find the universal unfolding of $(I^*, R^*) = (2, 3)$ by choosing the parameters A and c as bifurcation parameters in a small neighbourbood of $(\beta, v, a, \mu, k) = (1/2, 2, 1/2, 1, 1/4)$. Let $A = 19 + \lambda_1$ and $c = 8 + \lambda_2$. We have

$$\begin{aligned} \frac{dx}{dt} &= \frac{1}{2}(19 + \lambda_1 - x - y)x - 3x - \frac{(8 + \lambda_2)x}{1 + \frac{1}{2}x}, \\ \frac{dy}{dt} &= \frac{1}{2}x + \frac{(8 + \lambda_2)x}{4(1 + \frac{1}{2}x)} - y. \end{aligned} \tag{3.17}$$

To translate (x^*, y^*) to the origin, we set $X = x - 2$,$Y = y - 3$ and rename X,Y as x,y respectively. Then

$$\begin{aligned} \frac{dx}{dt} &= \frac{1}{2}((19 + \lambda_1) - (x + 2) - (y + 3))(x + 2) - 3(x + 2) - \frac{(8 + \lambda_2)(x + 2)}{1 + \frac{1}{2}(x + 2)}, \\ \frac{dy}{dt} &= \frac{1}{2}(x + 2) + \frac{(8 + \lambda_2)(x + 2)}{4(1 + \frac{1}{2}(x + 2))} - (y + 3). \end{aligned} \tag{3.18}$$

Using the Taylor expansion for (3.18), we have

$$\begin{aligned}\frac{dx}{dt} &= \lambda_1 - \lambda_2 - y + (-\frac{1}{4}\lambda_2 + \frac{1}{2}\lambda_1 + 1 - \frac{1}{2}y)x + \frac{1}{16}\lambda_2 x^2 + (-\frac{1}{8} - \frac{1}{64}\lambda_2)x^3 \\ &\quad + (\frac{1}{32} + \frac{1}{256}\lambda_2)x^4 + O(|x,y|^5), \\ \frac{dy}{dt} &= \frac{1}{4}\lambda_2 - y + (\frac{1}{16}\lambda_2 + 1)x + (-\frac{1}{8} - \frac{1}{16}\lambda_2)x^2 + (\frac{1}{32} + \frac{1}{256}\lambda_2)x^3 \\ &\quad + (-\frac{1}{128} - \frac{1}{1024}\lambda_2)x^4 + O(|x,y|^5).\end{aligned} \tag{3.19}$$

Let $X = x$,

$$\begin{aligned}Y &= \lambda_1 - \lambda_2 - y + (-\frac{1}{4}\lambda_2 + \frac{1}{2}\lambda_1 + 1 - \frac{1}{2}y)x + \frac{1}{16}\lambda_2 x^2 + (-\frac{1}{8} - \frac{1}{64}\lambda_2)x^3 \\ &\quad + (\frac{1}{32} + \frac{1}{256}\lambda_2)x^4 + O(|x,y|^5)\end{aligned}$$

and rename X,Y as x,y respectively. Then we obtain

$$\begin{aligned}\frac{dx}{dt} &= y, \\ \frac{dy}{dt} &= a_0 + a_1 x + a_2 y + a_3 x^2 + a_4 xy + a_5 y^2 + O(|x,y,\lambda|^3),\end{aligned}$$

where $a_0 = \lambda_1 - 5/4\lambda_2$,$a_1 = 1/2\lambda_1 - 7/16\lambda_2$,$a_2 = 1/4\lambda_2$,$a_3 = -3/8$,$a_4 = -1/2$ and $a_5 = 1/2$. By setting $X = x + a_2/a_4$ (i.e. $X = x - 1/2\lambda_2$) and rewriting X as x, we have

$$\begin{aligned}\frac{dx}{dt} &= y, \\ \frac{dy}{dt} &= b_0 + b_1 x + a_3 x^2 + a_4 xy + a_5 y^2 + O(|x,y,\lambda|^3),\end{aligned}$$

where $b_0 = \lambda_1 - 5/4\lambda_2 + 1/4\lambda_1\lambda_2 - 5/16\lambda_2^2$,$b_1 = 1/2\lambda_1 - 13/16\lambda_2$,$a_3 = -3/8$,$a_4 = -1/2$ and $a_5 = 1/2$. By rewriting the equation using the new time τ with $dt = (1 - a_5 x)d\tau$ (i.e.$dt = (1 - 1/2x)d\tau$) and then rewriting τ as t , we obtain

$$\begin{aligned}\frac{dx}{dt} &= y(1 - \frac{1}{2}x), \\ \frac{dy}{dt} &= (1 - \frac{1}{2}x)(b_0 + b_1 x + a_3 x^2 + a_4 xy + a_5 y^2 + O(|x,y,\lambda|^3)).\end{aligned}$$

Carrying out the transformation $X = x$, $Y = y(1 - \frac{1}{2}x)$, and then renaming X,Y as x,y respectively, we have

$$\begin{aligned}\frac{dx}{dt} &= y, \\ \frac{dy}{dt} &= b_0 + c_1 x + c_2 x^2 + a_4 xy + O(|x,y,\lambda|^3),\end{aligned}$$

where $b_0 = \lambda_1 - 5/4\lambda_2 + 1/4\lambda_1\lambda_2 - 5/16\lambda_2^2$,$c_1 = -1/2\lambda_1 + 7/16\lambda_2$,$c_2 = -3/8$,$a_4 = -1/2$.

By the change of variables $X = a_4^2/c_2 x$, $Y = a_4^3/c_2^2 y$, $\tau = c_2/a_4 t$, and then renaming X, Y, as x, y, t respectively, we obtain

$$\begin{aligned} \frac{dx}{dt} &= y, \\ \frac{dy}{dt} &= \tau_1 + \tau_2 x + x^2 + xy + O(|x, y, \lambda|^3), \end{aligned}$$

where $\tau_1 = b_0 a_4^4/c_2^2$, $\tau_2 = c_1 a_4^2/c_2^2$. By putting $\tau_1 = 1/4\tau_2^2$ and simplifying it, system (3.12) has a saddle-node bifurcation, and the saddle-node bifurcation curve is given by $-384\lambda_1 + 480\lambda_2 + 16\lambda_1\lambda_2 - 64\lambda_1^2 + 71\lambda_2^2 + O(|\lambda_1, \lambda_2|^2) = 0$.

Theorem 3.2. *At the Bogdanov point, the model* (3.2) *with* $A = 19$, $c = 8$ *and* $(\beta, v, a, \mu, k) = (1/2, 2, 1/2, 1, 1/4)$, *in a small neighbourhood of* $(I^*, R^*) = (2, 3)$, *has the following bifurcation :*

(a) saddle-node bifurcation: the saddle-node bifurcation curve is given by

$$-384\lambda_1 + 480\lambda_2 + 16\lambda_1\lambda_2 - 64\lambda_1^2 + 71\lambda_2^2 + O(|\lambda_1, \lambda_2|^2) = 0,$$

(b) Hopf bifurcation : the Hopf bifurcation curve is given by

$$16\lambda_1 - 20\lambda_2 + 4\lambda_1\lambda_2 - 5\lambda_2^2 + O(|\lambda_1, \lambda_2|^2)) = 0,$$

(c) Homoclinic bifurcation : the homoclinic bifurcation curve is given by

$$-600\lambda_1 + 750\lambda_2 - 318\lambda_1\lambda_2 + 96\lambda_1^2 + 261\lambda_2^2 + O(|\lambda_1, \lambda_2|^2) = 0.$$

Figure 3.2 shows the homoclinic bifurcation when $\lambda_1 = 0.05$ and $\lambda_2 = 0.03997138969$ for system (3.17).

From the result in Theorem 3.2, we study the bifurcation curves near the origin on the (λ_1, λ_2) plane. The curves pass through the origin and there are four regions separated by these bifurcation curves. If we take $\lambda_1 \approx 0.2$, we obtain the region as shown in Figure 3.3.

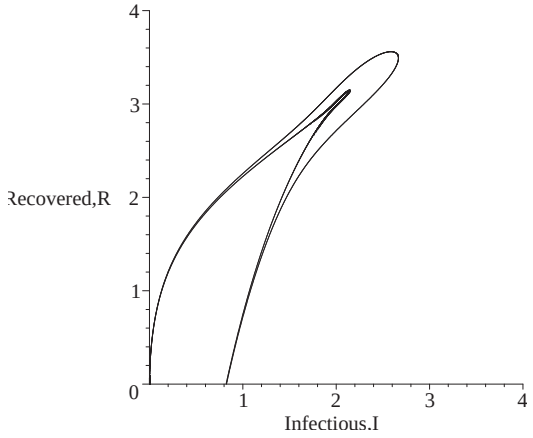

Figure 3.2: The homoclinic bifurcation when $\lambda_1 = 0.05$, $\lambda_2 = 0.03997138969$

The Jacobian matrix for system (3.17) is

$$M = \begin{pmatrix} M_{11} & -\frac{x}{2} \\ M_{21} & -1 \end{pmatrix},$$

where

$$M_{11} = \frac{1}{2(2+x)^2}\left(-2x^3 + (5+\lambda_1 - y)x^2 + (4\lambda_1 + 44 - 4y)x - 8\lambda_2 - 12 - 4y\right)$$

and

$$M_{12} = \frac{1}{2(2+x)^2}\left(x^2 + 4x + 2\lambda_1 + 20\right).$$

If we take$\lambda_1 = 0.2$, after some simple calculation, we obtain the result as shown in Table 3.1.

When (λ_1, λ_2) lies in the region I as in Figure 3.3, there is no limit cycle or homoclinic orbit and E_2 is a stable focus. If (λ_1, λ_2) lies in the region II, there is a unique limit cycle inside the positive orbits of the system (3.17) and the orbits approach E_2 as t tends to infinity. In this situation, the disease is persistent inside the cycle. When (λ_1, λ_2) lies in the region III, E_2 becomes an unstable focus and the limit cycle disappears. In this stage, at finite time, any positive orbits, except for the two equilibria E_1 and E_2 , will tend to the axis $R = 0$, i.e. the disease becomes extinct. When (λ_1, λ_2) lies in the region IV, there is no positive equilibrium and the disease will disappear. The classification of the equilibrium points can be easily checked by the eigenvalues of the Jacobian matrix,M.

Table 3.1: The classification of equilibrium points

	λ_2	E_i	$det(M)$	$tr(M)$	Q	Conclusion
I	0.1590	E_1	(-)	(+)	(+)	Unstable saddle
		E_2	(+)	(-)	(-)	Stable focus
II	0.1596	E_1	(-)	(+)	(+)	Unstable saddle
		E_2	(+)	(-)	(-)	Stable focus
III	0.1602	E_1	(-)	(+)	(+)	Unstable saddle
		E_2	(+)	(+)	(-)	Unstable focus
IV	0.1610	No positive equilibrium				

$$Q = (tr(M))^2 - 4(det(M)).$$

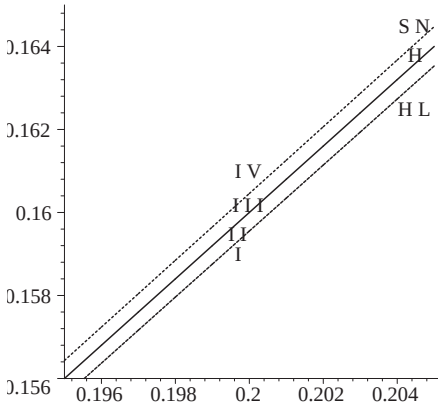

Figure 3.3: The four typical regions separated by the bifurcation curves. The horizontal axis is the λ_1-axis and the vertical axis is the λ_2-axis

3.5 Concluding remarks

In this chapter, we have proposed an epidemic model with sub-optimal immunity and saturated treatment/recovery rate. Through global analysis, the system in (3.2) has been shown to have rich dynamical behaviour including Hopf bifurcation, Bogdonov-Takens bifurcation and its associated homoclinic bifurcation. We also show that when the bifurcation parameters are within certain regions, the disease will be persistent or extinct.

Chapter 4

Bifurcation of an Epidemic Model Taking into Account Nonlinear Incidence

In this chapter, we study the bifurcation of an epidemic model with sub-optimal immunity, nonlinear incidence rate and saturated treatment/recovery rate. Due to the combination of the nonlinearities in both incidence rate and recovery rate, the analysis of equilibrium involves a cubic polynomial. By carrying out the bifurcation analysis of the model, we show that there exist some values of the model parameters such that Hopf bifurcation, Bogdanov-Takens bifurcation and its associated homoclinic bifurcation occur. By studying the bifurcation curves, one can predict the persistence or extinction of diseases.

4.1 General

In recent years, intensive research has been carried out in mathematical epidemiology to develop more realistic epidemic models. For compartmental ordinary differential equation (ODE) models, various new forms of incidence rate and treatment/recovery rate were introduced recently. A number of analytical techniques have been developed to study the underlying ODE models and it has been shown that the dynamics for some of these epidemic models is rich and challenging.

In a seminal paper, Ruan and Wang [83] presented a SIR epidemic model with

the specific nonlinear incidence rate $(\beta SI^2)/(1+aI^2)$, namely

$$\begin{aligned}
\frac{dS}{dt} &= A - \frac{\beta SI^2}{1+aI^2} - \mu S + wR, \\
\frac{dI}{dt} &= \frac{\beta SI^2}{1+aI^2} - (\mu+\gamma)I, \\
\frac{dR}{dt} &= \gamma I - (\mu+w)R,
\end{aligned} \tag{4.1}$$

where A is the recruitment rate of susceptible population,β is the disease transmission rate, μ is the natural death rate, γ is the recovery rate of infective individuals, w is the rate of removed individuals who lose immunity and return to susceptible class. In the paper, the authors consider a reduced system and perform an elaborative analysis of the state equilibrium through a quadratic equation. By transformation of the underlying differential equations to the normal form, they show that the model undergoes Hopf bifurcation, Bogdanov-Takens bifurcation and its associated homoclinic bifurcation. Following this work, various attempts have been made to study the problem with different assumptions on the form of the incidence rate, for example, the form of $(\beta SI)/(1+aI+bI^2)$[103], $(\beta SI^2)/(1+aI+bI^2)$ [85] ,$(\beta_1 I+\beta_2 I)S^p$ [17] and sigmoidal function [50].

Different forms of the treatment/recovery rate were proposed in the attempts to simulate the dynamics of the disease transmission more accurately. In [91], a constant removal rate, r, due to the treatment of infectives is used in the model, namely

$$\begin{aligned}
\frac{dS}{dt} &= A - \beta SI - \mu S, \\
\frac{dI}{dt} &= \beta SI - (\mu+\gamma)I - h(I), \\
\frac{dR}{dt} &= \gamma I + h(I) - \mu R,
\end{aligned} \tag{4.2}$$

with $h(I) = r$, for $I > 0$ and $h(I) = 0$, for $I = 0$. The authors showed the existence of Hopf bifurcation and Bogdanov-Takens bifurcation. In [99], the authors established a model with a saturated incidence rate and a saturated treatment rate; while, in [55], the authors proposed a model with a saturated incedence rate and a treatment function with low capacity. Both authors show that the backward bifurcation exists in their proposed models.

In this chapter, we analyze a more general epidemic model with sub-optimal immunity, nonlinear incidence rate and saturated treatment/recovery rate, namely

$$\begin{aligned}\frac{dS}{dt} &= A - \beta SI^2 + \sigma T(I) - \mu S,\\ \frac{dI}{dt} &= \beta SI^2 - T(I) - \mu I,\\ \frac{dR}{dt} &= (1-\sigma)T(I) - \mu R,\end{aligned} \tag{4.3}$$

where all the parameters are positive, A is the recruitment rate of susceptible population, β is the disease transmission rate, μ is the natural death rate and $T(I)$ is the recovery rate. We take $T(I) = vI + cI/(1+aI)$ as the recovery rate function in which $c/(1+aI)$ and v are respectively the recovery rate of the infected population with and with no treatment. In comparison with previous works, our work presented here has various new features and contributions. Firstly, it is more general and includes some previous models as special cases. For example, if the nonlinear incidence rate βSI^2 is replaced by a bilinear function, then it reduces to the sub-optimal immunity model [76], while it reduces to the nonlinear SIR model if $T(I)$ is taken to be zero. It should also be addressed that $\sigma = 1$ corresponds to the SIS model in which immunity is assumed not to protect against reinfection, while $\sigma = 0$ corresponds to the SIR model in which immunity is assumed to be fully protective and prevents any reinfection. The sub-optimal immunity model where $\sigma \in [0, 1]$ are more appropriate for the study of microparasite infections which usually occur during childhood. After a primary infection, one may get temporary immunity (immune protection will wane over time) or partial immunity (immunity that may not fully protective). Examples of this kind of diseases include Pertussis (temporary immunity) and Influenza A (partial immunity) [35]. Secondly, due to the combination of the nonlinearities in both incidence rate and recovery rate, the work involves more complex analysis of equilibrium through a higher order polynomial and thus, it is hard to obtain exact solution in simple form. Hence, some analysis using numerical results are required. In similar scenario,the authors in [102] obtained positive real equilibrium from a cubic equation which derives from a mathematical model of Schistosoma Mansoni. Throughout the chapter, we choose some specific values

for the parameters as in [103]. The values can be easily replaced by other values whenever necessary as long as the conditions are fulfilled.

The rest of the chapter is organized as follows. In Section 4.2, we discuss the existence of equilibria. In Section 4.3 and 4.4, we study the Hopf bifurcation and Bogdanov-Takens Bifurcation. Some conclusions are given in Section 4.5.

4.2 Existence of equilibria

Summing up the three equations in (4.3), we obtain $dN/dt = A - \mu N(t)$,where $N(t) = S(t) + I(t) + R(t)$ which gives $N(t) = A/\mu(1 - e^{-\mu t}) + N_0 e^{-\mu t}$ implying that $N(t)$ tends to a constant value, A/μ , as $t \to \infty$. Let $S + I + R = A/\mu$ and $k = 1 - \sigma$, we can obtain from (4.3) the following reduced system

$$\begin{aligned} \frac{dI}{dt} &= \beta(\frac{A}{\mu} - I - R)I^2 - vI - \frac{cI}{1+aI} - \mu I, \\ \frac{dR}{dt} &= k(vI + \frac{cI}{1+aI}) - \mu R. \end{aligned} \tag{4.4}$$

We have the following lemma.

Lemma 4.1. *Let* $K = \frac{\beta(kv+kc+\mu-Aa)}{\beta a(kv+\mu)}$, $M = \frac{-\beta A+v\mu a+\mu^2 a}{\beta a(kv+\mu)}$,$N = \frac{c\mu+\mu^2+v\mu}{\beta a(kv+\mu)}$ *and* $q = M - \frac{1}{3}K^2$, $p = \frac{2}{27}K^3 - \frac{1}{3}KM + N$,$\triangle = \frac{p^2}{4} + \frac{q^3}{27}$. *Suppose* $a > \frac{1}{A}(kv + kc + \mu)$ *or* $a < \frac{\beta A}{v\mu+\mu^2}$. *If* $\triangle < 0$, *system* (4.4) *has two positive equilibria,* $E_j\left(I_j, \frac{kI_j(v+vaI_j+c)}{(1+aI_j)\mu}\right)$ *for* $j = 1, 2$. *If* $\triangle = 0$, *system* (4.4) *has a unique positive equilibrium,* $E^*\left(I^*, \frac{kI^*(v+vaI^*+c)}{(1+aI^*)\mu}\right)$. *If* $\triangle > 0$, *system* (4.4) *has no positive equilibrium.*

Proof. Assume equilibrium occurs at t_e , then $dI/dt_e = 0$, $dR/dt_e = 0$ and $N(t_e) = A/\mu(1 - e^{-\mu t_e}) + N_0 e^{-\mu t_e} := A_e$. Thus from the second equation of (4.4), we obtain $R = \frac{kI(v(1+aI)+c)}{\mu(1+aI)}$. After some algebra work, we obtain

$$[\beta a(kv+\mu)]I^3 + [\beta(kv+kc+\mu-Aa)]I^2 + [-\beta A+v\mu a+\mu^2 a]I + [c\mu+\mu^2+v\mu] = 0, \tag{4.5}$$

which can be written as

$$I^3 + KI^2 + MI + N = 0, \tag{4.6}$$

where $K = \frac{\beta(kv+kc+\mu-Aa)}{\beta a(kv+\mu)}$, $M = \frac{-\beta A+v\mu a+\mu^2 a}{\beta a(kv+\mu)}$,and $N = \frac{c\mu+\mu^2+v\mu}{\beta a(kv+\mu)}$. As all the parameters are positive, N is positive. By the Descartes' rule of sign for the roots of cubic equations, if both of K and M are positive, then there is no positive root; or otherwise there is no positive root or have two positive roots (i.e. at most two positive roots) if

$$a > \frac{1}{A}(kv + kc + \mu) \qquad \text{or} \qquad a < \frac{\beta A}{v\mu + \mu^2}. \tag{4.7}$$

Further from (4.6), let $I = x - \frac{K}{3}$, we obtain

$$x^3 + qx + p = 0,$$

where $q = M - \frac{1}{3}K^2$,and $p = \frac{2}{27}K^3 - \frac{1}{3}KM + N$. Let

$$\triangle = \frac{p^2}{4} + \frac{q^3}{27}. \tag{4.8}$$

Then we have

(a) If $\triangle > 0$, there is one real root.

(b) If $\triangle = 0$, there are two distinct real roots (or all roots are real, and two equal).

(c) If $\triangle < 0$, there are three distinct real roots.

Combining the result from the Descartes' rule of sign, (4.7) and (4.8), we have the following conclusion. If $\triangle < 0$, system (4.4) has two positive equilibria, $E_j\left(I_j, \frac{kI_j(v+vaI_j+c)}{(1+aI_j)\mu}\right)$ for $j = 1, 2$. If $\triangle = 0$, system (4.4) has a unique positive equilibrium, $E^*\left(I^*, \frac{kI^*(v+vaI^*+c)}{(1+aI^*)\mu}\right)$. If $\triangle > 0$, system (4.4) has no positive equilibrium. □

Remark 4.1. *Graphically, the surface* $\triangle = p^2/4 + q^3/27 = 0$ *or* $1/108(4K^3N - K^2M^2 - 18KMN + 27N^2 + 4M^3)$ *is a saddle node bifurcation surface. That is, on one side of the surface, there are two positive equilibria. On the surface of the curve, there is only one positive equilibrium, and on the other side of surface, the system has no positive equilibrium. We will show that this is the saddle node bifurcation curve by difference analysis in Section 4.4 later.*

Let the basic reproduction number be $R_0 = \beta A/(\mu(c+\mu+v))$, the Jacobian matrix for (4.4) is

$$M = \begin{pmatrix} -\beta I^2 + 2\beta I(\frac{A}{\mu} - I - R) - v - \frac{c}{1+aI} + \frac{caI}{(1+aI)^2} - \mu & -\beta I^2 \\ k\left(v + \frac{c}{1+aI} - \frac{caI}{(1+aI)^2}\right) & -\mu \end{pmatrix}.$$

At the disease free equilibrium, $O(0,0)$, the eigenvalues are $-\mu$ and $-\mu - v - c$ which are less than 0. So O is locally asymptotically stable. At endemic equilibrium, $E(I,R)$, the characteristic polynomial is $\lambda^2 + P_1\lambda + P_2$ where

$$P_1 = -2\beta I(\frac{A}{\mu} - I - R) + \beta I^2 + v + \frac{c}{(1+aI)^2} + 2\mu,$$

$$P_2 = \left(-2\beta I(\frac{A}{\mu} - I - R) + \beta I^2 + v + \frac{c}{(1+aI)^2} + \mu\right)\mu + \beta I^2 k\left(v + \frac{c}{(1+aI)^2}\right).$$

If $P_2 > 0$, after some algebra work, we can show that the eigenvalues have negative real part if

$$\frac{1}{c+\mu+v}\left(R\beta + \frac{3\beta I^2 + v + 2\mu}{2I} + \frac{c}{2I(1+aI)^2}\right) > R_0,$$

So $E(I,R)$ is locally asymptotically stable when

$$\frac{1}{c+\mu+v}\left(R\beta + \frac{3\beta I^2 + v + 2\mu}{2I} + \frac{c}{2I(1+aI)^2}\right) > R_0,$$

and $P_2 > 0$.

Example 4.1. *Let* $(\beta, v, c, a, \mu, k, A) = (1/2, 1.27, 2, 4, 1, 1/2, 6)$ *in system* (4.4)*. From* (4.8)*, we have* $\triangle = -0.0414 < 0$ *which concludes that there are two positive equilibria. Solving* (4.5)*, we obtain* $E_1(I_1, R_1) = (1.615353698, 1.242243888)$ *and* $E_2(I_2, R_2) = (2.046474276, 1.522295468)$*. For* $E_2(I_2, R_2)$ *, we have* $P_2 = 0.766804631 > 0$ *and*

$$\frac{1}{c+\mu+v}\left(R\beta + \frac{3\beta I^2 + v + 2\mu}{2I} + \frac{c}{2I(1+aI)^2}\right) = 0.7261661363 > R_0,$$

where $R_0 = 0.7025761124$*. It means that the conditions for existence and asymptotically stable as discussed above are satisfied. Figure 4.1 shows the stable endemic equilibrium when the parameters are taken as* $(\beta, v, c, a, \mu, k, A) = (1/2, 1.27, 2, 4, 1, 1/2, 6)$.

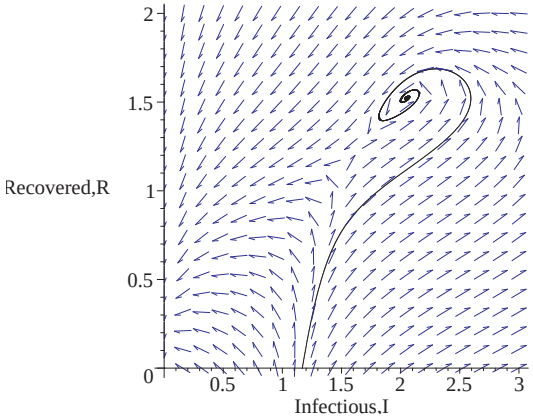

Figure 4.1: Stable endemic equilibrium when the parameters are taken as $(\beta, v, c, a, \mu, k, A) = (1/2, 1.27, 2, 4, 1, 1/2, 6)$ for model (4.4). The values of (I, R) at equilibrium are $(2.046474276, 1.522295468)$.

4.3 Hopf bifurcation

In this section, we will show that the model in (4.4) undergoes Hopf bifurcation for some values. For simplicity, let $\mu = 1$. The Jacobian matrix for (4.4) is

$$M = \begin{pmatrix} -\beta I^2 + 2\beta I(A - I - R) - v - \frac{c}{1+aI} + \frac{caI}{(1+aI)^2} - 1 & -\beta I^2 \\ k\left(v + \frac{c}{1+aI} - \frac{caI}{(1+aI)^2}\right) & -1 \end{pmatrix}.$$

Theorem 4.1. *Suppose that the condition of* (4.7) *are satisfied and let* $\mu = 1$. *If there exists a limit cycle for* (4.4)*, it must include a positive equilibrium,* $E^+(I^+, R^+)$.

Proof. If a limit cycle exists, we have $tr(M) = 0$, then we obtain

$$-\beta I^2 + 2\beta I(A - I - R) - v - \frac{c}{1 + aI} + \frac{caI}{(1 + aI)^2} - 2 = 0.$$

At equilibrium,$R = kI(v(1 + aI) + c)/(\mu(1 + aI))$. So we get

$$A = \frac{P_3}{2\beta I(1 + aI)^2},$$

where

$$P_3 = a^2\beta(2kv + 3)I^4 + \beta a(6 + 4kv + 2kc)I^3$$
$$+ (\beta(2kc + 2kv + 3) + a^2(2 + v))I^2 + 2a(2 + v)I + 2 + v + c.$$

Substituting the above into (4.5), after some algebra work, we obtain

$$\frac{1}{2(1 + aI)}\left(-a^2\beta I^4 - 2\beta a I^3 + (va^2 - \beta)I^2 + 2a(c + v)I + v + c\right) = 0.$$

By the Descartes rule of sign, we will have at most one positive root (real or imaginary root). Since all the parameters are real and positive and the quartic equation has real coefficients, the complex value roots will be in conjugate pair. Hence, we can rule out the case of having any complex root with a positive real part. In other words, if there exists a limit cycle in (4.4), it must include a positive equilibrium,$E^+(I^+, R^+)$, if (4.7) is satisfied. □

With Theorem 4.1 and avoiding the condition in (4.7), let (β, v, c, a, μ, k) $= (1/2, 8, 8, 3, 1, 1/2)$, then the positive real root is approximated to 4.270040762 or $\frac{12571}{2944}$. Hence, we find that the positive endemic equilibrium $E^+(I^+, R^+)$ is $(\frac{12571}{2944}, \frac{548108171}{29923552})$. With the parameters as mentioned, we obtain $A = \frac{3312503940005049139}{122351215219281152}$, or ≈ 27.07373142.

Writing I and R in term of x and y, then $(I^+, R^+) = (x^+, y^+) = (\frac{12571}{2944}, \frac{548108171}{29923552})$ and we have

$$\begin{aligned} \frac{dx}{dt} &= \frac{1}{2}\left(\frac{3312503940005049139}{122351215219281152} - x - y\right)x^2 - 9x - \frac{8x}{1+3x}, \\ \frac{dy}{dt} &= 4x + \frac{4x}{1+3x} - y. \end{aligned} \tag{4.9}$$

To translate (x^+, y^+) to the origin, we set $X = x - \frac{12571}{2944}$ and $Y = y - \frac{548108171}{29923552}$, then rename X,Y as x,y respectively. Hence

$$\begin{aligned} \frac{dx}{dt} &= \frac{1}{2}\left(\frac{3312503940005049139}{122351215219281152} - (x + \frac{12571}{2944}) - (y + \frac{548108171}{29923552})\right)(x + \frac{12571}{2944})^2 \\ &\quad - 9(x + \frac{12571}{2944}) - \frac{8(x + \frac{12571}{2944})}{1 + 3(x + \frac{12571}{2944})}, \\ \frac{dy}{dt} &= 4(x + \frac{12571}{2944}) + \frac{4(x + \frac{12571}{2944})}{1 + 3(x + \frac{12571}{2944})} - (y + \frac{548108171}{29923552}). \end{aligned} \tag{4.10}$$

Using the Taylor expansion for (4.10), we have

$$\begin{aligned}
\frac{dx}{dt} &= -\frac{2331843754045}{168711259576927780864} - \frac{158030041}{17334272}y + (1 - \frac{12571}{2944}y)x \\
&\quad - (\frac{20072413090211610137691}{9948866714340627593728} + \frac{1}{2}y)x^2 - \frac{2743198563151458625}{5464762783327478402}x^3 \\
&\quad + \frac{47768629289768976384}{1110904302408726446950 57}x^4 + O(|x,y|^5), \\
\frac{dy}{dt} &= -y + \frac{6646635140}{1652991649}x - \frac{306192580608}{67205681473393}x^2 + \frac{2704292871929856}{2732381391663739201}x^3 \\
&\quad - \frac{23884314644884488192}{1110904302408726446950 57}x^4 + O(|x,y|^5).
\end{aligned} \tag{4.11}$$

The Jacobian matrix for (4.11) at$(x, y) = (0, 0)$ is

$$M = \begin{pmatrix} m_{11} & m_{12} \\ m_{21} & m_{22} \end{pmatrix} = \begin{pmatrix} 1 & -\frac{158030041}{17334272} \\ \frac{6646635140}{1652991649} & -1 \end{pmatrix}$$

and thus $tr(M) = 0$ and $det(M) \approx 35.65770109 > 0$. In this case, the eigenvalues are $\pm\frac{\sqrt{71075066462383315864674}}{44645939584}i$ (or $\pm 5.971406960i$). Hence Hopf bifurcation occurs. By taking transformation $X = x$, $Y = m_{11}x + m_{12}y$,where $Y = x - \frac{158030041}{17334272}y$, and then renaming X,Y as x,y respectively, (4.11) becomes

$$\begin{aligned}
\frac{dx}{dt} &= -\frac{2331843754045}{168711259576927780864} + y - \frac{24732259340632230237275}{9948866714340627593728}x^2 \\
&\quad + \frac{5888}{12571}xy - \frac{48087162365680388356575 0297}{86359668670451552829467 4482}x^3 + \frac{8667136}{158030041}x^2y \\
&\quad + \frac{47768629289768976384}{1110904302408726446950 57}x^4 + O(|x,y|^5), \\
\frac{dy}{dt} &= -\frac{2331843754045}{168711259576927780864} - \frac{255428654207186553}{7163351714373632}x \\
&\quad - \frac{24319025069373392327771}{9948866714340627593728}x^2 + \frac{5888}{12571}xy \\
&\quad - \frac{48866377569279616060631 2473}{86359668670451552829467 4482}x^3 + \frac{8667136}{158030041}x^2y \\
&\quad + \frac{265512946592970178560}{1110904302408726446950 57}x^4 + O(|x,y|^5).
\end{aligned} \tag{4.12}$$

Let $k_1 = \frac{255428654207186553}{7163351714373632}$. Making the change of variables $u = -x$, $v = \frac{1}{\sqrt{k_1}}y$, we obtain

$$\begin{aligned}
\frac{du}{dt} &= -\sqrt{k_1}v + F_1(u,v), \\
\frac{dv}{dt} &= \sqrt{k_1}u + F_2(u,v),
\end{aligned} \tag{4.13}$$

where

$$
\begin{aligned}
F_1(u,v) &= \frac{2331843754045}{168711259576927780864} + \frac{24732259340632230237275}{9948866714340627593728}u^2 \\
&+ \frac{5888}{12571}\sqrt{k_1}uv - \frac{4808716236568038835657502 97}{8635966867045155282946744 82}u^3 \\
&- \frac{8667136}{158030041}\sqrt{k_1}u^2v - \frac{47768629289768976384}{1110904302408726446950 57}u^4 + O(|x,y|^5), \\
F_2(u,v) &= -\frac{2331843754045}{168711259576927780864\sqrt{k_1}} - \frac{24319025069373392327771}{9948866714340627593728\sqrt{k_1}}u^2 \\
&- \frac{5888}{12571}uv + \frac{48866377569279616060631 2473}{8635966867045155282946744 82\sqrt{k_1}}u^3 \\
&- \frac{8667136}{158030041}u^2v + \frac{265512946592970178560}{1110904302408726446950 57}u^4 + O(|x,y|^5).
\end{aligned}
\tag{4.14}
$$

We can get the first Liapunov constant, σ , by

$$
\begin{aligned}
\sigma &= \frac{1}{16}\left[\frac{\partial^3 F_1}{\partial u^3} + \frac{\partial^3 F_1}{\partial u \partial v^2} + \frac{\partial^3 F_2}{\partial u^2 \partial v} + \frac{\partial^3 F_2}{\partial v^3}\right] \\
&+ \frac{1}{16\sqrt{k_1}}\left[\frac{\partial^2 F_1}{\partial u \partial v}\left(\frac{\partial^2 F_1}{\partial u^2} + \frac{\partial^2 F_1}{\partial v^2}\right) - \frac{\partial^2 F_2}{\partial u \partial v}\left(\frac{\partial^2 F_2}{\partial u^2} + \frac{\partial^2 F_2}{\partial v^2}\right)\right] \\
&+ \frac{1}{16\sqrt{k_1}}\left[-\frac{\partial^2 F_1}{\partial u^2}\frac{\partial^2 F_2}{\partial u^2} + \frac{\partial^2 F_1}{\partial v^2}\frac{\partial^2 F_2}{\partial v^2}\right] = -0.01781784460.
\end{aligned}
$$

Hence, there is a stable periodic orbit when A increases from $\frac{3312503940005049139}{122351215219281152}$ (≈ 27.07373142) .

Figure 4.2 shows a stable orbit for system (4.4) when $(\beta, v, c, a, \mu, k) = (1/2, 8, 8, 3, 1, 1/2)$ while $(I^+, R^+) = (\frac{12571}{2944}, \frac{548108171}{29923552})$ and $A = 27.1$.

In the following, we choose A as a bifurcation parameter. Let $A = A_0 + \epsilon$, where $A_0 = \frac{3312503940005049139}{122351215219281152}$. From (4.9), we obtain,

$$
\begin{aligned}
\frac{dI}{dt} &= \beta(\frac{A_0+\epsilon}{\mu} - I - R)I^2 - vI - \frac{cI}{1+aI} - \mu I, \\
\frac{dR}{dt} &= k(vI + \frac{cI}{1+aI}) - \mu R.
\end{aligned}
\tag{4.15}
$$

Let $\mu = 1$, similar to (4.5), we obtain

$$[\beta a(kv+1)]I^3 + [\beta(kv+kc+1-(A_0+\epsilon)a)]I^2 + [-\beta(A_0+\epsilon)+va+a]I + [c+1+v] = 0.$$

Write I and R as x and y, and $(\beta, v, c, a, \mu, k) = (1/2, 8, 8, 3, 1, 1/2)$, then from

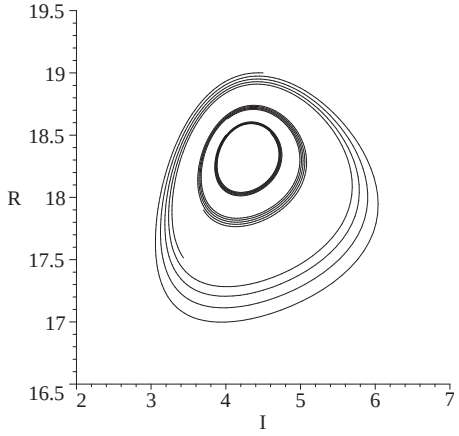

Figure 4.2: A stable orbit for system (4.4) when $(\beta, v, c, a, \mu, k) = (1/2, 8, 8, 3, 1, 1/2)$ while $(I^+, R^+) = (\frac{12571}{2944}, \frac{548108171}{29923552})$ and $A = 27.1$

(4.9), we obtain,

$$\begin{aligned} \frac{dx}{dt} &= \frac{1}{2}(A_0 + \epsilon - x - y)x^2 - 9x - \frac{8x}{1+3x}, \\ \frac{dy}{dt} &= 4x + \frac{4x}{1+3x} - y. \end{aligned} \tag{4.16}$$

In this case, let (x^+, y^+) be the positive equilibrium of the system (4.16). The Jacobian matrix is

$$M = \begin{pmatrix} m_{11} & -\frac{(x^+)^2}{2} \\ m_{21} & -1 \end{pmatrix},$$

where

$$m_{11} = x^+(A_0 + \epsilon - x^+ - y^+) - 9 - \frac{(x^+)^2}{2} - \frac{8}{1+3x^+} + \frac{24x^+}{(1+3x^+)^2},$$

$$m_{21} = 4 + \frac{4}{1+3x^+} - \frac{12x^+}{(1+3x^+)^2}.$$

Hence, the characteristic equation is given by

$$\lambda^2 + (1 - m_{11})\lambda - m_{11} + \frac{(x^+)^2}{2}m_{21} = 0,$$

which gives $\lambda = \frac{1}{2}(m_{11} - 1) \pm \sqrt{m_{11}^2 + 2m_{11} + 1 - 2m_{21}(x^+)^2}$.

We can obtain the following values

(a) $Re\lambda(\epsilon) = 0$ when $\epsilon = 0$.

(b) $Im\lambda(\epsilon) = 5.971406945 \neq 0$ when $\epsilon = 0$.

(c) $Re\dfrac{d}{d\epsilon}\lambda(\epsilon) = -0.3575405923 \neq 0$ when $\epsilon = 0$.

Therefore, by the Hopf bifurcation theory, we obtain the following result

Theorem 4.2. *There exist a* $\sigma_1 > 0$ *and a function* $\epsilon = \epsilon(x_1)$ *defined on* $0 < x_1 - \frac{12571}{2944} \leq \sigma_1$ *, which satisfy* $\epsilon(\frac{12571}{2944}) = 0$ *and when* $\epsilon = \epsilon(x_1) < 0$*, system* (4.16) *has a unique stable limit cycle which passes through* $(x_1, \frac{548108171}{29923552})$.

4.4 Bogdanov-Takens bifurcation

In this section, we will study the Bogdanov-Takens bifurcation for some values of the model in (4.4). Let $\mu = 1$, the Jacobian matrix for (4.4) is

$$M = \begin{pmatrix} -\beta I^2 + 2\beta I(A - I - R) - v - \frac{c}{1+aI} + \frac{caI}{(1+aI)^2} - 1 & -\beta I^2 \\ k\left(v + \frac{c}{1+aI} - \frac{caI}{(1+aI)^2}\right) & -1 \end{pmatrix}.$$

Theorem 4.3. *Suppose that we choose* $(\beta, c, a, \mu, k) = (1/2, 2, 4, 1, 1/2)$*. Then there exists a positive equilibrium,* (I^+, R^+)*, when Bogdanov-Takens bifurcation occurs.*

Proof. We choose $(\beta, c, a, \mu, k) = (1/2, 2, 4, 1, 1/2)$ for (I^+, R^+) and set $tr(M) = 0$, $det(M) = 0$. Knowing $R = \frac{kI(v(1+aI)+c)}{\mu(1+aI)} = \frac{I(4vI+v+2)}{2(1+4I)}$, we get

$$A = \frac{1}{2I^3(16I^2 + 8I + 1)}\left(48I^6 + 32I^5 + 131I^4 + 64I^3 + 136I^2 + 64I + 8\right),$$

$$v = \frac{2}{I^2(16I^2 + 8I + 1)}\left(31I^2 + 16I + 2\right).$$

Substituting the above into (4.5) , after some algebra work, we obtain

$$-\frac{1}{4I^2(4I + 1)}\left(16I^6 + 8I^5 + I^4 - 32I^3 - 128I^2 - 64I - 8\right) = 0.$$

By the Descartes rule of sign, we will have at most one positive root (real or imaginary root) for the polynomial of degree six above. Since all the coefficients of the polynomial equation are real, the complex value root will be in conjugate pair. Hence, we can rule out there is any complex root with positive real part. In other words, the positive root in the six degree polynomial is a real root. □

By setting $A = \frac{1}{2I^3(16I^2+8I+1)}\,(48I^6 + 32I^5 + 131I^4 + 64I^3 + 136I^2 + 64I + 8)$, $v = \frac{2}{I^2(16I^2+8I+1)}\,(31I^2 + 16I + 2)$, and $(\beta, c, a, \mu, k) = (1/2, 2, 4, 1, 1/2)$. we obtain $(I^+, R^+) = (x^+, y^+) = (\frac{31623}{17444}, \frac{212322110622679}{163787945597952})$. Writing I and R in term of x and y, we have

$$\begin{aligned} \frac{dx}{dt} &= \frac{1}{2}(A - x - y)x^2 - vx - \frac{2x}{1+4x} - x, \\ \frac{dy}{dt} &= \frac{1}{2}(vx + \frac{2x}{1+4x}) - y. \end{aligned} \tag{4.17}$$

To translate (x^+, y^+) to the origin, we set $X = x - \frac{31623}{17444}$, $Y = y - \frac{212322110622679}{163787945597952}$ and rename X,Y as x,y respectively. Then

$$\begin{aligned} \frac{dx}{dt} &= \frac{1}{2}\left(A - (x + \frac{31623}{17444}) - (y + \frac{212322110622679}{163787945597952})\right)(x + \frac{31623}{17444})^2 \\ &\quad - v(x + \frac{31623}{17444}) - \frac{2(x + \frac{31623}{17444})}{1 + 4(x + \frac{31623}{17444})} - (x + \frac{31623}{17444}), \\ \frac{dy}{dt} &= \frac{1}{2}\left(v(x + \frac{31623}{17444}) + \frac{2(x + \frac{31623}{17444})}{1 + 4(x + \frac{31623}{17444})}\right) - (y + \frac{212322110622679}{163787945597952}). \end{aligned} \tag{4.18}$$

Using the Taylor expansion for (4.18), we have

$$\begin{aligned} \frac{dx}{dt} &= \epsilon - \frac{1000014129}{608586272}y + (1 - \frac{31623}{17444}y)x \\ &\quad - (-\frac{3679158776793358777092660900 25}{80321834349300801352439719 0656} - \frac{1}{2}y)x^2 \\ &\quad - \frac{26559071628444065}{52394750189570048}x^3 + \frac{1577358583287077801}{471343172705372151808}x^4 + O(|x, y|^5), \\ \frac{dy}{dt} &= -y + \frac{608586272}{1000014129}x - \frac{82938897881}{11648454910976}x^2 + \frac{361696533659041}{104789500379140096}x^3 \\ &\quad - \frac{1577358583287077801}{9426863454107443036 16}x^4 + O(|x, y|^5), \end{aligned} \tag{4.19}$$

where $\epsilon = \frac{22145673427690019}{6792195847043662205369856} \approx 0.326 \times 10^{-8}$.

The Jacobian matrix for (4.19) at $(x, y) = (0, 0)$ is

$$M = \begin{pmatrix} 1 & -\frac{1000014129}{608586272} \\ \frac{608586272}{1000014129} & -1 \end{pmatrix}.$$

We have $tr(M) = 0$ and $det(M) = 0$. Clearly, the matrix M has two zero eigenvalues, and thus the Bogdanov-Takens bifurcation occurs.

Let $\epsilon = 0$, by carrying out transformation $X = x$, $Y = m_{11}x + m_{12}y$, (i.e. $Y = x - \frac{1000014129}{608586272}y$) and renaming X, Y as x, y respectively, (4.19) becomes

$$\begin{aligned}
\frac{dx}{dt} &= y - \frac{1254064616501840497000262174761}{80321834349300801352439719065 6}x^2 + \frac{34888}{31623}xy \\
&\quad - \frac{42502809726687967683784913}{52395490474995476435208192}x^3 + \frac{304293136}{1000014129}x^2y \\
&\quad + \frac{1577358583287077801}{471343172705372151808}x^4 + O(|x,y|^5), \\
\frac{dy}{dt} &= -\frac{61275924689377761682143125312 77}{39543056910425009896585707847 68}x^2 + \frac{34888}{31623}xy \\
&\quad - \frac{21070759084088779625673586 1}{25794703003074696091179417 6}x^3 + \frac{304293136}{1000014129}x^2y \\
&\quad - \frac{14145463004235472301}{2320458696395678285824}x^4 + O(|x,y|^5).
\end{aligned} \tag{4.20}$$

In order to obtain the canonical normal forms, set $u = x + Kx^2 + Lxy$,$v = y + Mx^2 + Nxy$ where $K = -\frac{17444}{31623}$, $M = -\frac{1254064616501840497000262174761}{80321834349300801352439719065 6}$, $L = N = 0$, and make the change of variables . In the selection of the value for K, L, M and N, we follow the procedures in [80] and we obtain

$$\begin{aligned}
\frac{du}{dt} &= v + O(|u,v|^3), \\
\frac{dv}{dt} &= \frac{34888}{31623}uv - \frac{61275924689377761682143125312 77}{39543056910425009896585707847 68}u^2 + O(|u,v|^3).
\end{aligned} \tag{4.21}$$

This implies that $(I^+, R^+) = (\frac{31623}{17444}, \frac{212322110622679}{163787945597952})$ is a cusp of dimension 2.

In the following, we find the universal unfolding of $(x^+, y^+) = (\frac{31623}{17444}, \frac{212322110622679}{163787945597952})$ by choosing the parameters A and v as bifurcation parameters in a small neighbourbood of $(\beta, c, a, \mu, k) = (1/2, 2, 4, 1, 1/2)$. Let $A = A_0 + \lambda_1$ and $v = v_0 + \lambda_2$, where $A_0 = \frac{41358974198917582274599129 27}{71428932280391997645566668 8}$ and $v_0 = \frac{769008283214884223}{647433275455504512}$. Then, we have,

$$\begin{aligned}
\frac{dx}{dt} &= \frac{1}{2}\left(A_0 + \lambda_1 - x - y\right)x^2 - (v_0 + \lambda_2)x - \frac{2x}{1+4x} - x, \\
\frac{dy}{dt} &= \frac{1}{2}\left((v_0 + \lambda_2)x - \frac{2x}{1+4x}\right) - y.
\end{aligned} \tag{4.22}$$

To translate (x^+, y^+) to the origin, we set $X = x - \frac{31623}{17444}$,$Y = y - \frac{212322110622679}{163787945597952}$

and rename X,Y as x,y respectively. Then

$$\begin{aligned}\frac{dx}{dt} &= \frac{1}{2}\left(A_0+\lambda_1-(x+\frac{31623}{17444})-(y+\frac{212322110622679}{163787945597952})\right)(x+\frac{31623}{17444})^2\\ &\quad-(v_0+\lambda_2)(x+\frac{31623}{17444})-\frac{2(x+\frac{31623}{17444})}{1+4(x+\frac{31623}{17444})}-(x+\frac{31623}{17444}),\\ \frac{dy}{dt} &= \frac{1}{2}\left((v_0+\lambda_2)(x+\frac{31623}{17444})-\frac{2(x+\frac{31623}{17444})}{1+4(x+\frac{31623}{17444})}\right)\\ &\quad-(y+\frac{212322110622679}{163787945597952}).\end{aligned} \tag{4.23}$$

Using the Taylor expansion for (4.23), we have

$$\begin{aligned}\frac{dx}{dt} &= \frac{1000014129}{608586272}(\lambda_1-y)-\frac{31623}{17444}\lambda_2+\epsilon_1+\left(\frac{31623}{17444}(\lambda_1-y)-\lambda_2+1\right)x\\ &\quad+\left(-\frac{1}{2}y+\frac{1}{2}\lambda_1-\frac{367915877679335877709266090025}{803218343493008013524397190656}\right)x^2\\ &\quad+(\frac{26559071628444065}{52394750189570048})x^3+\frac{1577358583287077801}{471343172705372151808}x^4+O(|x,y|^5),\\ \frac{dy}{dt} &= \frac{31623}{34888}\lambda_2-y+(\frac{1}{2}\lambda_2+\frac{608586272}{1000014129})x-\frac{82938897881}{11648454910976}x^2\\ &\quad+\frac{361696533659041}{104789500379140096}x^3-\frac{1577358583287077801}{942686345410744303616}x^4+O(|x,y|^5),\end{aligned} \tag{4.24}$$

where $\epsilon_1=\frac{22145673427690019}{679219584704366220536985 6}\approx 0.3260\times 10^{-8}$.

Let $X=x$,

$$\begin{aligned}Y &= \frac{1000014129}{608586272}(\lambda_1-y)-\frac{31623}{17444}\lambda_2+\epsilon_1+\left(\frac{31623}{17444}(\lambda_1-y)-\lambda_2+1\right)x\\ &\quad+\left(-\frac{1}{2}y+\frac{1}{2}\lambda_1-\frac{367915877679335877709266090025}{803218343493008013524397190656}\right)x^2\\ &\quad+(\frac{26559071628444065}{52394750189570048})x^3+\frac{1577358583287077801}{471343172705372151808}x^4+O(|x,y|^5),\end{aligned}$$

and rename X,Y as x,y respectively. Then we obtain

$$\begin{aligned}\frac{dx}{dt} &= y,\\ \frac{dy}{dt} &= a_0+a_1x+a_2y+a_3x^2+a_4xy+a_5y^2+O(|x,y,\lambda|^3),\end{aligned}$$

where $a_0=\frac{1000014129}{608586272}\lambda_1-\frac{70114094160279}{21232357857536}\lambda_2$,$a_1=\frac{31623}{17444}\lambda_1-\frac{4217214931}{1217172544}\lambda_2$,$a_2=\lambda_2$,$a_3=-\frac{61275924689377761682143125312 77}{39543056910425009896585707847 68}$,$a_4=-\frac{81099024709058818735476413239 3}{40160917174650400676219859532 8}$ and $a_5=\frac{34888}{31623}$.

By setting $X = x + \frac{a_2}{a_4}$ and rewriting X as x, we have

$$\begin{aligned}\frac{dx}{dt} &= y,\\ \frac{dy}{dt} &= b_0 + b_1 x + a_3 x^2 + a_4 xy + a_5 y^2 + O(|x, y, \lambda|^3),\end{aligned}$$

where

$b_0 = a_0 + \frac{728049004708764973964744678976}{8109902470905881873547641323 93}\lambda_1\lambda_2$
$-\frac{601125570758367413052772427546167815747614227251359633272893424 2}{2868252293800468362298091248846586563534736985872087577144024089}\lambda_2^2,$
$b_1 = \frac{31623}{17444}\lambda_1 - \frac{123377373645863571094924599894873779920 1}{2467787655526099556147367223861851544 48}\lambda_2,$
and a_3,a_4 and a_5 still remain the same.

By rewriting the equation using the new time τ with $dt = (1 - a_5 x)d\tau$ and then rewriting τ as t , we obtain

$$\begin{aligned}\frac{dx}{dt} &= y\,(1 - a_5 x)\,,\\ \frac{dy}{dt} &= (1 - a_5 x)\left(b_0 + b_1 x + a_3 x^2 + a_4 xy + a_5 y^2 + O(|x, y, \lambda|^3)\right).\end{aligned}$$

Carrying out the transformation $X = x$, $Y = y(1 - a_5 x)$, and then renaming X,Y as x,y respectively, we have

$$\begin{aligned}\frac{dx}{dt} &= y,\\ \frac{dy}{dt} &= b_0 + c_1 x + c_2 x^2 + a_4 xy + O(|x, y, \lambda|^3),\end{aligned}$$

where b_0 and a_4 remain the same and $c_1 = -\frac{31623}{17444}\lambda_1$
$+\frac{705428789154491802231205198064286749 11}{308473456940762444518420902982731443 06}\lambda_2$,$c_2 = -\frac{612759246893777616821431253 1277}{395430569104250098965857078476 8}$.

By the change of variables $X = a_4^2/c_2 x$, $Y = a_4^3/c_2^2 y$, $\tau = c_2/a_4 t$, and then renaming X, Y, as x, y, t respectively, we obtain

$$\begin{aligned}\frac{dx}{dt} &= y,\\ \frac{dy}{dt} &= \tau_1 + \tau_2 x + x^2 + xy + O(|x, y, \lambda|^3),\end{aligned}$$

where $\tau_1 = b_0 a_4^4/c_2^3$, $\tau_2 = c_1 a_4^2/c_2^2$. By putting $\tau_1 = 1/4\tau_2^2$ and simplifying it, system (4.17) has a saddle-node bifurcation, and the saddle-node bifurcation curve is given by $-10.18506042\lambda_1 + 20.46853347\lambda_2 + 2.726814689\lambda_1\lambda_2 - 3.286351254\lambda_1^2 +$

$7.760920653\lambda_2^2 + O(|\lambda_1, \lambda_2|^2) = 0$. It can be easily checked that the curve is well approximated by using $\triangle = p^2/4 + q^3/27 = 0$ as shown in (4.8). By using the same parameters, the curve is represented by $-7.342993075\lambda_1 + 14.75693746\lambda_2 + 7.956010841\lambda_1\lambda_2 - 1.520873020\lambda_1^2 - 9.869429450\lambda_2^2 - 0.000000271 + O(|\lambda_1, \lambda_2|^2) = 0$.

Theorem 4.4. *At the Bogdanov point, the model* (4.4) *with* $(\beta, c, a, \mu, k) = (1/2, 2, 4, 1, 1/2)$, $A = \frac{4135897419891758227459912927}{7142893228039199764556666688}$ *and* $v = \frac{769008283214884223}{647433275455504512}$ *, in a small neighbourhood of* $(x^+, y^+) = (\frac{31623}{17444}, \frac{212322110622679}{163787945597952})$ *, has the following bifurcation :*
(i) saddle-node bifurcation and the saddle-node bifurcation curve is given by

$$-10.18506042\lambda_1 + 20.46853347\lambda_2 + 2.726814689\lambda_1\lambda_2 - 3.286351254\lambda_1^2 + 7.760920653\lambda_2^2 + O(|\lambda_1, \lambda_2|^2) = 0,$$

(ii) Hopf bifurcation and the Hopf bifurcation curve is given by

$$1.643175627\lambda_1 - 3.302228355\lambda_2 + 0.8977284342\lambda_1\lambda_2 - 2.095790430\lambda_2^2 + O(|\lambda_1, \lambda_2|^2) = 0,$$

(iii) Homoclinic bifurcation and the homoclinic bifurcation curve is given by

$$-63.65662763\lambda_1 + 127.9283342\lambda_2 - 84.52577134\lambda_1\lambda_2 + 19.71810752\lambda_1^2 + 112.5686913\lambda_2^2 + O(|\lambda_1, \lambda_2|^2) = 0.$$

Figure 4.3(a) shows the homoclinic bifurcation when $\lambda_2 = 0.02477285891$, $\lambda_1 = 0.05$ for system (4.22). Figure 4.3(b) shows a detail look for the phase portrait in Figure 4.3(a).

From the above results, we study the bifurcation curves near the origin on the (λ_1, λ_2) plane. The curves pass through the origin and there are four regions separated by these bifurcation curves. If we take $\lambda_1 \approx 0.1$, we obtain the region as in Figure 4.4.

The Jacobian matrix for system (4.22) is

$$M = \begin{pmatrix} M_{11} & -\frac{x^2}{2} \\ M_{21} & -1 \end{pmatrix},$$

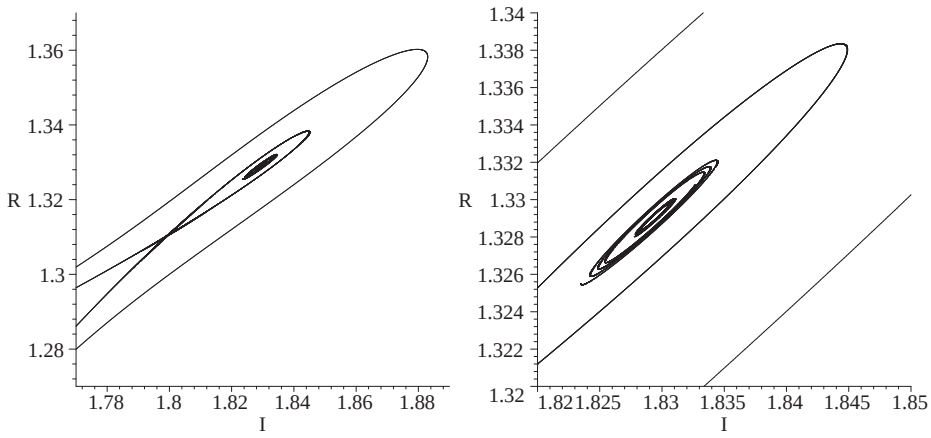

Figure 4.3: (a)Homoclinic bifurcation when $\lambda_1 = 0.05$, $\lambda_2 = 0.02477285891$ for system (4.22), (b)A detail look for the phase portrait in (a)

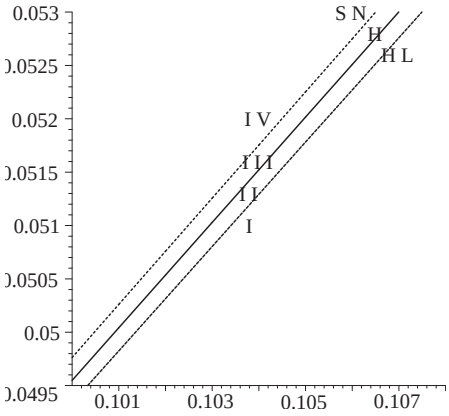

Figure 4.4: The four typical regions separated by the bifurcation curves. The horizontal axis is the λ_1-axis and the vertical axis is the λ_2-axis

Table 4.1: The classification of equilibrium points

	λ_2	E_i	$det(M)$	$tr(M)$	Q	Conclusion
I	0.0493	E_1	(-)	(+)	(+)	Unstable saddle
		E_2	(+)	(-)	(-)	Stable focus
II	0.0495	E_1	(-)	(+)	(+)	Unstable saddle
		E_2	(+)	(-)	(-)	Stable focus
III	0.0497	E_1	(-)	(+)	(+)	Unstable saddle
		E_2	(+)	(+)	(-)	Unstable focus
IV	0.05	No positive equilibrium				

$$Q = (tr(M))^2 - 4(det(M)).$$

where

$$M_{11} = -\frac{x^2}{2} + (A_0 + \lambda_1 - x - y)x - v_0 + \lambda_2 - \frac{2}{1+4x} + \frac{8x}{(1+4x)^2} - 1,$$

and

$$M_{12} = \frac{1}{2}v_0 + \frac{1}{2}\lambda_2 + \frac{1}{1+4x} - \frac{4x}{(1+4x)^2}.$$

Figure 4.4 shows the four typical regions separated by the bifurcation curves. The horizontal axis is the λ_1-axis and the vertical axis is the λ_2-axis.

If we take$\lambda_1 = 0.1$, after some simple calculation, we obtain the result as shown in Table 4.1.

When (λ_1, λ_2) lies in the region I as in Figure 4.4, there is no limit cycle or homoclinic orbit and E_2 is a stable focus. If (λ_1, λ_2) lies in the region II, there is a unique limit cycle inside the positive orbits of system (4.22) and the orbits approach E_2 as t tends to infinity. In this situation, the disease is persistent inside the cycle. When (λ_1, λ_2) lies in the region III, E_2 becomes an unstable focus and the limit cycle disappears. In this stage, at finite time, any positive orbits, except for the two equilibria E_1 and E_2 , will tend to the axis $R = 0$, i.e. the disease becomes extinct. When (λ_1, λ_2) lies in the region IV, there is no positive equilibrium and the disease will disappear. The classification of the equilibrium points can be easily checked by the eigenvalues of the Jacobian matrix,M.

4.5 Concluding remarks

In this chapter, we have proposed an epidemic model with sub-optimal immunity, nonlinear incidence rate and saturated treatment/recovery rate. The model leads to an elaborative analysis of equilibrium through a third and forth orders polynomial. By carrying out global analysis, the system in (4.4) has been shown to have rich dynamical behaviour which include Hopf bifurcation, Bogdanov-Takens bifurcation and its associated homoclinic bifurcation. We also show that when the bifurcation parameters are within certain regions, the disease will be persistent or extinct.

Chapter 5

Computation of the Domain of Attraction for the Epidemic Models using the Maximal Lyapunov Function

In this chapter, we are concerned with the estimation of the domain of attraction (DOA) for compartmental ODE epidemic models, expressed by autonomous dynamical systems. Based on the definition of the DOA and the maximal Lyapunov function, a theorem and subsequently a numerical procedure are established to determine the maximal Lyapunov function in the form of rational function and the DOA. Determination of the domain of attraction for epidemic models are very important for understanding the dynamic behaviour of the disease transmission as a function of the state of population distribution in different categories of disease state. We focus on the sub-optimal immunity model with saturated treatment rate which we study in Chapter Three and Four.

5.1 General

The computing of domain of attraction (DOA), i.e. the region where the dynamical system is asymptotically stable, is an interesting research topic in the stability analysis of nonlinear systems such as the systems for the compartmental ODE epidemic models. In other words, the mathematical analysis of epidemic models often

involves computing the asymptotic stability region for both the disease free equilibrium and the endemic equilibrium. The set of initial states whose corresponding trajectories converge to an asymptotically stable equilibrium point as time increases is known as the stability region or domain of attraction (DOA), of the equilibrium under study. If the initial state lies within the DOA, the disease will evolve towards an endemic state. On the contrary, if the initial state is outside the DOA, the system will converge to a disease free state. Therefore, it is important to study the DOA of endemic equilibrium.

Lyapunov's second method (the direct method) is generally used to analyze the stability of epidemic models. In this method, the asymptotic stability of the origin can be examined if a positive definite function whose derivative along the solutions of the system is negative definite. However, it is not only difficult to construct the Lyapunov Function, but also it is hard to guarantee the asymptotical stability of the equilibrium. Apart from that, it is known that if the Lyapunov function exists to an autonomous ODE, then it is not unique. A maximal Lyapunov function is a special Lyapunov function on S (where S denotes the DOA) which indicates the DOA for a given locally asymptotical stable equilibrium point.

Considerable work on DOA estimation and optimized DOA for epidemic dynamical models has been done. In [60], the authors had computed the DOA in epidemiological models with constant removal rates of infected individuals. An optimization approach for finding the DOA of a class of SIR models, based on the moment theory, is presented in [49]. Recently, the authors in [101] had adopted a recurrence formulae established by E. Kaslik et. al. [47] by using an R-Analytical function and the sequence of its Taylor polynomial to construct Lyapunov function, and solved the Linear Matrix Inequality (LMI) relaxations of a global optimization problem to obtain the DOA. However, all the epidemic models in the papers mentioned above are limited to relatively simple epidemic models, without taking into account nonlinear incidence rates or saturated recovery rates. In this chapter, we study the DOA for the models we proposed previously, namely the sub-optimal immunity models with nonlinear incidence rates and saturated recovery rates, by

using the maximal Lyapunov function derived by A. Vannelli and M. Vidyasagar [88]. Although the method is relatively old and complex, but the advantage is that it does not require to obtain the exact solution of the autonomous system $\dot{\mathbf{x}} = f(\mathbf{x})$. Furthermore, as the Lyapunov function candidates are rational functions, the Lyapunov function, $V(\mathbf{x}) = \frac{N(\mathbf{x})}{D(\mathbf{x})}$, tends to ∞ as $\mathbf{x}$ approaches ∂S (the boundary of DOA), i.e. $D(\mathbf{x})$ tends to 0. Hence, it will lead to a larger DOA especially if the number of terms in the Lyapunov Function candidates is increased.

Throughout the chapter, we focus on DOA for the sub-optimal immunity models. These sub-optimal immunity models will be more appropriate for the study of microparasite infections which usually occurs during childhood. After a primary infection, one may get temporary immunity (immune protection will wane over time) or partial immunity (immunity that may not fully protective). Examples of this kind of diseases include Pertussis (temporary immunity) and Influenza (partial immunity)

The remaining part of the chapter is structured as follows. In Section 5.2, we will establish a theorem which is based on [88] and an iterative procedure for the construction of the maximal Lyapunov function. In Section 5.3, two examples are given to demonstrate the validity of the procedure and we will focus on the sub-optimal immunity models which we study in Chapter Three and Four. We give a conclusion of this chapter in Section 5.4.

5.2 The maximal Lyapunov function

Consider the following system

$$\dot{\mathbf{x}} = f(\mathbf{x}), \tag{5.1}$$

where $f : \mathbb{R}^n \to \mathbb{R}^n$ is an analytical function with the following properties.

(a) $f(\mathbf{0}) = \mathbf{0}$, i.e. $\mathbf{x} = \mathbf{0}$ is an equilibrium point of system (5.1),

(b) all the eigenvalues of the Jacobian matrix at $\mathbf{x} = \mathbf{0}$, i.e. $\frac{\partial f}{\partial \mathbf{x}}(\mathbf{0})$, has negative real parts , namely $\mathbf{x} = \mathbf{0}$ is an asymptotically stable equilibrium point.

It is well known that in the Lyapunov sense, if there exists a Lyapunov function for the equilibrium point $\mathbf{x} = \mathbf{0}$ of the system (5.1), then $\mathbf{x} = \mathbf{0}$ is asymptotically stable.

Definition 5.1. *(Lyapunov Function). Let $V(\mathbf{x})$ be a continuously differentiable real-valued function defined on a domain $R(\mathbf{0}) \subseteq \mathbb{R}^n$ containing the equilibrium point $\mathbf{x} = \mathbf{0}$. The function $V(\mathbf{x})$ is a Lyapunov function of the equilibrium $\mathbf{x} = \mathbf{0}$ of the system* (5.1) *if the following conditions hold:*

(a) $V(\mathbf{x})$ is positive definite on $R(\mathbf{0})$.

(b) The time derivative of $V(\dot{\mathbf{x}})$ is negative definite on $R(\mathbf{0})$.

If $V(\mathbf{x})$ is a Lyapunov function which fulfills the conditions in the Definition 5.1, the estimation of DOA is given by the following definition.

Definition 5.2. *Given an autonomous system* (5.1) *where $\mathbf{x} \in \mathbb{R}^n$ and $f(\mathbf{0}) = \mathbf{0}$, the domain of attraction (DOA) of $\mathbf{x} = \mathbf{0}$ is $S_A = \{\mathbf{x}^0 \in \mathbb{R}^n : \lim_{t\to\infty} \mathbf{x}(t, \mathbf{x}^0) = \mathbf{0}\}$, where $\mathbf{x}(\cdot, \mathbf{x}^0)$ denotes the solution of the autonomous system corresponding to the initial condition $\mathbf{x}(0) = \mathbf{x}^0$.*

The Lyapunov function is not unique. A maximal Lyapunov function, $V(\mathbf{x})$, is a special Lyapunov function on S (where S denotes the DOA) which indicates the DOA for a given locally asymptotically stable equilibrium point.

Definition 5.3. *(Maximal Lyapunov function, [88]). A function $V_m(\mathbf{x}) : \mathbb{R}^n \to \mathbb{R}^+ \cup \{\infty\}$ is called a maximal Lyapunov function for the system* (5.1) *if*

(a) $V_m(\mathbf{0}) = 0$, $V_m(\mathbf{x}) > 0, \forall \mathbf{x} \in S, \mathbf{x} \neq 0$,

(b) $V_m(\mathbf{x}) < \infty$ if and only if $\mathbf{x} \in S$,

(c) $V_m(\mathbf{x}) \to \infty$ as $\mathbf{x} \to \partial S$ and/or $\|\mathbf{x}\| \to \infty$,

(d) $\dot{V}_m$ is well defined and negative definite over S,

where S denotes the DOA.

We have the following definition for the DOA of an asymptotically stable equilibrium point which derives from the maximal Lyapunov function.

Definition 5.4. *Suppose we can find a set $E \subseteq \mathbb{R}^n$ containing the origin in its interior and a continuous function $V(\mathbf{x}) : E \to \mathbb{R}^+$ such that*

(a) $V(\mathbf{x})$ is positive definite on E,

(b) $\dot{V}(\mathbf{x})$ is negative definite on E,

(c) $V(\mathbf{x}) \to \infty$ as $\mathbf{x} \to \partial S$ and/or as $\|\mathbf{x}\| \to \infty$,

then $E = S$ where S denotes the DOA.

From the above definition, based on the work in [88],we derive the following theorem,

Theorem 5.1. *Consider the nonlinear system of equations $\dot{\mathbf{x}} = f(\mathbf{x}) = \sum_{i=1}^{\infty} F_i(\mathbf{x})$, where $F_i(\mathbf{.})$ is a homogeneous function of degree i. Suppose that the linearized system $\dot{\mathbf{x}} = F_1(\mathbf{x}) = A\mathbf{x}$ is asymptotically stable at $\mathbf{x} = \mathbf{0}$. Let R_i, Q_i are homogeneous function of degree i, and the function R_i and Q_i satisfy the following recursive equations.*

$$(\nabla R_2)^T F_1 = -\mathbf{x}^T Q \mathbf{x}, \tag{5.2}$$

$$\begin{aligned}(\nabla R_2)^T F_{k-1} + \sum_{j=3}^{k} \left((\nabla R_j)^T + \sum_{i=1}^{j-2} (Q_i (\nabla R_{j-i})^T - (\nabla Q_i)^T R_{j-i}) \right) F_{k-j+1} \\ = -x^T Q x \left(2Q_{k-2} + \sum_{i=1}^{k-3} Q_i Q_{k-2-i} \right),\end{aligned} \tag{5.3}$$

where Q is a fixed positive definite matrix and $k \geq 3$. Then, we have the following Lyapunov Function

$$V_n(\mathbf{x}) = \frac{R_2(\mathbf{x}) + R_3(\mathbf{x}) + \ldots + R_n(\mathbf{x})}{1 + Q_1(\mathbf{x}) + \ldots + Q_{n-2}(\mathbf{x})}. \tag{5.4}$$

Proof. Rewrite

$$V_n(\mathbf{x}) = \frac{R_2(\mathbf{x}) + R_3(\mathbf{x}) + \ldots + R_n(\mathbf{x})}{1 + Q_1(\mathbf{x}) + \ldots + Q_{n-2}(\mathbf{x})} = \frac{\sum_{i=2}^{\infty} R_i(\mathbf{x})}{1 + \sum_{i=1}^{\infty} Q_i(\mathbf{x})}, \tag{5.5}$$

which satisfies condition (a) in the Definition 5.3. Differentiating (5.5) with respect to $\mathbf{x}$, we have

$$\begin{aligned}
&\dot{V}_n(\mathbf{x}) \\
&= \left(\frac{\left(1 + \sum_{i=1}^{\infty} Q_i(\mathbf{x})\right) \sum_{i=1}^{\infty} (\nabla R_i(\mathbf{x}))^T - \left(\sum_{i=1}^{\infty} (\nabla Q_i(\mathbf{x}))^T\right) \sum_{i=2}^{\infty} R_i(\mathbf{x})}{\left(1 + \sum_{i=1}^{\infty} Q_i(\mathbf{x})\right)^2} \right) \sum_{i=1}^{\infty} F_i(\mathbf{x}).
\end{aligned} \tag{5.6}$$

One of the choices to ensure that $\dot{V}_n(\mathbf{x})$ is negative definite is $\dot{V}_n(\mathbf{x}) = -\mathbf{x}^T Q \mathbf{x}$. Then from (5.6), we have

$$\begin{aligned}
&\left(\left(1 + \sum_{i=1}^{\infty} Q_i(\mathbf{x})\right) \sum_{i=1}^{\infty} (\nabla R_i(\mathbf{x}))^T - \left(\sum_{i=1}^{\infty} (\nabla Q_i(\mathbf{x}))^T\right) \sum_{i=2}^{\infty} R_i(\mathbf{x}) \right) \sum_{i=1}^{\infty} F_i(\mathbf{x}) \\
&= -\mathbf{x}^T Q \mathbf{x} \left(1 + \sum_{i=1}^{\infty} Q_i(\mathbf{x})\right)^2.
\end{aligned} \tag{5.7}$$

Equating the coefficients of the same degrees k of the two sides of (5.7), we get the following recursive relations. For $k = 2$,

$$(\nabla R_2)^T F_1 = -\mathbf{x}^T Q \mathbf{x},$$

$$\begin{aligned}
&(\nabla R_2)^T F_{k-1} + \sum_{j=3}^{k} \left((\nabla R_j)^T + \sum_{i=1}^{j-2} (Q_i (\nabla R_{j-i})^T - (\nabla Q_i)^T R_{j-i}) \right) F_{k-j+1} \\
&\quad = -\mathbf{x}^T Q \mathbf{x} \left(2Q_{k-2} + \sum_{i=1}^{k-3} Q_i Q_{k-2-i} \right),
\end{aligned}$$

where Q is a fixed positive definite matrix, and $k \geq 3$. □

Based on Theorem 5.1, the procedure for obtaining the maximal Lyapunov function and calculating the DOA is established as follows :

Consider the nonlinear system of equations $\dot{\mathbf{x}} = f(\mathbf{x}) = \sum_{i=1}^{\infty} F_i(\mathbf{x})$.

Step 1: From the linearized system, $F_1 = A\mathbf{x}$, find $P > 0$ such that $A^T P + PA = -Q$, then set

$$V_2(\mathbf{x}) = R_2 = \mathbf{x}^T P \mathbf{x},$$

where $R_2 = a_1x^2 + a_2xy + a_3y^2$. In this case, Q is a fixed positive definite matrix. Hence, one of the good choices for Q is the identity matrix.

Step 2: For $n = 3$, using (5.3) where $k = 3$, we have

$$(\nabla R_2)^T F_2 + \left((\nabla R_3)^T + Q_1(\nabla R_2)^T - (\nabla Q_1)^T R_2\right), F_1 = -\mathbf{x}^T Q \mathbf{x}(2Q_1), \tag{5.8}$$

where $R_3 = a_1x^3 + a_2x^2y + a_3xy^2 + a_4y^3$ and $Q_1 = b_1x + b_2y$. Equating the coefficients of same degree in (5.8), we will obtain a system of linear equations in terms of a_1,a_2,a_3,a_4, b_1 and b_2. The solution of these linear equations will be used as constraints in the minization problem to get $e_n(y)$ in the later step.

Step 3: For $n = 4$, using (5.3) where $k = 4$, we have

$$\begin{aligned}
&(\nabla R_2)^T F_3 + \left((\nabla R_3)^T + Q_1(\nabla R_2)^T - (\nabla Q_1)^T R_2\right) F_2 \\
&+ \left((\nabla R_4)^T + Q_1(\nabla R_3)^T - (\nabla Q_1)^T R_3 - Q_2(\nabla R_2)^T - (\nabla Q_2)^T R_2\right) F_1 \\
&= -\mathbf{x}^T Q \mathbf{x}(2Q_2 + Q_1^2),
\end{aligned} \tag{5.9}$$

where $R_4 = a_1x^4 + a_2x^3y + a_3x^2y^2 + a_4xy^3 + a_4y^4$ and $Q_2 = b_1x^2 + b_2xy + b_3y^2$. Hence, one need to solve the system of linear equations in this step as in Step 2.

Step 4: (optional) For $n = 5$, which can be extended to $n = 5$ or more when necessary

$$\begin{aligned}
&(\nabla R_2)^T F_4 + \left((\nabla R_3)^T + Q_1(\nabla R_2)^T - (\nabla Q_1)^T R_2\right) F_3 \\
&+ \left((\nabla R_4)^T + Q_1(\nabla R_3)^T - (\nabla Q_1)^T R_3 + Q_2(\nabla R_2)^T - (\nabla Q_2)^T R_2\right) F_2 \\
&+ \{(\nabla R_5)^T + Q_1(\nabla R_4)^T - (\nabla Q_1)^T R_4 + Q_2(\nabla R_3)^T - (\nabla Q_2)^T R_3 \\
&+ Q_3(\nabla R_2)^T - (\nabla Q_3)^T R_2\} F_1 \\
&= -\mathbf{x}^T Q \mathbf{x}(2Q_3 + 2Q_1Q_2),
\end{aligned} \tag{5.10}$$

where $R_5 = a_1x^5 + a_2x^4y + a_3x^3y^2 + a_4x^2y^3 + a_5xy^4 + a_6y^5$ and $Q_3 = b_1x^3 + b_2x^2y + b_3xy^2 + b_4y^3$. Hence, one needs to solve the system of linear equations in this step as in Step 2.

For each of the steps 2 to 4, one will lead to a number of choices for the value of the coefficients for R_n and Q_{n-2}. Consider

$$\dot{V}_n(\mathbf{x}) = -\mathbf{x}^T Q\mathbf{x} + \frac{e_n(y)}{\left(1 + \sum_{i=1}^{n-2} Q_i(\mathbf{x})\right)^2}, \tag{5.11}$$

where $e_n(y)$ is the squared 2-norm of the coefficients of degree greater than or equal to $n+1$ in the expression of $\dot{V}_n$. This ensures that $\dot{V}_n(\mathbf{x})$ is negative definite over a neighbourhood of the origin. To have it as similar as possible to $\dot{V}_2(\mathbf{x}) = -\mathbf{x}^T Q\mathbf{x}$, we take $e_n(y)$ as small as possible. Hence, it creates a new condition that can be formulated as a minimization problem where the constraints are obtained from the recursive relations in each of the steps above.

Step 5: Once we get $e_n(y)$ sufficiently small, say at step 3, we obtain the maximal Lyapunov function as

$$V_4(\mathbf{x}) = \frac{R_2(\mathbf{x}) + R_3(\mathbf{x}) + R_4(\mathbf{x})}{1 + Q_1(\mathbf{x}) + Q_2(\mathbf{x})}. \tag{5.12}$$

To obtain the DOA, one needs to find the largest possible value C^* when $V_4(\mathbf{x}) = C^*$ such that the interior of the resulting ellipsoid is entirely fix in the region given by $\Omega = \{\mathbf{x} : \dot{V}_n(\mathbf{x}) \leq 0\}$. In this case, one can determine C^* by solving an optimization problem.

$$\begin{aligned} V_4(\mathbf{x}) = \frac{R_2(\mathbf{x}) + R_3(\mathbf{x}) + R_4(\mathbf{x})}{1 + Q_1(\mathbf{x}) + Q_2(\mathbf{x})} &= C^*, \\ C^* &= \min V_4(\mathbf{x}), \\ \text{subject to the constraints} \dot{V}_4(\mathbf{x}) &= 0. \end{aligned} \tag{5.13}$$

Then, the set $S_A = \{\mathbf{x} : V_4(\mathbf{x}) < C^*\}$ is contained in the DOA S. Appropriate C^* also can be determined manually as suggested in [82]. In this case, one can choose the largest positive value C^* such that the sublevel set

$S_A = \{\mathbf{x} : V_4(\mathbf{x}) < C^*\}$ is contained in the region given by $\{\mathbf{x} : \dot{V}_4(\mathbf{x}) < 0\}$. Hence, we obtain the DOA in the form of S_A.

For the problem in (5.11), we perform the calculation using the Optimization packages in Maple 14 as follows:

> with(Optimization):

> objective := ;

> constraints := ;

> bounds := ;

> solution := NLPSolve(objective,constraints,bounds);

5.3 Numerical examples

Example 1: We consider the following reduced system for the sub-optimal immunity model in Chapter Three.

$$\begin{aligned} \frac{dI}{dt} &= \beta(\frac{A}{\mu} - I - R)I - vI - \frac{cI}{1+aI} - \mu I, \\ \frac{dR}{dt} &= k(vI + \frac{cI}{1+aI}) - \mu R, \end{aligned} \tag{5.14}$$

where $(A, \beta, v, c, a, \mu, k) = (19.2, 0.5, 1, 10, 0.5, 1, 0.25)$. Rewrite X and Y for I and R, and translate the equilibrium point to the origin by using $x = X + 4.549349206$ and $y = Y + 4.424023809$ .By using the numerical procedure in Sec-

tion 5.2, we have the following result

$$
\begin{aligned}
V_4(\mathbf{x}) &= \frac{R_2(\mathbf{x}) + R_3(\mathbf{x}) + R_4(\mathbf{x})}{1 + Q_1(\mathbf{x}) + Q_2(\mathbf{x})}, \\
R_2 &= 0.3022747584x^2 - 0.5489131064xy + 0.7627668376y^2, \\
R_3 &= -0.1906560890547x^3 + 0.4815774872748x^2y - 0.6165924190417xy^2 \\
&\quad + 0.4585192403196y^3, \\
R_4 &= 0.007811814325017x^4 - 0.03492153517471x^3y - 0.05336496715089x^2y^2 \\
&\quad + 0.04128157637850xy^3 - 0.06092067012745y^4, \\
Q_1 &= -0.06282269989259x + 0.1095295671604y, \\
Q_2 &= -0.2970068157810x^2 + 0.3716413661196xy - 0.4183114315558y^2,
\end{aligned}
$$

and $C^* = 0.284$. Thus,$S_A = \{x : V_4(x) < 0.284\}$ is an estimate of S for the system (5.14) when $(A, \beta, v, c, a, \mu, k) = (19.2, 0.5, 1, 10, 0.5, 1, 0.25)$. This estimate and its phase portrait are given in Figure 5.1.

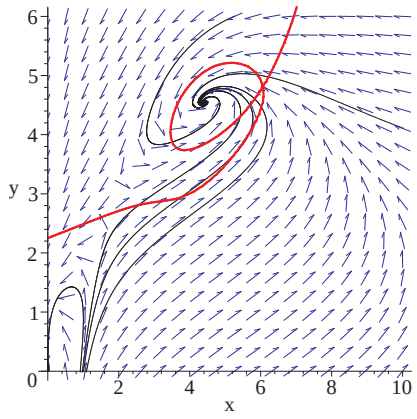

Figure 5.1: The DOA when $(A, \beta, v, c, a, \mu, k) = (19.2, 0.5, 1, 10, 0.5, 1, 0.25)$ for the model (5.14)

Consider smaller k, which means the model is more toward the SIS model. Let $(A, \beta, v, c, a, \mu, k) = (19.2, 0.5, 1, 10, 0.5, 1, 0.15)$. Rewrite X and Y for I and R, and translate the equilibrium point to the origin by using $x = X + 7.494893880$ and $y = Y + 3.492315487$. By using the numerical procedure as given in Section

5.2, we have the following result

$$V_4(\mathbf{x}) = \frac{R_2(\mathbf{x}) + R_3(\mathbf{x}) + R_4(\mathbf{x})}{1 + Q_1(\mathbf{x}) + Q_2(\mathbf{x})},$$

$$R_2 = 0.4648333096x^2 - 0.07770850670xy + 0.2509240187y^2,$$

$$R_3 = -0.0103476214205x^3 + 0.0197320143477x^2y - 0.0291440548148xy^2 + 0.0390387604663y^3,$$

$$R_4 = 0.000967433200671x^4 - 0.00183392836942x^3y - 0.000331164573248x^2y^2 - 0.00185999715174xy^3 + 0.00320488908290y^4,$$

$$Q_1 = -0.0153579530898x + 0.0484049077942y,$$

$$Q_2 = -0.0188227332305x^2 + 0.0118205411592xy - 0.00704546632408y^2,$$

and $C^* = 0.4$. Thus,$S_A = \{x : V_4(x) < 0.4\}$ is an estimate of S for the system (5.14) when $(A, \beta, v, c, a, \mu, k) = (19.2, 0.5, 1, 10, 0.5, 1, 0.15)$. This estimate and its phase portrait are given in Figure 5.2.

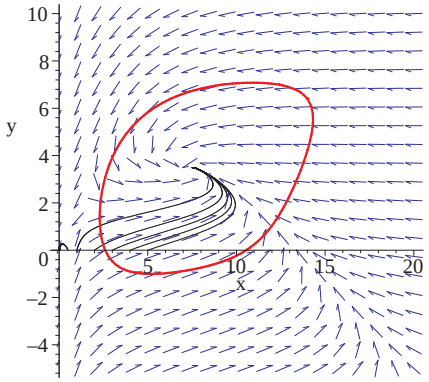

Figure 5.2: The DOA when $(A, \beta, v, c, a, \mu, k) = (19.2, 0.5, 1, 10, 0.5, 1, 0.15)$ for the model (5.14)

Example 2: We consider the following reduced system for the sub-optimal model in Chapter Four

$$\begin{aligned} \frac{dI}{dt} &= \beta(\frac{A}{\mu} - I - R)I^2 - vI - \frac{cI}{1+aI} - \mu I, \\ \frac{dR}{dt} &= k(vI + \frac{cI}{1+aI}) - \mu R. \end{aligned} \tag{5.15}$$

For this example, we consider the nonlinear incidence rate βSI^2. According to [58], one of the reasons to consider the nonlinear incidence rate, $\beta S^p I^q$, is to rep-

resent heterogeneous mixing. Take $(A, \beta, v, c, a, \mu, k) = (6, 0.5, 1.27, 2, 4, 1, 0.5)$. Rewrite X and Y for I and R, and translate the equilibrium point to the origin by using $x = X + 2.046474176$ and $y = Y + 1.522295468$. By using the numerical procedure in Section 5.2, we have the following result ,

$$
\begin{aligned}
V_5(\mathbf{x}) &= \frac{R_2(\mathbf{x}) + R_3(\mathbf{x}) + R_4(\mathbf{x}) + R_5(\mathbf{x})}{1 + Q_1(\mathbf{x}) + Q_2(\mathbf{x}) + Q_3(\mathbf{x})}, \\
R_2 &= 0.3762413699x^2 - 0.8519913644xy + 0.9464782714y^2, \\
R_3 &= -0.126181821512x^3 + 0.173193705351x^2y + 0.570250486120xy^2 \\
&\quad + 0.0690548525960y^3, \\
R_4 &= -0.105927461038x^4 + 0.356193079263x^3y - 0.518348042762x^2y^2 \\
&\quad + 0.765173017380xy^3 - 0.518220094340y^4, \\
R_5 &= -0.0125629412858x^5 - 0.278448382561x^4y + 0.788615459079x^3y^2 \\
&\quad - 1.85902079923x^2y^3 + 1.38491789447xy^4 - 1.09987599898y^5, \\
Q_1 &= 3.17302544294x - 4.63120513014y, \\
Q_2 &= -2.99749941519x^2 + 1.05587625048xy - 5.75817945157y^2, \\
Q_3 &= 1.48286905974x^3 - 11.5305874770x^2y + 10.9212904075xy^2 \\
&\quad - 11.6184182953y^3,
\end{aligned}
$$

and $C^* = 0.0002$. Thus,$S_A = \{x : V_5(x) < 0.0002\}$ is an estimate of S for the system (5.15) when $(A, \beta, v, c, a, \mu, k) = (6, 0.5, 1.27, 2, 4, 1, 0.5)$. This estimate and its phase portrait are given in Figure 5.3.

Here, we study the effect of the value a for the DOA. Let $(A, \beta, v, c, a, \mu, k) = (6, 0.5, 1.27, 2, 40, 1, 0.5)$ where the value of a is ten fold of the previous calculation. Rewrite X and Y for I and R, and translate the equilibrium point to the origin by using $x = X + 2.561174171$ and $y = Y + 1.651103929$. By using the numerical

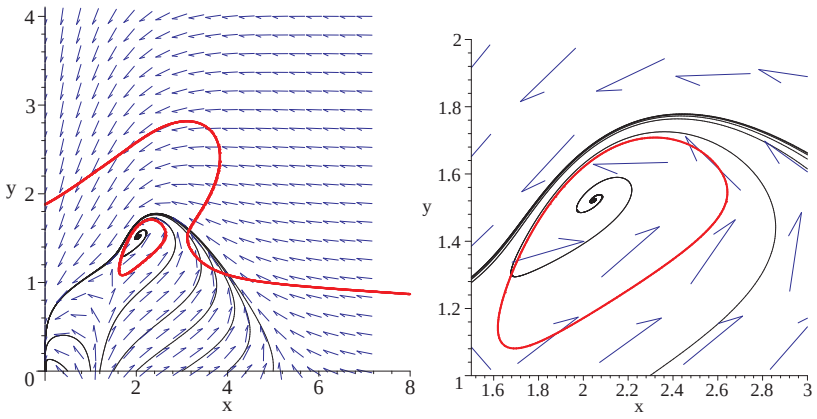

Figure 5.3: (a)The DOA when $(A, \beta, v, c, a, \mu, k) = (6, 0.5, 1.27, 2, 4, 1, 0.5)$ for the model (5.15), (b)A detail look for the phase portrait in (a)

procedure as in Section 5.2, we have the following results,

$$V_5(\mathbf{x}) = \frac{R_2(\mathbf{x}) + R_3(\mathbf{x}) + R_4(\mathbf{x}) + R_5(\mathbf{x})}{1 + Q_1(\mathbf{x}) + Q_2(\mathbf{x}) + Q_3(\mathbf{x})},$$

$$R_2 = 0.003578383960x^2 - 0.004275326810xy + 0.01184451697y^2,$$

$$R_3 = -0.00143947851169x^3 + 0.00137383162785x^2y + 0.00388197475475xy^2 + 0.000772525621974y^3,$$

$$R_4 = 0.000276577054304x^4 - 0.000324162597520x^3y - 0.000204916381848x^2y^2 + 0.000107606340123xy^3 - 0.0000451580448282y^4,$$

$$R_5 = 0.0000533208751600x^5 - 0.0000416190488560x^4y + 0.0000894460564105x^3y^2 - 0.000374374857674x^2y^3 - 0.000460737371773xy^4 - 0.000456992688012y^5,$$

$$Q_1 = 0.706952511101x - 0.577082269086y,$$

$$Q_2 = -0.104792704737x^2 - 0.246689057581xy - 0.104749443691y^2,$$

$$Q_3 = -0.00279459100782x^3 - 0.00352025797534x^2y - 0.00315115011888xy^2 - 0.0581955306735y^3,$$

and $C^* = 0.043$. Thus, $S_A = \{x : V_4(x) < 0.043\}$ is an estimate of the DOA for the system (5.15) when $(A, \beta, v, c, a, \mu, k) = (6, 0.5, 1.27, 2, 40, 1, 0.5)$. This estimate and its phase portrait are given in Figure 5.4.

By applying the same procedure, we calculate the DOA when $a = 12$, and we obtain the DOA as in Figure 5.5. It is clear that with $(A, \beta, v, c, a, \mu, k) =$

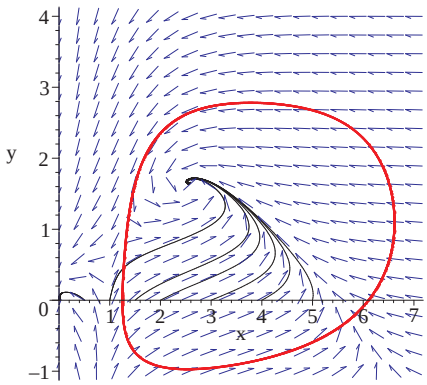

Figure 5.4: The DOA when $a = 40$ for the model given by (5.15)

$(6, 0.5, 1.27, 2, 12, 1, 0.5)$, increasing the value of a will increase the DOA for the this sub-optimal immunity model in (5.15).

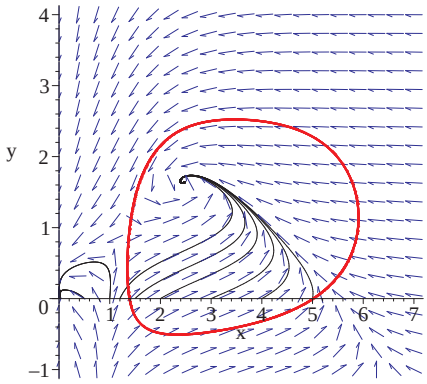

Figure 5.5: The DOA when $a = 12$ for model (5.15)

5.4 Concluding remarks

In this chapter, we deal with the problem of estimating the domain of attraction (DOA) for the sub-optimal immunity epidemic model. We establish a procedure to determine the maximal Lyapunov function in the form of rational functions and compute the domain of attraction for the epidemic models. Determination of the DOA is important in order to understand the dynamic behaviour of the transmission of diseases as a function of the initial population distribution. In our first example, we show that for certain values of the model parameters, larger k value (i.e. the

model is more toward the SIR model) leads to a smaller DOA. In our second example, we show that within certain values of the model parameters, decreasing the a value will yield a smaller DOA.

Chapter 6

Analytical Solution for the Spread of Epidemic Diseases in Community Clustered Networks

In this chapter, we present a bond percolation model for community clustered networks with an arbitrarily specified joint degree distribution. Our model is based on the probability generating function (PGF) method for multitype networks, but incorporate the free-excess degree distribution, which makes it applicable for clustered networks. In the context of contact network epidemiology, our model serves as a special case of community clustered networks which are more appropriate for modelling the disease transmission in community networks with clustering effects. Beyond the percolation threshold, we are able to obtain the probability that a randomly chosen community-i node leads to the giant component. In the context of contact network epidemiology, the probability refers to the probability that an individual in a community will be affected from the infective disease. Besides that, we also establish method to calculate the size of the giant component and the average small-component size (excluding the giant component). When the clustering effect is taken into account through the free-excess degree distribution, the model shows that the clustering effect will decrease the size of the giant component. In short, our model enables one to carry out numerical calculations to simulate the disease transmission in community networks with different community structure effects and clustering effects.

6.1 General

It has long been recognized that two of the key features of social networks are community structure and clustering effect. The former one emphasizes that the links are dense in a community but sparse between communities, while the later one refers to the relative number of triangles in a network. For the community structure effect, the links between communities will make the network less heterogeneous and result in larger epidemic prevalence in the exponential degree distribution networks [98]. For other types of degree distributions such as the power-law degree distribution, the authors of [95] developed an algorithm to obtain a social network model with a multiple-community structure with adjustable clustering coefficients and adjustable degree of community. They showed that the heterogeneous network is less efficient than the homogeneous network in spreading of epidemic. Different to [95], we study the bond percolation model of community clustered networks with an arbitrary joint degree distribution by using the probability generating function (PGF) formalism.

In a series of papers [62, 69, 74], M.E.J. Newman used probability generating function for random graphs with arbitrary distributions of vertex degree. With the mathematics of generating functions, the author managed to calculate exactly some statistical properties of such graphs in the limit of large numbers of vertices, including the mean of component size and the giant component. Using the combination of mapping to percolation models and the generating function method, Newman established the analytic expressions for the size of epidemic outbreaks and the mean degree of individuals affected in an epidemic.

Following Newman's work, many researchers consider more features to improve the percolation models based on the generating function method. For example, in [89], the author developed a model to represent heterogeneous populations so as to study the mixing patterns. Apart from that there are many other models, including percolation models for random directed networks [13], models for two competing disease spreading over the same network at the same time [46].

There are some other models which use other mathematical tools or simulation to predict the transmission of infectious diseases in social networks. One of the areas which get considerable attention from researchers is clustered networks. In [13], the author introduced a class of random clustered networks and showed that the clustered networks had small component sizes and bigger epidemic threshold in comparison to the same preferential mixing unclustered networks.

In this chapter, we present a bond percolation model of community clustered networks with an arbitrary joint degree distribution (i.e. the degree distribution can be specified arbitrarily). Our model is based on the probability generating function (PGF) formalism for multitype networks introduced by Antoine Allard et.al. [3]. Their multitype network model is the extension of the PGF formalism which investigated by M.E.J. Newman. In addition, we incorporate the free-excess degree distribution, which was introduced in [10] to make it applicable for clustered networks. We focus on complex networks with arbitrary joint degree distribution. In the context of contact network epidemiology, our model serves as a special case of community clustered networks which are more suitable for modelling the disease transmission in community networks with the clustering effect. For certain clustering coefficient and beyond the percolation threshold, we obtain the probability that a randomly chosen community-i node leads to the giant component. In the context of contact network epidemiology, this probability refers to the probability that an individual in a community is affected by the infectious disease. In addition, we derive formulae to calculate the size (i.e. fraction) of the giant component and the average small-component size (excluding the giant component) in the community structure network. If the disease transmission rate between each pair of communities is the same in both direction, the size of the giant component in each community-i is equivalent to the probability that a randomly chosen community-i node leads to the giant component. When the clustering effect is taken into account through the free-excess degree distribution , our model shows that the clustering effect leads to the reduce of the size of the giant component.

The rest of the chapter is organized as follows. In Section 6.2, we discuss

some assumptions to be used in our community clustered networks. In Section 6.3, we present the PGF formamlism for the proposed community clustered networks. In Sections 6.4 and 6.5, we focus on the calculation of the outbreak size distribution and the percolation threshold, followed by numerical simulations in Section 6.6. Some conclusions are given in Section 6.7.

6.2 Community clustered networks

We discuss a model with 2 communities which can be generalized to multi-communities. Throughout the discussion, we assume that

(a) there exist realizable degree sequences which lead to simple graphs (i.e. networks) with no self loop,

(b) the inter-community edges will be redistributed according to the three ways as explained in Section 6.3.1.3,

(c) the isolated nodes in each community will remain isolated,

(d) the highest degree is 8 for model 1, and 6 for model 2,

(e) it is possible for two nodes connecting to a mutual node to connect themselves, thereby forming a triangle. It is represented by the clustering coefficient, C,

(f) One link is counted as two edges.

Assumption (b) implies that power-law distribution will not be applied here. In other words, nodes with higher degree do not necessarily have more inter-community edges. In assumption (c), we assign some isolated nodes to each community. In a finite time, the isolated nodes remain isolated when we randomly connect the inter-community edges to the nodes with different degrees in each community. This can serve as a check point for our computer program when we use it to find distribution for the size of small component. There is no contact for every isolated node, namely there is no transmissibility of disease. Hence, the number of isolated nodes in each

community will remain the same. Apart from that, we set the highest degree at 8. In other words, the network is not a highly right skewed network and does not have super infection nodes.

In some of our analysis, we will further make the following assumptions.

(a) One of the communities has a low vaccination rate and thus a higher rate of disease transmissibility among their members.

(b) The rate of disease transmissibility along the inter-community edges is low, as sick individuals will travel less.

For our models, we assume that the exact number of nodes having degree k, denoted by n_k, is known. Hence, we can write the exact generating function for the probability distribution in the form of a finite polynomial.

6.3 Formalism

We now present a formalism that describes the bond percolation model of community networks. It is based on the probability generating function (PGF) formalism for multitype networks introduced by Antoine Allard et.al. [3]. Their multitype network model is the extension of the well-known PGF formalism introduced by MEJ Newman in a series of papers [62, 69, 74].

6.3.1 Degree distribution

First, we assume that the arbitrarily specified degree distribution will produce a realizable degree sequence. Let $P_{i=1}(k_1, k_2, ..., k_M)$ and $P_{i=2}(k_1, k_2, ..., k_M)$ be the probability degree distributions that a randomly chosen community-i node is connected to k_1 nodes, k_2 nodes, k_3 nodes and so on. Since we deal with community structure networks, among the edges of a node, there are some edges which may connect to nodes in other community.

For the sake of simplicity, we discuss the PGF formalism for the model with two communities. In this case, we have two ways to represent the degree distribution.

(a) Number of nodes in each community.

(b) Number of nodes connecting community-i node to community-j.

6.3.1.1 Degree distribution for number of nodes in each community

In the first way, we need to have degree distribution for the number of nodes in each community. As an example, we consider the following degree distribution,
$p_1(\mathbf{k}) = \{10, 10, 10, 45, 205, 135, 85\}$,
$p_2(\mathbf{k}) = \{10, 10, 5, 85, 110, 185, 135\}$,
where $\mathbf{k} = \{k_l\}_{l=0}^{6} = \{l\}_{l=0}^{6} = (0, 1, 2, 3, 4, 5, 6)$ and the value of $p_i(k_l)$ is the number of nodes with degree l in the community-i. In the above example, there are 10 nodes with 0 degree (i.e. isolated nodes) in community 1, 10 nodes with 1 degree, 10 nodes with 2 degree, 45 nodes with 3 degree and so on in community 1. Apart from that, we can get the information about the number of edges in each community, namely
$(10 \times 0) + (10 \times 1) + (10 \times 2) + (45 \times 3) + (205 \times 4) + (135 \times 5) + (85 \times 6) = 2170$
$(10 \times 0) + (10 \times 1) + (5 \times 2) + (85 \times 3) + (110 \times 4) + (185 \times 5) + (135 \times 6) = 2450$
There are 2170 and 2450 edges respectively in communities 1 and 2 in our model example and the total edges is 4620. Note that here one link is counted as two edges.

If we divide $P_i(\mathbf{k})$ by N_i where N_i denotes the number of nodes in community-i, we will have a probability degree distribution.
$P_1(\mathbf{k}) = \frac{1}{500}\{10, 10, 10, 45, 205, 135, 85\}$,
$P_2(\mathbf{k}) = \frac{1}{540}\{10, 10, 5, 85, 110, 185, 135\}$,
Without considering the rate of transmissibility of diseases, we have the following PGF

$$G_i(\mathbf{x}) = \sum_{k=0}^{\infty} P_i(k) \prod_{l=1}^{M} x_l^{k_l}, \tag{6.1}$$

where $i = 1, 2$; M denotes the number of communities which is 2 in this example and $x_l^{k_l}$ denotes node in community-l with degree k_l.

6.3.1.2 Degree distribution for number of nodes connecting community-i to community-j

The second way of representing the degree distribution is by considering the number of nodes connecting community-i to community-j. We have the following degree distribution:

$p_1(\mathbf{k}_1) = \{10, 10, 20, 80, 200, 120, 60\}$,

$p_1(\mathbf{k}_2) = \{420, 50, 20, 10, 0, 0, 0\}$,

$p_2(\mathbf{k}_1) = \{460, 50, 20, 10, 0, 0, 0\}$,

$p_2(\mathbf{k}_2) = \{10, 10, 10, 100, 140, 180, 90\}$,

where $p_i(\mathbf{k}_i)$ is as defined before, while $p_i(\mathbf{k}_{jl})$ denotes the number of nodes in community-i with $\mathbf{k}_{jl}$ edges linking to community j in which $\mathbf{k}_{jl} = l$ for $l = 0, 1, 2, \ldots$.

For the above example, $p_1(\mathbf{k}_1)$ shows that there are 10 nodes with 0 degree (i.e. isolated nodes) in community 1, 10 nodes with 1 degree, 20 nodes with 2 degree, 80 nodes with 3 degree and so on in community 1; The data of $p_1(\mathbf{k}_2)$ shows that there are 420 nodes in community 1 with no edge linking to community 2, 50 nodes in community 1 having one edge linking to community 2, 20 nodes in community 1 having two edges linking to community 2 and so on. The same will apply to the nodes in community 2. We can also get the information about the number of inter-community edges and the number of intra-community edges in each community. The number of intra-community edge is calculated as follows.

- Community 1:$(10\times0)+(10\times1)+(20\times2)+(80\times3)+(200\times4)+(120\times5)+(60\times6)+(420\times0)+(50\times1)+(20\times2)+(10\times3)+(0\times4)+(0\times5)+(0\times6) = 2170$,

- Community 2:$(460\times0)+(50\times1)+(20\times2)+(10\times3)+(0\times4)+(0\times5)+(0\times6)+(10\times0)+(10\times1)+(10\times2)+(100\times3)+(140\times4)+(180\times5)+(90\times6) = 2450$.

For the two communities model, $\mathbf{k} = \mathbf{k}_1 + \mathbf{k}_2$, hence the total edges must be the same as that by the first way mentioned in Section 6.3.1.1 (where it is 4620). The

number of inter-community edges for communities 1 and 2 must be the same, which is calculated as follows,

- Community 1: $(420 \times 0) + (50 \times 1) + (20 \times 2) + (10 \times 3) + (0 \times 4) + (0 \times 5) + (0 \times 6) = 120$,
- Community 2: $(460 \times 0) + (50 \times 1) + (20 \times 2) + (10 \times 3) + (0 \times 4) + (0 \times 5) + (0 \times 6) = 120$.

We can rewrite the degree distribution above as probability degree distribution as follows

$P_1(\mathbf{k}_1) = \frac{1}{500}\{10, 10, 20, 80, 200, 120, 60\}$,
$P_1(\mathbf{k}_2) = \frac{1}{500}\{420, 50, 20, 10, 0, 0, 0\}$,
$P_2(\mathbf{k}_1) = \frac{1}{540}\{460, 50, 20, 10, 0, 0, 0\}$,
$P_2(\mathbf{k}_2) = \frac{1}{540}\{10, 10, 10, 100, 140, 180, 90\}$,

Without considering the rate of transmissibility of diseases, let G_{ij} be the generating function where the subscript ij represents the chosen node in community-i connected to node in community-j, and let $P_i(k_{uv})$ be the probability that a randomly chosen community-i node with u edges connects to the nodes in community v. Then, we have the following PGF

$$\begin{aligned}
G_{11}(\mathbf{x}) &= P_1(k_{01}) + P_1(k_{11})x_1 + P_1(k_{21})x_1^2 + P_1(k_{31})x_1^3 + P_1(k_{41})x_1^4 \\
&\quad + P_1(k_{51})x_1^5 + P_1(k_{61})x_1^6 \\
&= \frac{10}{500} + \frac{10}{500}x_1 + \frac{20}{500}x_1^2 + \frac{80}{500}x_1^3 + \frac{200}{500}x_1^4 + \frac{120}{500}x_1^5 + \frac{60}{500}x_1^6, \\
G_{12}(\mathbf{x}) &= P_1(k_{02}) + P_1(k_{12})x_2 + P_1(k_{22})x_2^2 + P_1(k_{32})x_2^3 + P_1(k_{42})x_2^4 \\
&\quad + P_1(k_{52})x_2^5 + P_1(k_{62})x_2^6 \\
&= \frac{420}{500} + \frac{50}{500}x_2 + \frac{20}{500}x_2^2 + \frac{10}{500}x_2^3, \\
G_{21}(\mathbf{x}) &= P_2(k_{01}) + P_2(k_{11})x_1 + P_2(k_{21})x_1^2 + P_2(k_{31})x_1^3 + P_2(k_{41})x_1^4 \\
&\quad + P_2(k_{51})x_1^5 + P_2(k_{61})x_1^6 \\
&= \frac{460}{540} + \frac{50}{540}x_1 + \frac{20}{540}x_1^2 + \frac{10}{540}x_1^3,
\end{aligned}$$

$$G_{22}(\mathbf{x}) = P_2(k_{02}) + P_2(k_{12})x_2 + P_2(k_{22})x_2^2 + P_2(k_{32})x_2^3 + P_2(k_{42})x_2^4$$
$$+ P_2(k_{52})x_2^5 + P_2(k_{62})x_2^6$$
$$= \frac{10}{540} + \frac{10}{540}x_2 + \frac{10}{540}x_2^2 + \frac{100}{540}x_2^3 + \frac{140}{540}x_2^4 + \frac{180}{540}x_2^5 + \frac{90}{540}x_2^6,$$

and $\frac{dG_{11}(\mathbf{1})}{dx_1} = \frac{41}{10}$, $\frac{dG_{12}(\mathbf{1})}{dx_2} = \frac{6}{25}$, $\frac{dG_{21}(\mathbf{1})}{dx_1} = \frac{2}{9}$, $\frac{dG_{22}(\mathbf{1})}{dx_2} = \frac{233}{54}$,

where $\frac{dG_{ij}(\mathbf{1})}{d\mathbf{x}}$ denotes the average number of edges connecting nodes in community-i to nodes in community-j, and we represent it as z_{ij}.

Definition 6.1. *Let z_{ij} be the average number of edges connecting nodes in community-i to nodes in community-j, then*

$$z_{ij} = \sum_{k_1=0}^{\infty} \cdots \sum_{k_M=0}^{\infty} k_j P_i(k_1, k_2, \cdots, k_M) \equiv \sum_{k=0}^{\infty} k_j P_i(\boldsymbol{k}).$$

In matrix form, for two communities, we have

$$\mathbf{z} = \begin{pmatrix} z_{11} & z_{12} \\ z_{21} & z_{22} \end{pmatrix}.$$

Let the community-i nodes occupy a fraction w_i of the network, and define

$$\mathbf{w} = \begin{pmatrix} w_1 & 0 \\ 0 & w_2 \end{pmatrix}.$$

We have $\mathbf{wz} = (\mathbf{wz})^T$,$tr(\mathbf{w}) = 1$ and $w_1 = \frac{z_{21}}{z_{12}+z_{21}}$,$w_2 = \frac{z_{12}}{z_{12}+z_{21}}$. In our model, we have $w_1 = \frac{z_{21}}{z_{12}+z_{21}} = \frac{2/9}{6/25+2/9} = \frac{25}{52}$,$w_2 = \frac{z_{12}}{z_{12}+z_{21}} = \frac{6/25}{6/25+2/9} = \frac{27}{52}$. This means that we have $\frac{25}{52}$ fraction of nodes in community 1 and $\frac{27}{52}$ fraction of nodes in community 2. The followings two ways can be used to determine how strong the community structure is:

(a) Let Z be the number of edges connecting nodes in community-i to nodes in community-j, then we will have $Z = \frac{n}{2m}z$ where n is the number of nodes and m is the number of edges. Hence we can use the information to obtain the modularity which is given by $Q = Tr(\mathbf{Z}) - \|\mathbf{Z}^2\|$.

(b) In [59], the degree of community σ , is given by $\sigma = p/q$ where p is the probability for the event that there exist links within the community and q is the probability for the event that there exist links between the communities. In this work, we redefine $\sigma = \frac{tr(z)}{\sum_{i\neq j} z_{ij}}$ where $\sigma >> 1$ implies strong community. It is easy to show that our model has $Q = 0.446$ or $\sigma = 18.02$.

6.3.1.3 Algorithm for redistributing the intercommunity links

There are a few possible ways to consider the distribution of intercommunity links including

(i) the links are randomly attached to the nodes in each community.

(ii) the links are equally attached to the nodes in each community.

(iii) the links are preferably attached to the nodes with higher degrees in each community.

Consider the two communities model, where the links are equally attached to the nodes in each community. Let n be the number of intercommunity links, and let M be the highest degree of the nodes in the respectively community. If $n \bmod M = R$, then we have $YM + R = n$. Assuming that P and Q are the number of nodes with degree 1 and degree M, then we have

(a) The number of nodes with degree $M + 1$ is $Y + R$.

(b) The number of nodes with degree M is $P - R$ where P is the number of nodes with degree 1.

(c) The number of nodes with degree 1 is $Q - Y$ where Q is the number of nodes with degree M.

6.3.2 The occupied degree distribution

For the discussion of the PGF formalism involving rate of disease transmission, we should consider the occupied degree distribution. For the two communities model, we define a bond occupation probability matrix as

$$\mathbf{T} = \begin{pmatrix} T_{11} & T_{12} \\ T_{21} & T_{22} \end{pmatrix}.$$

Definition 6.2. *The probability that a randomly chosen degree-**k** node has $\tilde{\mathbf{k}}$ occupied edges is*

$$P_i(\tilde{\mathbf{k}}|\mathbf{k}) = \prod_{i=1}^{M} \binom{k_l}{\tilde{k}_l} (T_{il})^{\tilde{k}_l} (1 - T_{il})^{k_l - \tilde{k}_l}.$$

The occupied degree distribution, $\tilde{P}_i(\tilde{\mathbf{k}})$, is

$$\tilde{P}_i(\tilde{\mathbf{k}}) = \sum_{k=\tilde{k}}^{\infty} P_i(\tilde{\mathbf{k}}|\mathbf{k}) P_i(\mathbf{k}) = \sum_{k=\tilde{k}}^{\infty} P_i(\mathbf{k}) \prod_{l=1}^{M} \binom{k_l}{\tilde{k}_l} (T_{il})^{\tilde{k}_l} (1-T_{il})^{k_l - \tilde{k}_l}.$$

Hence, the PGF is

$$G_i(\mathbf{x};\mathbf{T}) = \sum_{\tilde{k}=0}^{\infty} \tilde{P}_i(\tilde{\mathbf{k}}) \prod_{l=1}^{M} x_l^{\tilde{k}_l} = \sum_{k=0}^{\infty} P_i(\mathbf{k}) \prod_{l=1}^{M} \sum_{\tilde{k}_l=0}^{k_l} \binom{k_l}{\tilde{k}_l} (x_l T_{il})^{\tilde{k}_l} (1-T_{il})^{k_l - \tilde{k}_l},$$

$$G_i(\mathbf{x};\mathbf{T}) = \sum_{k=0}^{\infty} P_i(\mathbf{k}) \prod_{l=1}^{M} \left[1-(x_l-1)T_{il}\right]^{k_l},$$

where $G_i(1;\mathbf{T}) = 1$ if $P_i(\mathbf{k})$ is properly normalized.

From Definition 6.2, we can get the average occupied degree connecting nodes in community-i to nodes in community-j as $\tilde{z}_{ij} = \frac{\partial G_i(\mathbf{1};\mathbf{T})}{\partial x_j} = T_{ij} \sum_{k=0}^{\infty} k_j P_i(\mathbf{k}) = T_{ij} z_{ij}$. For example,$\frac{\partial G_1(\mathbf{x};\mathbf{T})}{\partial x_2}|_{x_1=1,x_2=1}$ gives $T_{12} z_{12}$.

For two communities (we assume each node has at most degree 6 as for in model 2) , we have the following generating functions when we consider the rate of transmissibility,

$$\begin{aligned}
G_1(\mathbf{x};\mathbf{T}) = {} & P_1(k_0) \left[\frac{L_{11}}{L_1}(1-(x_1-1)T_{11})\frac{L_{12}}{L_1}(1-(x_2-1)T_{12})\right]^{k_0} \\
& + P_1(k_1) \left[\frac{L_{11}}{L_1}(1-(x_1-1)T_{11})\frac{L_{12}}{L_1}(1-(x_2-1)T_{12})\right]^{k_1} \\
& + P_1(k_2) \left[\frac{L_{11}}{L_1}(1-(x_1-1)T_{11})\frac{L_{12}}{L_1}(1-(x_2-1)T_{12})\right]^{k_2} \\
& + P_1(k_3) \left[\frac{L_{11}}{L_1}(1-(x_1-1)T_{11})\frac{L_{12}}{L_1}(1-(x_2-1)T_{12})\right]^{k_3} \\
& + P_1(k_4) \left[\frac{L_{11}}{L_1}(1-(x_1-1)T_{11})\frac{L_{12}}{L_1}(1-(x_2-1)T_{12})\right]^{k_4} \\
& + P_1(k_5) \left[\frac{L_{11}}{L_1}(1-(x_1-1)T_{11})\frac{L_{12}}{L_1}(1-(x_2-1)T_{12})\right]^{k_5} \\
& + P_1(k_6) \left[\frac{L_{11}}{L_1}(1-(x_1-1)T_{11})\frac{L_{12}}{L_1}(1-(x_2-1)T_{12})\right]^{k_6},
\end{aligned}$$

$$
\begin{aligned}
G_2(\mathbf{x};\mathbf{T}) = {} & P_2(k_0)\left[\frac{L_{21}}{L_2}(1-(x_1-1)T_{21})\frac{L_{22}}{L_2}(1-(x_2-1)T_{22})\right]^{k_0} \\
& + P_2(k_1)\left[\frac{L_{21}}{L_2}(1-(x_1-1)T_{21})\frac{L_{22}}{L_2}(1-(x_2-1)T_{22})\right]^{k_1} \\
& + P_2(k_2)\left[\frac{L_{21}}{L_2}(1-(x_1-1)T_{21})\frac{L_{22}}{L_2}(1-(x_2-1)T_{22})\right]^{k_2} \\
& + P_2(k_3)\left[\frac{L_{21}}{L_2}(1-(x_1-1)T_{21})\frac{L_{22}}{L_2}(1-(x_2-1)T_{22})\right]^{k_3} \\
& + P_2(k_4)\left[\frac{L_{21}}{L_2}(1-(x_1-1)T_{21})\frac{L_{22}}{L_2}(1-(x_2-1)T_{22})\right]^{k_4} \\
& + P_2(k_5)\left[\frac{L_{21}}{L_2}(1-(x_1-1)T_{21})\frac{L_{22}}{L_2}(1-(x_2-1)T_{22})\right]^{k_5} \\
& + P_2(k_6)\left[\frac{L_{21}}{L_2}(1-(x_1-1)T_{21})\frac{L_{22}}{L_2}(1-(x_2-1)T_{22})\right]^{k_6},
\end{aligned}
$$

where L_1 and L_2 are the total number of edges in communities 1 and 2 respectively and L_{ij} is the total number of edges which link nodes in community-i to nodes in community-j. Note that $G_1(\mathbf{1};\mathbf{T}) = 1$ and $G_2(\mathbf{1};\mathbf{T}) = 1$.

6.3.3 The occupied excess degree distribution

Definition 6.3. *The occupied excess degree distribution is given by*

$$
\tilde{Q}_{ij}(\tilde{\mathbf{k}}) = \frac{1}{z_{ji}}\sum_{k=\tilde{k}}^{\infty}(k_i+1)P_j(\mathbf{k}+\boldsymbol{\delta}_i)\prod_{l=1}^{M}\binom{k_l}{\tilde{k}_l}(T_{jl})^{\tilde{k}_l}(1-T_{jl})^{k_l-\tilde{k}_l}.
$$

Hence, the PGF is given by

$$
F_{ij}(\mathbf{x};\mathbf{T}) = \sum_{\tilde{k}=0}^{\infty}\tilde{Q}_{ij}(\tilde{\mathbf{k}})\prod_{l=1}^{M}x_l^{\tilde{k}_l} = \frac{1}{z_{ji}}\sum_{k=0}^{\infty}k_iP_j(\mathbf{k})\prod_{l=1}^{M}\left[1-(x_l-1)T_{jl}\right]^{k_l-\delta_{il}},
$$

where the ij represents the chosen edges connecting community-i and community-j.

For our 2-community model, we can obtain $F_{ij}(\mathbf{x};\mathbf{T})$ by

$$
F_{ij}(\mathbf{x};\mathbf{T}) = \frac{1}{\tilde{z}_{ji}}\frac{\partial G_j(\mathbf{x};\mathbf{T})}{\partial x_i}. \tag{6.2}
$$

For two communities networks with nodes of at most degree 6, using (6.2),

after some algebra work, we have

$$\begin{aligned}F_{11}(x_1,x_2;\mathbf{T}) &= p_0 + p_{01}x_2 + p_{02}x_2^2 + p_{03}x_2^3 + p_{04}x_2^4 + p_{05}x_2^5 \\ &+ p_{10}x_1 + p_{11}x_1x_2 + p_{12}x_1x_2^2 + p_{13}x_1x_2^3 + p_{14}x_1x_2^4 \\ &+ p_{20}x_1^2 + p_{21}x_1^2x_2 + p_{22}x_1^2x_2^2 + p_{23}x_1^2x_2^3 + p_{30}x_1^3 + p_{31}x_1^3x_2 + p_{32}x_1^3x_2^2 \\ &+ p_{40}x_1^4 + p_{41}x_1^4x_2 + p_{50}x_1^5,\end{aligned}$$

where the parameter p_{uv} denotes the probability that a node with excess degree v is reached by following a randomly chosen edge with excess degree u. Similar formulae can be established for $F_{12}(x_1,x_2;\mathbf{T})$, $F_{21}(x_1,x_2;\mathbf{T})$ and $F_{22}(x_1,x_2;\mathbf{T})$ where the parameter p in the above equation will be replaced by q,r,and s respectively.

6.3.4 The occupied free-excess degree distribution

In order to consider the clustered network ($C > 0$), we apply the free-excess degree distribution concept introduced in [12]. Analogously to the excess degree, we follow one of the edges of node v_0 to reach a neighbour v_1 having degree $d(v_1) = i + 1$(i is the excess degree). We are interested in calculating the probability that the node has k neighbours that are not connected back to v_0 (via a triangle), which is given by $\binom{i}{k}(1-C)^k C^{i-k}$

Definition 6.4. *The free excess degree distribution is given by*

$$\begin{aligned}G_c(x) &= \sum_{k=0}^{\infty} e_k x^k = \sum_{k=0}^{\infty}\sum_{i=0}^{\infty} q_i \binom{i}{k} C^i \left(\frac{1-C}{C}\right)^k x^k \\ &= \sum_{i=0}^{\infty} q_i C^i \sum_{k=0}^{\infty}\binom{i}{k}\left(\frac{1-C}{C}x\right)^k = \sum_{i=0}^{\infty} q_i C^i \left(1+\frac{1-C}{C}x\right)^i \\ &= \sum_{i=0}^{\infty} q_i \left[C+(1-C)x\right]^i = G_1\left[C+(1-C)x\right], \\ e_k &= \sum_{i=0}^{\infty} q_i \binom{i}{k}(1-C)^k C^{i-k} = \sum_{i=0}^{\infty} q_i \binom{i}{k} C^i \left(\frac{1-C}{C}\right)^k.\end{aligned}$$

By Definition 6.4, we use the generating function associated with the occupied excess degree distribution as given in Definition 6.3. Thus, we have the following relationship

$$Fc_{ij}(\mathbf{x};\mathbf{T}) = F_{ij}(C+(1-C)\mathbf{x};\mathbf{T}). \tag{6.3}$$

6.4 Outbreak size distribution

In this section, we discuss an iteration method to obtain the probability that a randomly chosen community-i node leads to the giant component. Although the discussion applies to the model without considering the clustering coefficient C, for the model with clustering coefficient C, we will have Fc_{ij} instead of F_{ij} as in (6.3).

Let $H_{ij}(\mathbf{x};\mathbf{T})$ be the generating function for the size distribution of the component reached by following an $i \to j$ edge.

$$H_{ij}(\mathbf{x};\mathbf{T}) = x_j F_{ij}(\mathbf{H}_j(\mathbf{x};\mathbf{T});\mathbf{T}). \tag{6.4}$$

The solution for the equation (6.4) can be found by seeking the stable fixed point of the mapping

$$H_{ij}^{(n)}(\mathbf{x};\mathbf{T}) = x_j F_{ij}(\mathbf{H}_{jM}^{(n-1)}(\mathbf{x};\mathbf{T});\mathbf{T}), \tag{6.5}$$

as $i = 1 \ldots M$ and $n \to \infty$ for initial conditions $H_{ij}^{0}(\mathbf{x};\mathbf{T}) = x_j$. The equation says that when we follow an $i \to j$ edge, we find at least one node at the other end (the factor of x_1 , x_2 on the RHS), plus some other clusters of nodes (each represented by $H_{ij}(\mathbf{x};\mathbf{T})$) which are reachable by following other edges attached to that node. The number of the clusters is distributed according to the coefficients of x_1 , x_2 in $F_{ij}(\mathbf{x};\mathbf{T}) = \frac{1}{\tilde{z}_{ij}} \frac{\partial G_j(\mathbf{x};\mathbf{T})}{\partial x_i}$, and hence the appearance of $F_{ij}(\mathbf{x};\mathbf{T})$.

For our model, using (6.4) and (6.5), we have the following iteration process

$$\begin{aligned}
H_{11}^{(n)}(x_1,x_2;\mathbf{T}) &= x_1 F_{11}(H_{11}^{(n-1)}(x_1,x_2;\mathbf{T}), H_{12}^{(n-1)}(x_1,x_2;\mathbf{T});\mathbf{T}) \\
H_{12}^{(n)}(x_1,x_2;\mathbf{T}) &= x_2 F_{12}(H_{21}^{(n-1)}(x_1,x_2;\mathbf{T}), H_{22}^{(n-1)}(x_1,x_2;\mathbf{T});\mathbf{T}) \\
H_{21}^{(n)}(x_1,x_2;\mathbf{T}) &= x_1 F_{21}(H_{11}^{(n-1)}(x_1,x_2;\mathbf{T}), H_{12}^{(n-1)}(x_1,x_2;\mathbf{T});\mathbf{T}) \\
H_{22}^{(n)}(x_1,x_2;\mathbf{T}) &= x_2 F_{22}(H_{21}^{(n-1)}(x_1,x_2;\mathbf{T}), H_{22}^{(n-1)}(x_1,x_2;\mathbf{T});\mathbf{T}),
\end{aligned}$$

where the initial condition is given by $H_{11}^{(0)}(x_1,x_2;\mathbf{T}) = p_0 x_1$, $H_{12}^{(0)}(x_1,x_2;\mathbf{T}) = q_0 x_2$, $H_{21}^{(0)}(x_1,x_2;\mathbf{T}) = r_0 x_1$, and $H_{22}^{(0)}(x_1,x_2;\mathbf{T}) = s_0 x_2$. For the first iteration in

our model 2, we have

$$
\begin{aligned}
&H_{11}^{(1)}(x_1, x_2; \mathbf{T}) \\
&= x_1 F_{11}(H_{11}^{(0)}(x_1, x_2; \mathbf{T}), H_{12}^{(0)}(x_1, x_2; \mathbf{T}); \mathbf{T}) \\
&= x_1 F_{11}(p_0 x_1, q_0 x_2; \mathbf{T}) \\
&= x_1 \{p_0 + p_{01}(q_0 x_2) + p_{02}(q_0 x_2)^2 + p_{03}(q_0 x_2)^3 + p_{04}(q_0 x_2)^4 + p_{05}(q_0 x_2)^5 \\
&+ p_{10}(p_0 x_1) + p_{11}(p_0 x_1)(q_0 x_2) + p_{12}(p_0 x_1)(q_0 x_2)^2 + p_{13}(p_0 x_1)(q_0 x_2)^3 \\
&+ p_{14}(p_0 x_1)(q_0 x_2)^4 + p_{20}(p_0 x_1)^2 + p_{21}(p_0 x_1)^2(q_0 x_2) + p_{22}(p_0 x_1)^2(q_0 x_2)^2 \\
&+ p_{23}(p_0 x_1)^2(q_0 x_2)^3 + p_{30}(p_0 x_1)^3 + p_{31}(p_0 x_1)^3(q_0 x_2) + p_{32}(p_0 x_1)^3(q_0 x_2)^2 \\
&+ p_{40}(p_0 x_1)^4 + p_{41}(p_0 x_1)^4(q_0 x_2) + p_{50}(p_0 x_1)^5\} \\
&= p_0 x_1 + p_{01} q_0 x_1 x_2 + p_{10} p_0 x_1^2 + O(x_1, x_2)^3.
\end{aligned}
$$

Similarly, we have

$$
\begin{aligned}
H_{11}^{(1)}(x_1, x_2; \mathbf{T}) &= q_0 x_2 + q_{10} r_0 x_1 x_2 + q_{01} s_0 x_2^2 + O(x_1, x_2)^3 \\
H_{21}^{(1)}(x_1, x_2; \mathbf{T}) &= r_0 x_1 + r_{01} q_0 x_1 x_2 + r_{10} p_0 x_1^2 + O(x_1, x_2)^3 \\
H_{22}^{(1)}(x_1, x_2; \mathbf{T}) &= s_0 x_2 + s_{10} r_0 x_1 x_2 + s_{01} s_0 x_2^2 + O(x_1, x_2)^3.
\end{aligned}
$$

For the second iteration, we have

$$
\begin{aligned}
&H_{11}^{(2)}(x_1, x_2; \mathbf{T}) \\
&= x_1 F_{11}(H_{11}^{(1)}(x_1, x_2; \mathbf{T}), H_{12}^{(1)}(x_1, x_2; \mathbf{T}); \mathbf{T}) \\
&= x_1 F_{11}(p_0 x_1 + p_{01} q_0 x_1 x_2 + p_{10} p_0 x_1^2, q_0 x_2 + q_{10} r_0 x_1 x_2 + q_{01} s_0 x_2^2; \mathbf{T}).
\end{aligned}
$$

After some algebra work, we obtain

$$
\begin{aligned}
H_{11}^{(2)}(x_1, x_2; \mathbf{T}) = p_0 x_1 &+ p_{01} q_0 x_1 x_2 + p_{10} p_0 x_1^2 + (p_{01} q_{01} s_0 + p_{02} q_0^2) x_1 x_2^2 \\
&+ (p_{10} p_{01} q_0^2 + p_{11} p_0 q_0 + p_{01} q_{10} r_0) x_1^2 x_2 + (p_{10}^2 p_0 + p_{20} p_0^2) x_1^3 \\
&+ O(x_1, x_2)^4.
\end{aligned}
$$

Similarly, we have

$$
\begin{aligned}
H_{12}^{(2)}(x_1, x_2; \mathbf{T}) &= x_2 F_{12}(H_{21}^{(1)}(x_1, x_2; \mathbf{T}), H_{22}^{(1)}(x_1, x_2; \mathbf{T}); \mathbf{T}) \\
H_{21}^{(2)}(x_1, x_2; \mathbf{T}) &= x_1 F_{21}(H_{11}^{(1)}(x_1, x_2; \mathbf{T}), H_{12}^{(1)}(x_1, x_2; \mathbf{T}); \mathbf{T}) \\
H_{22}^{(2)}(x_1, x_2; \mathbf{T}) &= x_2 F_{22}(H_{21}^{(1)}(x_1, x_2; \mathbf{T}), H_{22}^{(1)}(x_1, x_2; \mathbf{T}); \mathbf{T}),
\end{aligned}
$$

and the iteration process continues until obtaining $H_{ij}^{(4)}(x_1, x_2; \mathbf{T})$ for model 2. Denoting $K_i(\mathbf{x}; \mathbf{T})$ as the generating function for the size distribution of the whole component, we have the

$$K_i(\mathbf{x}; \mathbf{T}) = x_i G_i(\mathbf{H}_i(\mathbf{x}; \mathbf{T}); \mathbf{T}), \tag{6.6}$$

now we can have the following definition.

Definition 6.5. *Let $K_i(\mathbf{x}; \mathbf{T})$ be the total number of nodes reachable from a randomly chosen vertex in community-i , i.e. the size of the component to which such a node belongs, is generated by*

$$K_i(\mathbf{x}; \mathbf{T}) = x_i G_i(\mathbf{H}_i(\mathbf{x}; \mathbf{T}); \mathbf{T}).$$

Since type-i nodes occupy a fraction w_i of the network, the size distribution of the component reached from a randomly chosen node is generated by

$$K(\mathbf{x}; \mathbf{T}) = \sum_{i=1}^{M} w_i K_i(\mathbf{x}; \mathbf{T}) = \sum_{i=1}^{M} w_i x_i G_i(\mathbf{H}_i(\mathbf{x}; \mathbf{T}); \mathbf{T}). \tag{6.7}$$

For our 2-communities model, using (6.7), we have

$$K_1(x_1, x_2; \mathbf{T}) = x_1 G_1(H_{11}^{(n)}(x_1, x_2; \mathbf{T}), H_{12}^{(n)}(x_1, x_2; \mathbf{T}); \mathbf{T}),$$
$$K_2(x_1, x_2; \mathbf{T}) = x_2 G_2(H_{21}^{(n)}(x_1, x_2; \mathbf{T}), H_{22}^{(n)}(x_1, x_2; \mathbf{T}); \mathbf{T}).$$

Above the percolation threshold, we will find the giant component. Hence the probability that a randomly chosen community-i node leads to the giant component is

$$P_i = 1 - K_i(\mathbf{1}; \mathbf{T}). \tag{6.8}$$

According to [3], for symmentric transmissibility $\mathbf{T} = \mathbf{T}^T$, the size of the giant component, S, is equal to P.

6.5 Percolation threshold

Using the moment property of the PGF, the average number of community-i nodes in the small component reached from a randomly chosen node is obtained by differentiating $H_{ij}^{(n)}(\mathbf{x}; \mathbf{T})$ with respect to x_i . Hence, the average number of community-i

nodes in the small component, $\langle s_i \rangle$,is given by

$$\langle s_i \rangle = w_i + \sum_{l=1}^{M} w_l \sum_{j=1}^{M} \tilde{z}_{lj} \alpha_{lj}^{(i)}, \tag{6.9}$$

where $\alpha_{lj}^{(i)} \equiv \frac{\partial H_{lj}(\mathbf{x};\mathbf{T})}{\partial x_i}|_{\mathbf{x}=\mathbf{1}}$. $\alpha_{lj}^{(i)}$ is well approximated by the solution of $\alpha_{lj}^{(i)} = \delta_{ij} + \sum_{n=1}^{M} T_{jn} \beta_{lj}^{(n)} \alpha_{jn}^{(i)}$ and where the average excess degree is given by $B_{lj}^{(n)} = \frac{1}{T_{jn}} \frac{\partial F_{lj}(\mathbf{x};\mathbf{T})}{\partial x_n}|_{\mathbf{x}=\mathbf{1}}$.

Define $[A_{ij}]_{\mu v} = T_{ij} \beta_{\mu v}^{(j)} \delta_{iv}$. If there are only two communities, A can be obtained by

$$A = \begin{pmatrix} T_{11}\beta_{11}^{(1)} & 0 & T_{12}\beta_{11}^{(2)} & 0 \\ T_{11}\beta_{21}^{(1)} & 0 & T_{12}\beta_{21}^{(2)} & 0 \\ 0 & T_{21}\beta_{12}^{(1)} & 0 & T_{22}\beta_{12}^{(2)} \\ 0 & T_{21}\beta_{22}^{(1)} & 0 & T_{22}\beta_{22}^{(2)} \end{pmatrix}, \tag{6.10}$$

with the average of s given by

$$\langle s \rangle = \sum_{i=1}^{M} \langle s_i \rangle \propto \frac{1}{det(I - A)}. \tag{6.11}$$

Hence, the phase transition occurs when $det(I - A) = 0$.

6.6 Numerical simulations

Model 1 :We summarize the model 1 as follows : There are two communities (i.e. $M = 2$) with probability degree distribution: $P_i(k_1, k_2) \equiv P_i(\mathbf{k})$ as shown below :

$P_1(\mathbf{k}_1) = \frac{1}{5700}\{10, 2910, 2120, 480, 10, 70, 60, 20, 20\}$

$P_1(\mathbf{k}_2) = \frac{1}{5700}\{5300, 300, 100, 0, 0, 0, 0, 0, 0\}$

$P_2(\mathbf{k}_1) = \frac{1}{5900}\{5500, 300, 100, 0, 0, 0, 0, 0, 0\}$

$P_2(\mathbf{k}_2) = \frac{1}{5900}\{10, 3010, 2210, 450, 40, 80, 60, 20, 20\}$.

After redistributing the intercommunity links, we obtain

$P_1(\mathbf{k}) = \frac{1}{5700}\{10, 2910 - Y, 2120, 480, 10, 70, 60, 20, 20 - Y, Y + R\}$

$P_2(\mathbf{k}) = \frac{1}{5900}\{10, 3010 - Y, 2210, 450, 40, 80, 60, 20, 20 - Y, Y + R\}$,

where $Y = 62$ and $R = 4$. We have average edges $z = \begin{pmatrix} \frac{482}{285} & \frac{5}{57} \\ \frac{5}{59} & \frac{100}{59} \end{pmatrix}$ and the distribution of nodes among the communities is $w = \begin{pmatrix} \frac{57}{116} & 0 \\ 0 & \frac{59}{116} \end{pmatrix}$. More details are shown in Table 6.1.

Table 6.1: Number of edges in each community in model 1

	Community 1	Community 2
Total nodes	5700	5900
Total inter community edges	9640	10000
Total intra community edges	500	500

The modularity for this model is $\sigma = 19.634$ or $Q = 0.451$. First, we study the effect of transmissibility rate. In this case, we have the same transmissibility rate for all the links, namely either inter or intra community edges within the same community have the same transmissibility rate. For example, $T = 0.1$ means that $T = \begin{pmatrix} 0.1 & 0.1 \\ 0.1 & 0.1 \end{pmatrix}$. Figure 6.1 shows the probability, P, that a randomly chosen community-i node (community 1 + community 2) leads to the giant component versus transmissibility rate, T, and the fraction of the giant component , in communities 1 and 2 ($S1$ and $S2$) versus transmissibility rate, T.

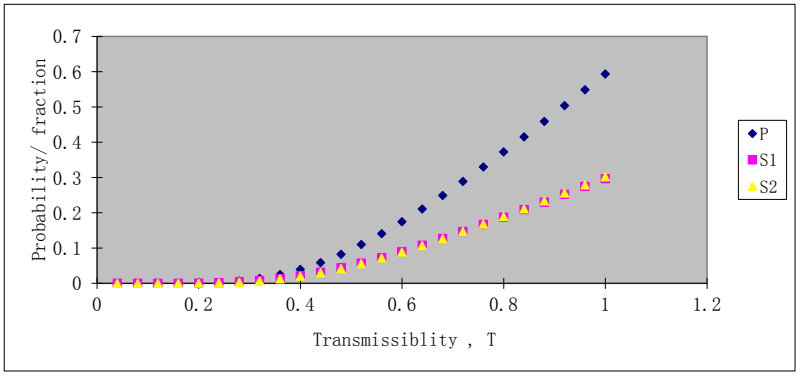

Figure 6.1: Diagram showing the probability, P, that a randomly chosen community-i node leads to the giant component versus tranmissiblity rate, T, for model 1. The diagram also shows the fraction of giant component in communities 1 and 2 ($S1$ and $S2$) versus tranmissiblity rate, T. The epidemic threshold in this example is 0.599.

Secondly, we study the effect of clustering in this mode. Using (6.11), the epidemic threshold is determined to be 0.599. Above the epidemic threshold, clustering will reduce the probability that a randomly chosen community-i node leads

to the giant component. In this case we use $T = \begin{pmatrix} 0.64 & 0.64 \\ 0.64 & 0.64 \end{pmatrix}$. Figure 6.2 shows the probabability, P, that a randomly chosen community-i node (community 1 + community 2) leads to the giant component versus clustering coefficient, C. The fraction of the giant component in communities 1 and 2 ($S1$ and $S2$) versus the clustering coefficient,C, is also show in Figure 6.2.

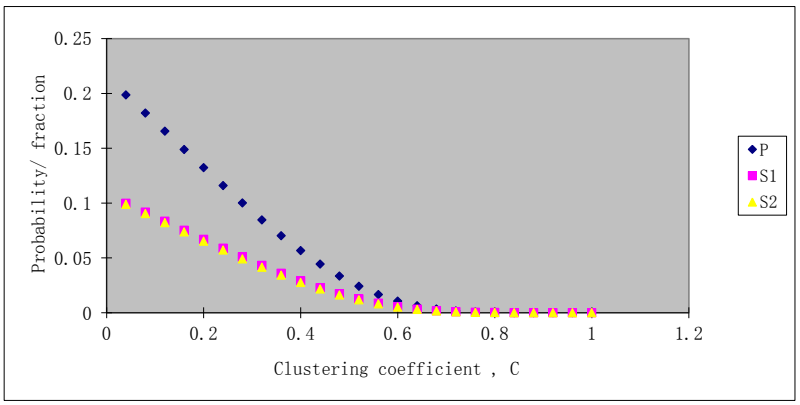

Figure 6.2: The probability, P, that a randomly chosen community-i node leads to the giant component versus clustering coefficients, C, for model 1 when $T = 0.64$. $S1$ and $S2$ are the fraction of giant component in communities 1 and 2 respectively

Thirdly, by using (6.9), we determine the average number of community-i nodes in the small component, $\langle s_i \rangle$, reached from a randomly chosen node for different clustering coefficient, C, in Figure 6.3.

Model 2 :We summarize the model 2 as follows : There are two communities (i.e. $M = 2$) with probability degree distribution: $P_i(k_1, k_2) \equiv P_i(\mathbf{k})$ as shown below :

$P_1(\mathbf{k}_1) = \frac{1}{500}\{10, 10, 20, 80, 200, 120, 60\}$

$P_1(\mathbf{k}_2) = \frac{1}{500}\{420, 50, 20, 10, 0, 0, 0\}$

$P_2(\mathbf{k}_1) = \frac{1}{540}\{460, 50, 20, 10, 0, 0, 0\}$

$P_2(\mathbf{k}_2) = \frac{1}{540}\{10, 10, 10, 100, 140, 180, 90\}$.

For analysis, we distribute the inter-community edges randomly across nodes in each community, we get

$P_1(\mathbf{k}) = \frac{1}{500}\{10, 10, 10, 45, 205, 135, 85\}$

$P_2(\mathbf{k}) = \frac{1}{540}\{10, 10, 5, 85, 110, 185, 135\}$.

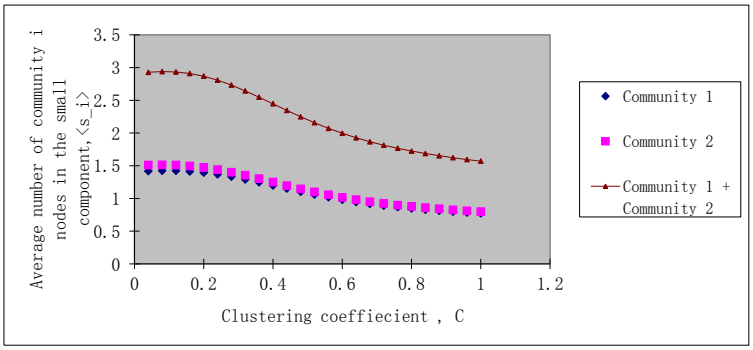

Figure 6.3: A diagram showing the average number of community-i nodes in the small component, $\langle s_i \rangle$, reached from a randomly chosen node for different clustering coefficient, C, for model 1 when $T = 0.64$.

Table 6.2: Number of edges in each community in model 2

	Community 1	Community 2
Total nodes	500	540
Total inter community edges	2050	2330
Total intra community edges	120	120

We have average edges $z = \begin{pmatrix} \frac{41}{10} & \frac{6}{25} \\ \frac{2}{9} & \frac{233}{54} \end{pmatrix}$ and the distribution of nodes among the community is $w = \begin{pmatrix} \frac{25}{52} & 0 \\ 0 & \frac{27}{52} \end{pmatrix}$. More details are shown in Table 6.2.

The modularity for this model is $\sigma = 18.20$ or $Q = 0.446$. For transmissibility, $T = \begin{pmatrix} \frac{3}{10} & \frac{1}{5} \\ \frac{1}{5} & \frac{6r}{10} \end{pmatrix}$. Using (6.11), we obtain $det(I - A) = -0.0464 + 0.1002r$. When $r = 0.4633$, phase transition occurs, namely the giant component first appears. If $r = 1$, that is when $T = \begin{pmatrix} \frac{3}{10} & \frac{1}{5} \\ \frac{1}{5} & \frac{6}{10} \end{pmatrix}$, there exists a giant component. (i.e. outbreak of disease)

Figure 6.4 shows the probabability, P, that a randomly chosen community-i node (community 1 + community 2) leads to the giant component versus the clustering coefficient,C. The fraction of the giant component in communities 1 and 2 ($S1$ and $S2$) versus the clustering coefficient,C, is also shown.

Figure 6.5 shows the average number of community-i nodes in the small com-

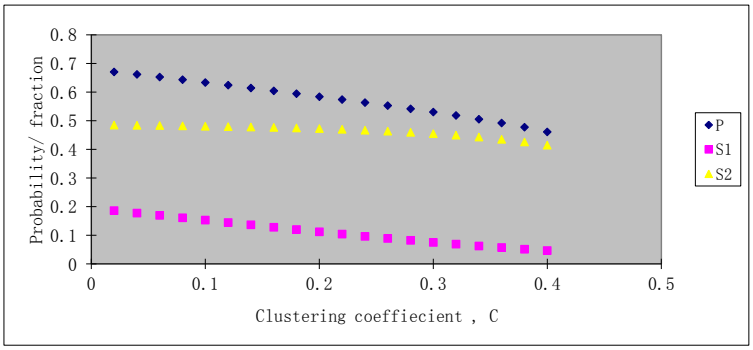

Figure 6.4: The probability,P, that a randomly chosen community-i node leads to the giant component versus the clustering coefficient,C, for model 2. $S1$ and $S2$ are the fraction of the giant component in communities 1 and 2 respectively.

ponent, $\langle s_i \rangle$, by using (6.11), reached from a randomly chosen node for different values of the clustering coefficient, C.

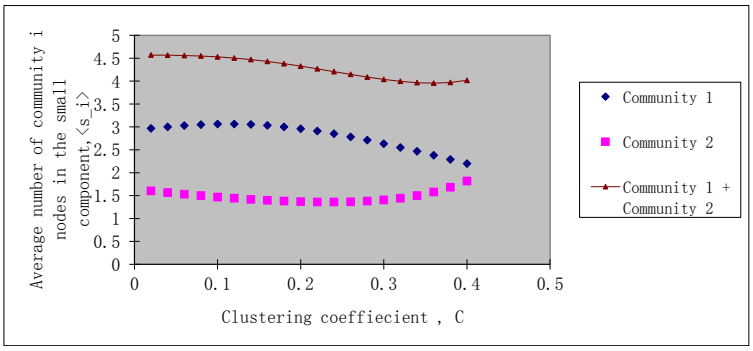

Figure 6.5: A diagram showing the average number of community-i nodes in the small component, $\langle s_i \rangle$, reached from a randomly chosen node for different clustering coefficient, C, for model 2.

6.7 Concluding remarks

In this chapter, we focus on complex networks with an arbitrary joint degree distribution. We study community clustered networks which are more suitable for modelling the disease transmission in community networks with clustering effects.

With certain clustering coefficient and beyond the percolation threshold, we obtain the probability that a randomly chosen community-i node leads to the giant component. In the context of contact network epidemiology, this probability refers to the probability that an individual in a community is affected by the infectious disease. We have also derived formulae to calculate the size of the giant component and the average small-component size (excluding the giant component). Taking into account the clustering effect through the free-excess degree distribution, the model shows that the clustering effect will decrease the size of the giant component.

Chapter 7

Conclusions and Further Work

7.1 Summary of research

This study mainly consists of three parts. In the first part of the research, we focus on the bifurcation analysis of an epidemic model with sub-optimal immunity and saturated treatment/recovery rate. Furthermore, nonlinear incidence rate is also taken into account as an additional feature in Chapter Four. Due to the combination of the nonlinearities in both incidence rate and recovery rate, the analysis of equilibrium involves a cubic polynomial instead of a quadratic polynomial as in previous works. Different from classical models, sub-optimal immunity models are more realistic to model the microparasite infectious diseases such as Pertussis and Influenza A. By carrying out the bifurcation analysis of the models, we have shown that for certain values of the model parameters, Hopf bifurcation, Bogdanov-Takens bifurcation and its associated homoclinic bifurcation occur. By studying the bifurcation curves, one can predict the persistence or extinction of diseases. The main results and key findings in this part are summarized below.

(a) For the sub-optimal immunity epidemic model with saturated treatment/recovery rate, the reduced system is given by

$$\begin{aligned} \frac{dI}{dt} &= \beta(\frac{A}{\mu} - I - R)I - vI - \frac{cI}{1+aI} - \mu I, \\ \frac{dR}{dt} &= k(vI + \frac{cI}{1+aI}) - \mu R, \end{aligned} \tag{7.1}$$

where $k = 1 - \sigma$.

(i) The system (7.1) has a unique positive equilibrium $E^*(I^*, R^*)$ under any of the three conditions in Lemma 3.1 and the type of unique positive equilibrium is shown in Lemma 3.2.

(ii) With $(\beta, v, c, a, \mu, k) = (1/2, 8, 8, 3, 1, 1/4)$, the system (7.1) has an unstable periodic orbit as A increases from $51/2$.

(iii) With $(\beta, v, a, \mu, k) = (1/2, 2, 1/2, 1, 1/4)$,$c = 8$ and $A = 19$, the system (7.1) has the bifurcation as shown in Theorem 3.2.

(b) For the sub-optimal immunity epidemic model with nonlinear incidence rate and saturated treatment/recovery rate, the reduced system is given by

$$\begin{aligned} \frac{dI}{dt} &= \beta(\frac{A}{\mu} - I - R)I^2 - vI - \frac{cI}{1+aI} - \mu I, \\ \frac{dR}{dt} &= k(vI + \frac{cI}{1+aI}) - \mu R, \end{aligned} \tag{7.2}$$

where $k = 1 - \sigma$.

(i) The system (7.2) has no, or unique, or two positive equilibria under the conditions given in Lemma 4.1.

(ii) With $(\beta, v, c, a, \mu, k, A) = (1/2, 1.27, 2, 4, 1, 1/2, 6)$, the system (7.2) has an stable orbit as A increases from 27.07373142.

(iii) With $(\beta, c, a, \mu, k) = (1/2, 2, 4, 1, 1/2)$ and setting A and v to the values according to Theorem 4.3, the system (7.2) has the bifurcation as shown in Theorem 4.4.

The second part of the research focuses on the problem of estimating the domain of attraction (DOA) for compartmental ODE epidemic models, which is one of the examples of autonomous dynamical systems. In this contribution, we have established a procedure to determine the maximal Lyapunov function in the form of rational functions. The estimation of the domain of attraction for epidemic models are very important for understanding the dynamic behaviour of the transmission of diseases as a function of the initial population distribution. For the calculation of

the DOA, we focus on the sub-optimal immunity models which we study in the first part. The main results and key findings in this part are summarized below.

(i) We have established a numerical procedure based on the work in [88] to determine the maximal Lyapunov function in the form of rational functions in Section 5.2.

(ii) We have showed that for certain values of the parameters, larger k value (i.e. the model is more toward the SIR model) leads to a smaller DOA in the model (7.1) and smaller a value will yield a smaller DOA in the model (7.2).

In the third part of the research, we establish a bond percolation model of community clustered networks with an arbitrary joint degree distribution (i.e. the degree distribution is arbitrarily specified). Our model is based on the PGF formalism for multitype networks and incorporates the free-excess degree distribution, which makes it applicable for clustered networks. In the context of contact network epidemiology, our model serves as a special case of community clustered networks which are more suitable for modelling the disease transmission in community networks with clustering effects. Beyond the percolation threshold, we obtain the probability that a randomly chosen community-i node leads to the giant component. In the context of the contact network epidemiology, the probability refers to the probablity that an individual in a community is affected by the infectious disease. Besides that, we derive formulae to calculate the size of the giant component and the average small-component size (excluding the giant component). When taking into account the clustering effect through the free-excess degree distribution, our model shows that the clustering effect will lead to a significant decrease in the size of the giant component. In short, our model enables one to carry out numerical calculations to study the disease transmission in community networks taking into account the community structure effects and clustering effects. The main results and key findings in this part are summarized below.

(i) We presented a bond percolation model for community clustered networks with an arbitrary joint degree distribution. The model is based on the proba-

bility generating function (PGF) method for multitype networks, but incorporates the free-excess degree distribution, which makes it applicable for clustered community structure networks.

(ii) The clustering effect will lead to a significant decrease in the size of the giant component as shown in Figure 6.2 and 6.4.

(iii) Our model enables us to numerically simulate the disease transmission in community networks taking into account the community structure effects and clustering effects.

7.2 Future works

A potential extension of our sub-optimal immunity models in Chapter Three and Four is to include the effect of delay in the models. Many researches have been carried out to consider the delay in epidemic models [1, 30, 67, 96]. There are various biological reasons for the introduction of time delays in epidemic models, including results from assumptions on the sojourn time in a certain epidemiological state, e.g., the infective state [5]. Apart from that, the effect of vaccination in the susceptible individuals in which the vaccine waning time is arbitrarily distributed also contribute to the time delay in epidemic models. Besides, to study the effect of delay in our sub-optimal immunity models with saturated recovered rate or /and nonlinear incidence rate, it is important to compare the sub-optimal immunity models with parameter, σ, as in (7.3) and the time delay as in the equation (7.4).

$$\frac{dR}{dt} = (1-\sigma)T(I) - \mu R, \tag{7.3}$$

$$\frac{dR}{dt} = e^{-\mu_1 \tau}T(t-\tau) - \mu R, \tag{7.4}$$

where $\tau \geq 0$ is a constant representing the time delay which may represent the length of the immunity period, and μ_1 addresses that an individual has survived natural death in a recovery pool before becoming susceptible.

Another possible extension for our sub-optimal immunity model is developing a discrete-type epidemic model which can be obtained from the forward Euler

method. Discrete models are more appropriate to directly fit the statistical data concerning infectious diseases with a latent period, such as malaria [29]. One of the possible studies in this field is to study the conditions of existence for the Neimark-Sacker bifurcation which are derived from the bifurcation theory in [97].

In Chapter Five, we use Maple 14-Optimization package for solving the optimization problem which is needed in the process of estimating the DOA. Researches in this computation area is still an important area and many computation techniques have been developed such as the sum-of-square optimization [45] and the global optimization approach [61].

For our bond percolation model using PGF in Chapter Six, we dealt with two communities only. Hence, the obvious extension is to apply the method to the cases with more than two communities. Better algorithms for the redistribution of community links are also deserve to have more specific study. Apart from that, we have to consider the overlapping community as introduced in [48] and its effect in disease transmission in our Chapter Six model.

Apart from that, in the PhD study, we also attempt to relate the bialternate matrix product method with the concept of subresultant by John Guckenheimer et.al. [40] for computing the Hopf bifurcations, which we briefly explained in Section 2.2.1. It is important to know if periodic solutions exist in the compartmental epidemic models. We have obtained an additional condition which is applicable for dimension up to 3. Further work can be done to solve this problem for higher dimension.

Bibliography

[1] M. Agarwal and V. Verma. Stability and Hopf bifurcation analysis of a SIRS epidemic model with time delay. *International Journal of Applied Mathematics and Mechanics*, 8(9):1–16, 2012.

[2] M. E. Alexander and S. M. Moghadas. Periodicity in an epidemic model with a generalized nonlinear incidence. *Mathematical Biosciences*, 189(1):75–96, 2004.

[3] Antoine Allard, Pierre-Andre Noël, and Louis J. Dube. Heterogeneous bond percolation on multitype networks with an application to epidemic dynamics. *Physical Review E*, 79(3):036113, 2009.

[4] Roy M. Anderson and Robert M. May. *Infectious diseases of humans: dynamics and control*. Oxford University Press, 1992.

[5] J. Arino and P. van den Driessche. *Delay differential equations and applications*, chapter 13 time delays in epidemic models : modeling and numerical considerations, pages 539–578. Springer, 2006.

[6] Albert-László Barabási and Réka Albert. Emergence of scaling in random networks. *Science*, 286(5439):509–512, 1999.

[7] Albert-László Barabási, Réka Albert, and Hawoong Jeong. Mean-field theory for scale-free random networks. *Physica A*, 272(1-2):173–187, 1999.

[8] Marc Barthélemy, Alain Barrat, Romualdo Pastor-Satorras, and Alessandro Vespignani. Velocity and hierarchical spread of epidemic outbreaks in scale-free networks. *Physical Review Letters*, 92(17):178701, 2004.

[9] Marc Barthélemy, Alain Barrat, Romualdo Pastor-Satorras, and Alessandro Vespignani. Dynamical patterns of epidemic outbreaks in complex heterogeneous networks. *Journal of Theoretical Biology*, 235(2):275–288, 2005.

[10] Yakir Berchenko, Yael Artzy-Randrup, Mina Teicher, and Lewi Stone. Emergence and size of the giant component in clustered random graphs with a given degree distribution. *Physical Review Letters*, 102(13):138701, 2009.

[11] S. M. Blower, P. M. Small, and P. C. Hopewell. Control strategies for tuberculosis epidemics: new models for old problems. *Science*, 273(5274):497–500, 1996.

[12] Marián Boguná and Romualdo Pastor-Satorras. Epidemic spreading in correlated complex networks. *Physical Review E*, 66(4):047104, 2002.

[13] Marián Boguná and M. Angeles Serrano. Generalized percolation in random directed networks. *Physical Review E*, 72(1):016106, 2005.

[14] Katy Borner, Soma Sanyal, and Alessandro Vespignani. Network science. *Annual Review of Information Science Technology*, 41(1):537–607, 2007.

[15] Fred Brauer and Carlos Castillo-Chávez. *Mathematical models in population biology and epidemiology*. Springer, 2001.

[16] S. Busenbergand and P. van den Driessche. Analysis of a disease transmission model in a population with varying size. *Journal of Mathhematical Biology*, 29(3):257–270, 1990.

[17] Li Ming Cai, Xue Zhi Li, and Mini Ghosh. Global stability of a stage-structured epidemic model with a nonlinear incidence. *Applied Mathematics and Computation*, 214(1):73–82, 2009.

[18] Duncan S. Callaway, M.E.J. Newman, Steven H. Strogatz, and Duncan J. Watts. Network robustness and fragility: percolation on random graphs. *Physical Review Letters*, 85(25):5468, 2000.

[19] Vincenzo Capasso. *Mathematical structures of epidemic systems*. Springer-Verlag, 1993.

[20] Carlos Castillo-Chavez and Zhilan Feng. To treat or not to treat: the case of tuberculosis. *Journal of Mathematical Biology*, 35(6):629–656, 1997.

[21] M. Catanzaro and R. Pastor-Satorras. Analytic solution of a static scale-free network model. *The European Physical Journal B*, 44(2):241–248, 2005.

[22] Nakul Chitnis, J. M. Cushing, and J. M. Hyman. Bifurcation analysis of a mathematical model for Malaria transmission. *SIAM Journal on Applied Mathematics*, 67(1):24–45, 2006.

[23] Pascal Crépey, Fabián P. Alvarez, and Marc Barthélemy. Epidemic variability in complex networks. *Physical Review E*, 73(4):046131, 2006.

[24] Jingan Cui, Xiaoxia Xia, and Hui Wan. Saturation recovery leads to multiple endemic equilibria and backward bifurcation. *Journal of Theoretical Biology*, 254(2):275–283, 2008.

[25] W. R. Derrick and P. van den Driessche. A disease transmission model in a nonconstant population. *Journal of Mathematical Biology*, 31(5):495–512, 1993.

[26] O. Diekman and J. A. P. Heesterbeek. *Mathematical epidemiology of infectious disease, model building, analysis and interpretation*. Wiley, 2000.

[27] O. Diekmann, J. A. P. Heesterbeek, and J.A.J. Metz. On the definition and the computation of the basic reproduction ratio R_0 in models for infectious diseases. *Journal of Mathematical Biology*, 35(4):503–522, 1990.

[28] S. N. Dorogovtsev and J. F. F. Mendes. Evolution of networks. *Advances In Physics*, 51(4):1079–1187, 2002.

[29] Yoichi Enatsu, Yukihiko Nakata, and Yoshiaki Muroya. Global stability for a class of discrete SIR epidemic models. *Mathematical Bioscience and Engineering*, 7(2):347–361, 2010.

[30] Yoichi Enatsu, Yukihiko Nakata, and Yoshiaki Muroyac. Lyapunov functional techniques for the global stability analysis of a delayed SIRS epidemic model. *Nonlinear Analysis: Real World Applications*, 13(5):2120–2133, 2012.

[31] Stephen Eubank, Hasan Guclu, V. S. Anil Kumar, Madhav V. Marathe, Aravind Srinivasan, Zoltán Toroczkai, and Nan Wang. Modeling disease outbreaks in realistic urban social networks. *Nature*, 429:180–184, 2004.

[32] Zhilan Fang and Horst R. Thieme. Recurrent outbreaks of childhood disease revisited: the impact of isolation. *Mathematical Biosciences*, 128(1-2):93–129, 1995.

[33] Zhilan Feng and Jorge X. Velasco-Hernández. Competitive exclusion in a vector-host model for the dengue fever. *Journal of Mathematical Biology*, 35(5):523–544, 1997.

[34] M. Girvan and M.E.J. Newman. Community structure in social and biological networks. *Proceedings of the National Academy of Sciences*, 99(12):7821–7826, 2002.

[35] M. G. M. Gomes, L. J. White, and G. F. Medley. Infection, reinfection, and vaccination under suboptimal immune protection: epidemiological perspectives. *Journal of Theoretical Biology*, 228(4):539–549, 2004.

[36] W. Govaerts, Yu. A. Kuznetsov, and B. Sijnave. Implementation of Hopf and double-Hopf continuation using bordering methods. *ACM Transactions on Mathematical Software*, 24(4):418–436, 1998.

[37] A. Grabowski and R. A. Kosinski. The SIS model of epidemic spreading in

a hierarchical social network. *Acta Physica Polonica B*, 36(5):1579–1593, 2005.

[38] Thilo Gross and Bernd Blasius. Adaptive coevolutionary networks : a review. *Journal of The Royal Society Interface*, 5(20):259–271, 2007.

[39] Thilo Gross and Ulrike Feudel. Analytical search for bifurcation surfaces in parameter space. *Physica D*, 195(3-4):292–302, 2004.

[40] John Guckenheimer, Mark Myers, and Bernd Sturmfels. Computing Hopf bifurcation I. *SIAM Journal on Numerical Analysis*, 34(1):1–21, 1997.

[41] J.M. Hefferman, R.J. Smith, and L.M. Wahl. Perspectives on the basic reproduction ratio. *Journal of the Royal Society Interface*, 2(4):281–293, 2005.

[42] H. W. Hethcote and P. van den Driessche. Some epidemiologic models with nonlinear incidence. *Journal of Mathematical Biology*, 29(3):271–287, 1991.

[43] H.W. Hethcote and Yi Li. Hopf bifurcation in models for Pertussis epidemiology. *Mathematical and Computer Modelling*, 30(11-12):29–45, 1999.

[44] John A. Jacquez. *Compartmental analysis in biology and medicine*. BioMedware, 3rd edition, 1996.

[45] Yuanwei Jing, Xiangyong Chen, Chunji Li, Vesna M. Ojleska, and Georgi. M. Dimirovski. Domain of attraction estimation for SIRS epidemic models via sum-of-square optimization. 18th IFAC World Congress. Milano,Italy, pages 14289–14294, 2011.

[46] Brian Karrer and M.E.J. Newman. Competing epidemic on complex networks. *Physical Review E*, 84(3):036106, 2011.

[47] E. Kaslik, A.M. Balint, and St. Balint. Methods for determination and approximation of the domain of attraction. *Nonlinear Analysis*, 60(4):703–717, 2005.

[48] Andrea Lancichinetti, Santo Fortunato, and Janos Kertesz. Detecting the overlapping and hierarchical community structure in complex networks. *New Journal of Physics*, 11(3):033015, 2009.

[49] Chunji Li, Lili Cao, Ning Li, and Xiangyong Chen. Estimation the domain of attraction of a class of SIR epidemic model. Chinese Control and Decision Conference, pages 5010–5013, 2008.

[50] Gui Hua Li and Wen Di Wang. Bifurcation analysis of an epidemic model with nonlinear incidence. *Applied Mathematics and Computation*, 214(2):411–423, 2009.

[51] Jianquan Li, Yicang Zhou, Jianhong Wu, and Zhien Ma. Complex dynamics of a simple epidemic model with a nonlinear incidence. *Discrete and Continuous Dynamical Systems -Series B*, 8(1):161–173, 2007.

[52] Michael Y. Li and James S. Muldowney. Global stability for the SEIR model in epidemiology. *Mathematical Biosciences*, 125(2):155–164, 1995.

[53] Michael Y. Li and James S. Muldowney. A geometric approach to the global stability problems. *SIAM Journal on Mathematical Analysis*, 27(4):1070–1083, 1996.

[54] Michael Y Li and Liancheng Wang. A criterion for stability of matrices. *Journal of Mathematical Analysis and Applications*, 225(1):225–249, 1998.

[55] Xue Zhi Li, Wen Sheng Li, and Mini Ghosh. Stability and bifurcation of an SIR epidemic model with nonlinear incidence and treatment. *Applied Mathematics and Computation*, 210(1):141–150, 2009.

[56] Jingzhou Liu, Yifa Tang, and Z. R. Yang. The spread of disease with birth and death on networks. *Journal of Statistical Mechanics: Theory and Experiment*, 2004(8):08008, 2004.

[57] Wei Min Liu, Herbert W. Hethcote, and Simon A. Levin. Dynamical behavior of epidemiologic model with nonlinear incidence rates. *Journal of Mathematical Biology*, 25(4):359–380, 1987.

[58] Wei Min Liu, Simon A. Levin, and Yoh Iwasa. Influence of nonlinear incidence rates upon the behavior of SIRS epidemiologic models. *Journal of Mathematical Biology*, 23(2):187–204, 1986.

[59] Zonghua Liu and Bambi Hu. Epidemic spreading in community networks. *Europhysics Letters*, 72(2):315–321, 2005.

[60] Luis G. Matallana, Anibal M. Blanco, and J. Alberto Bandoni. Estimation of domains of attraction in epidemiological models with constant removal rates of infected individuals. *Journal of Physics: Conference Series*, 90(1):012052, 2007.

[61] Luis G. Matallana, Anibal M. Blanco, and J. Alberto Bandoni. Estimation of domains of attraction: a global optimization approach. *Mathematical and Computer Modelling*, 52(3-4):574–585, 2010.

[62] Cristopher Moore and M. E. J. Newman. Epidemics and percolation in small-world networks. *Physical Review E*, 61(5):5678–5682, 2000.

[63] Y. Moreno, R. Pastor-Satorras, and A. Vespignani. Epidemic outbreaks in complex heterogeneous networks. *The European Physical Journal B*, 26(4):521–529, 2002.

[64] Stefano Mossa, Marc Barthélémy, H. Eugene Stanley, and Luis A. Nunes Amaral. Truncation of power law behavior in scale-free network models due to information filtering. *Physical Review Letters*, 88(13):138701, 2002.

[65] D. Moulay, M.A. Aziz-Alaoui, and M. Cadivel. The Chikungunya disease: modeling, vector and transmission global dynamics. *Mathematical Biosciences*, 229(1):50–63, 2011.

[66] J.D. Murray. *Mathematical biology : I. an introduction*. Springer, 3 edition, 2001.

[67] Ram Naresh, Agraj Tripathi, J.M. Tchuenchec, and Dileep Sharmaaa. Stability analysis of a time delayed SIR epidemic model with nonlinear incidence rate. *Computers and Mathematics with Applications*, 58(2):348–359, 2009.

[68] M. E. J. Newman. Models of small world. *Journal of Statistical Physics*, 101(3-4):819–841, 2000.

[69] M. E. J. Newman. Spread of epidemic disease on networks. *Physical Review E*, 66(1):016128, 2002.

[70] M. E. J. Newman. Finding community structure in networks using the eigenvectors of matrices. *Physical Review E*, 74(3):036104, 2006.

[71] M. E. J. Newman. Modularity and community structure in networks. *Proceedings of the National Academy of Sciences*, 103(23):8577–8582, 2006.

[72] M. E. J. Newman, C. Moore, and D. J. Watts. Mean-field solution of the small-world network model. *Physical Review Letters*, 84(14):3201–3204, 2000.

[73] M. E. J. Newman and D. J. Watts. Scaling and percolation in the small-world network model. *Physical Review E*, 60(6):7332–7342, 1999.

[74] M.E.J. Newman, S. H. Strogatz, and D. J. Watts. Random graphs with arbitrary degree distribution and their application. *Physical Review E*, 64(2):026118, 2001.

[75] M. Nuno, Z. Feng, M. Martcheva, and C. Castillo-Chavez. Dynamics of two-strain influenza with isolation and partial cross immunity. *SIAM Journal on Applied Mathematics*, 65(3):964–982, 2005.

[76] Jian Hua Pang, Jing An Cui, and Jing Hui. Rich dynamics of an epidemic model with sub-optimal immunity and nonlinear recovery rate. *Mathematical and Computer Modelling*, 54(1-2):440–448, 2011.

[77] Romualdo Pastor-Satorras and Alessandro Vespignani. Epidemic spreading in scale-free networks. *Physical Review Letters*, 86(14):3200–3203, 2001.

[78] Romualdo Pastor-Satorras and Alessandro Vespignani. Epidemic dynamics in finite size scale free networks. *Physical Review E*, 65(3):035108, 2002.

[79] Romualdo Pastor-Satorras and Alessandro Vespignani. Immunization of complex networks. *Physical Review E*, 65(3):036104, 2002.

[80] Guo Jin Peng and Yao Lin Jiang. Practical computation of normal forms of the Bogdanov-Takens bifurcation. *Nonlinear Dynamics*, 66(1-2):99–132, 2011.

[81] Nandita Roy and Nilimesh Halder. Compartmental modeling of hand, foot and mouth infectious disease (HFMD). *Research Journal of Applied Sciences*, 5(3):177–182, 2010.

[82] Szabolcs Rozgonyi, Katalin M. Hangos, and Gábor Szederkényi. Determining the domain of attraction of hybrid non-linear systems using maximal Lyapunov functions. *Kybernetika*, 46(1):19–37, 2010.

[83] Shi Gui Ruan and Wen Di Wang. Dynamical behaviour of an epidemic model with a nonlinear incidence rate. *Journal of Differential Equations*, 188(1):135–163, 2003.

[84] S.Boccaletti, V.Latora, Y.Moreno, M.Chavez, and D.U.Hwang. Complex networks : structure and dynamics. *Physics Reports*, 424(4-5):175–308, 2006.

[85] Zigen Song, Jian Xu, and Qunhong Li. Local and global bifurcations in an SIR epidemic model. *Applied Mathematics and Computation*, 214(2):534–547, 2009.

[86] Steven H. Strogatz. Exploring complex networks. *Nature*, 410:268–276, 2001.

[87] P. van den Driessche and James Watmough. *Mathematical epidemiology*, volume 1945, chapter 6 Further notes on the basic reproduction number, pages 159–178. Springer, 2008.

[88] A. Vannelli and M. Vidyasagar. Maximal Lyapunov functions and domains of attraction for autonomous nonlinear systems. *Automatica*, 21(1):69–80, 1985.

[89] Alexei Vazquez. Spreading dynamics on heterogeneous populations : multitype network approach. *Physical Review E*, 74(6):066114, 2006.

[90] Wendi Wang. Backward bifurcation of an epidemic model with treatment. *Mathematical Biosciences*, 201(1-2):58–71, 2006.

[91] Wendi Wang and Shigui Ruan. Bifurcations in an epidemic model with constant removal rate of the infectives. *Journal of Mathematical Analysis and Applications*, 291(2):775–793, 2004.

[92] Duncan J. Watts and Steven H. Strogatz. Collective dynamics of small-world networks. *Nature*, 393:440–442, 1998.

[93] Marjorie J. Wonham, Tomás de Camino-Beck, and Mark A. Lewis. An epidemiological model for West Nile virus: invasion, analysis and control applications. *Proceedings of the Royal Society London B*, 271(1538):501–507, 2004.

[94] Lih-Ing Wu and Zhilan Feng. Homoclinic bifurcation in an SIQR model for childhood diseases. *Journal of Differential Equations*, 168(1):150–167, 2000.

[95] Xiaoyan Wu and Zonghua Liu. How community structure influences epidemic spread in social networks. *Physica A: Statistical Mechanics and its Applications*, 387(2-3):623–630, 2008.

[96] Rui Xu, Zhien Ma, and Zhiping Wang. Global stability of a delayed SIRS epidemic model with saturation incidence and temporary immunity. *Computers and Mathematics with Applications*, 59(9):3211–3221, 2010.

[97] Na Yi, Peng Liu, Qingling Zhang, and Shuhui Shi. Neimark-Sacker bifurcation and control of a discrete epidemic model. 2nd International Asia Conference on Informatics in Control, Automation and Robotics, pages 409–412, 2010.

[98] D. H. Zanette. Dynamics of rumor propagation on small-world networks. *Physical Review E*, 65(4):041908, 2002.

[99] Xu Zhang and Xianning Liu. Backward bifurcation of an epidemic model with saturated treatment function. *Journal of Mathematical Analysis and Applications*, 348(1):433–443, 2008.

[100] Zhonghua Zhang and Yaohong Suo. Qualitative analysis of a SIR epidemic model with saturated treatment rate. *Journal of Applied Mathematics and Computing*, 34(1-2):177–194, 2010.

[101] Zhonghua Zhang, Jianhua Wu, Yaohong Suo, and Xinyu Song. The domain of attraction for the endemic equilibrium of an SIRS epidemic model. *Mathematics and Computers in Simulation*, 81(9):1697–1706, 2011.

[102] Rui Jun Zhao and Fabio Augusto Milner. A mathematical model of schistosoma mansoni in biomphalaria glabrata with control strategies. *Bulletin of Mathematical Biology*, 70(7):1886–1905, 2008.

[103] Yu Gui Zhou, Dong Mei Xiao, and Yi Long Li. Bifurcation of an epidemic model with non-monotonic incidence rate of saturated mass action. *Chaos, Solitons and Fractals*, 32(5):1903–1915, 2007.

terial. I would be pleased to hear from any copyright owner who has been omitted or incorrectly acknowledged.